Bioelectromagnetics 10:197–202 (1989)

Radiofrequency Radiation-Induced Calcium Ion Efflux Enhancement From Human and Other Neuroblastoma Cells in Culture

S.K. Dutta, B. Ghosh, and C.F. Blackman

Departments of Botany and Radiotherapy and the Cancer Research Center, Howard University, Washington, DC (S.K.D., B.G.); Health Effects Research Laboratory, Environmental Protection Agency, Research Triangle Park, North Carolina (C.F.B.)

To test the generality of radiofrequency radiation-induced changes in $^{45}Ca^{2+}$ efflux from avian and feline brain tissues, human neuroblastoma cells were exposed to electromagnetic radiation at 147 MHz, amplitude-modulated (AM) at 16 Hz, at specific absorption rates (SAR) of 0.1, 0.05, 0.01, 0.005, 0.001, and 0.0005 W/kg. Significant $^{45}Ca^{2+}$ efflux was obtained at SAR values of 0.05 and 0.005 W/kg. Enhanced efflux at 0.05 W/kg peaked at the 13–16 Hz and at the 57.5–60 Hz modulation ranges. A Chinese hamster-mouse hybrid neuroblastoma was also shown to exhibit enhanced radiation-induced $^{45}Ca^{2+}$ efflux at an SAR of 0.05 W/kg, using 147 MHz, AM at 16 Hz. These results confirm that amplitude-modulated radiofrequency radiation can induce responses in cells of nervous tissue origin from widely different animal species, including humans. The results are also consistent with the reports of similar findings in avian and feline brain tissues and indicate the general nature of the phenomenon.

Key words: frequency windows, intensity windows, power line frequency

INTRODUCTION

Calcium ions are important in maintaining normal physiologic function in brain tissues. Therefore, radiation-enhanced calcium efflux may affect nervous system function. Bawin et al. [1975] and Blackman et al. [1979, 1980a, 1981] have studied radiofrequency (RF)-induced efflux of radioactive calcium ions with low-power 147 MHz carrier waves, sinusoidally amplitude-modulated (AM) at 16 Hz. All these studies at extremely low modulation frequencies were performed with freshly removed avian and feline brain tissues. We have tested the generality of the response by using cultured neural cells derived from human and another vertebrate sources. In a previous study [Dutta et al., 1984], we reported enhanced efflux of calcium ions

Received for review March 18, 1988; revision received September 19, 1988.

Address reprint requests to Dr. S.K. Dutta, Department of Botany, Howard University, Washington, DC 20059.

from human neuroblastoma cells in culture exposed to RF radiation at 915 MHz, AM at 16 Hz. This is a report of the effects of AM 147 MHz radiation, similar to the exposure used in the study by Bawin et al. [1975] and Blackman et al. [1979, 1980a, 1981], on neuroblastoma cells derived from humans and other vertebrates. Our studies confirm and extend the generality of RF-induced enhanced $^{45}Ca^{2+}$ efflux to mammalian neural cells.

MATERIALS AND METHODS

Human neuroblastoma cells (IMR 32) were obtained from the American Type Culture Collection (ATCC). This cell line was established from a neuroblastoma in a 13-month-old white male. In our routine microscopic examinations, this culture is a morphologically distinct cell type. The other cell line was the Chinese hamster-mouse hybrid neuroblastoma cell line NG-108 obtained from the U.S. National Institute of Health.

The cultures were grown in minimum essential medium (MEM-Eagle-Earles balanced salt solution, with nonessential amino acids and sodium pyruvate) supplemented with 10% fetal bovine serum, glutamine (0.02 mM), and gentamycin (1%). All media components were obtained from M.A. Bioproducts (Walkersville, MD). Each cell culture was seeded in T-flasks (25 cm^2 growth surface) with identical 5 ml aliquots of medium and was grown to a confluent monolayer containing about 2.0×10^7 cells.

The exposure system is the same as that described earlier by Dutta et al. [1984]. The exposure chamber, a Crawford cell (Instrument for Industry, Model BC-110), consisted of a transmission line tapered at each end to mate with a standard coaxial cable. A signal generator (Hewlett Packard, Model 8640) provided the 147 MHz carrier frequency, which was sinusoidally AM (80%) at low frequencies with a function generator (Krohn-Hite, Model 5200). The modulated signals were amplified with a linear amplifier (Amplifier Research, Model IW 1000). Two identical thermoelectric power meters (Hewlett-Packard, Model 432B) and sensors (Hewlett-Packard Model 478A), attached to 20 dB bidirectional couplers (Narda, Model 3020A), were used in conjunction with a switch (Sage Laboratories, Model STN2180A, Type 1P2T) to measure the forward, reflected, and transmitted powers.

Specific absorption rates (SARs) were determined from incident, reflected, and transmitted powers measured with 1) an empty Crawford cell, 2) a Crawford cell with an empty flask, and 3) a Crawford cell and flask with culture and 5 ml of growth medium. The reflected power was adjusted to zero with a tuner (Weinschel Engineering, model DS-109LL) for each measurement. SAR for a given incident power was determined as described previously [Dutta et al., 1984]. No attempt was made to estimate the local SAR in the monolayer of cells; it was assumed that the composition of the cells was sufficiently close to the medium so that the measured SAR was an adequate approximation for the cells as well. The measured SAR was then varied by increasing or decreasing the forward power once the percentage of absorption was determined. The static, local geomagnetic field (LGF) in the exposure system as measured by a gauss meter (Bell model 640) was 16 μT (0.16 gauss) at an inclination of 53°.

Procedures for cell labeling, exposures, and assay have been described previously [Dutta et al., 1984]. Four identical confluent flasks containing the cells of

TABLE 1. Calcium Ion Efflux in Two Cell Lines*

Cells	Release of calcium during exposure		Difference in release, paired samples	P value, for
	Control ± SEM(n)[a]	Exposed± SEM(n)[a]	mean ± SEM(n)[a]	paired samples
IMR-32[b]	2,192 ± 228 (14)	3,011 ± 282 (14)	818 ± 140 (14)	<0.001
NG-108[c]	2,230 ± 195 (10)	2,594 ± 229 (10)	365 ± 64 (10)	<0.001

*147 MHz electromagnetic radiation, amplitude modulated at 16 Hz, at an SAR of 0.05 W/kg.
[a]Mean counts per minute ± standard error of the mean (number of samples).
[b]Human neuroblastoma from ATCC.
[c]Hybrid (Chinese hamster-mouse) neuroblastoma cell line from NIH.

interest were selected. Old medium was replaced by 5 ml of fresh medium supplemented with $^{45}Ca^{2+}$ (E.I. Dupont; specific activity of 5 μCi/ml). Flasks were kept at 37 °C for 2 hr for optimum incorporation of the isotope. Cultures were washed three times with 5 ml of medium to remove unincorporated radioactivity; the washing process took 4–5 min. After washing, 6 ml of complete medium without radioactive calcium ions was added to the culture and mixed gently. One milliliter of medium was removed from each flask and kept in a microcentrifuge tube for an initial count. Two flasks were placed inside the Crawford cell and the other two were placed outside the Crawford cell but in the same incubator, which maintained them all at 37 °C. The flasks were exposed for 30 min to selected values of modulated RF radiation.

Following a 30-min exposure to various treatments, an aliquot of medium was removed from each flask, placed in a microcentrifuge tube along with the tubes containing the 1 ml aliquot representing the initial count, and centrifuged at 13,000*g* for 1 min to remove cell debris. A volume was withdrawn from each tube and counted in a scintillation counter to estimate the release of radioactive calcium ions from the cells in counts per minute (cpm). Sample channel ratios were used to monitor the counting efficiency between samples.

The data were analyzed by paired t test as follows. The radioactivity released before exposure was subtracted from that present after 30 min of treatment for each flask (exposure and control). The radioactivity released during the 30 min period was calculated for each exposed and control flask, and a mean difference in release between exposed and control flasks was calculated for the set. For a given exposure condition, additional sets of flasks were assayed to increase the sample size and were then analyzed by a paired t test (two-tailed) to determine if the exposure caused a statistically significant alteration in the release of radioactivity from the exposed samples.

Tests were done to compare the calcium ion efflux from cells in the incubator at 37 °C (controls) to those kept inside the Crawford cell unexposed (sham-treated). No differences were detected between control and sham-treated samples.

RESULTS

$^{45}Ca^{2+}$ Efflux in Different Cell Lines

Table 1 summarizes the results of RF-induced $^{45}Ca^{2+}$ efflux studies conducted with 147 MHz carrier waves, AM at 16 Hz, with two neuroblastoma cell lines of different origin. The SAR (0.05 W/kg) and AM frequency (16 Hz) were chosen

TABLE 2. Calcium Ion Efflux From Human Neuroblastoma Cells* Exposed to Different SARs of 147 MHz Radiation Amplitude Modulated at 16 Hz

SAR (W/kg)	Release of calcium during exposure: Control ± SEM (n)[a]	Release of calcium during exposure: Exposed ± SEM (n)[a]	Difference in release, paired samples mean ± SEM (n)[a]	*P* value, for paired samples
0.0001	1,314 ± 141 (9)	1,324 ± 88 (9)	10 ± 73 (9)	0.897
0.0005	1,299 ± 132 (5)	1,282 ± 136 (5)	− 17 ± 25 (5)	0.537
0.0007	2,391 ± 529 (4)	2,384 ± 459 (4)	− 7 ± 143 (4)	0.964
0.001	1,811 ± 206 (9)	1,795 ± 205 (9)	− 16 ± 92 (9)	0.861
0.002	1,948 ± 153 (11)	1,941 ± 128 (11)	− 6 ± 77 (11)	0.938
0.005	2,684 ± 141 (9)	3,402 ± 193 (9)	719 ± 170 (9)	<0.003
0.010	2,109 ± 128 (22)	2,032 ± 125 (22)	− 76 ± 39 (22)	0.066
0.050[b]	2,192 ± 228 (14)	3,011 ± 282 (14)	818 ± 140 (14)	<0.001
0.100	1,718 ± 114 (5)	1,808 ± 162 (5)	90 ± 95 (5)	0.400

*Human neuroblastoma, IMR-32, from ATCC.
[a]Mean counts per minute ± standard error of the mean (number of samples).
[b]Data from Table 1.

because of their previously determined effectiveness [Dutta et al., 1984]. Significant changes in $^{45}Ca^{2+}$ efflux, when compared with that in the corresponding unirradiated cells, were found under these exposure conditions in cells of both human and nonhuman origin.

$^{45}Ca^{2+}$ Efflux at Different SARs of 147 MHz, 16 Hz AM

Table 2 presents the composite data from numerous tests with the neuroblastoma cell line IMR-32 at SAR values between 0.0001 and 1 W/kg. Of 10 different dose rates tested, $^{45}Ca^{2+}$ efflux enhancement occurs only at unique SAR windows, unlike the standard dose-response curves normally seen with chemical agents. The percent changes in $^{45}Ca^{2+}$ efflux at SAR values of 0.05 and 0.005 W/kg are 37 and 27, respectively. These changes are statistically significant ($P < .003$) when compared to the efflux from unirradiated cells.

$^{45}Ca^{2+}$ Efflux as a Function of AM Frequencies

Additional tests were conducted with the neuroblastoma cell line IMR-32 at different AM frequencies. These results are summarized in Table 3. The efflux of calcium ions from brain cells was induced only by specific ELF frequencies, which is consistent with our previous report [Dutta et al., 1984] with 915 MHz carrier waves amplitude modulated near or at 16-Hz. Modulation frequencies centered on 16 Hz caused enhanced efflux with both 915 and 147 MHz carrier waves. In addition, in this study with 147 MHz carrier waves, significant $^{45}Ca^{2+}$ efflux was induced at AM frequencies centered near 60 Hz.

DISCUSSION

The purpose of this study was to determine whether cell culture systems would respond to modulated RF radiation under these conditions and in a manner similar to responses exhibited by the chick brain preparations of Bawin et al. [1975, 1978] and

TABLE 3. Calcium Ion Efflux From Human Neuroblastoma Cells* Exposed to 147 MHz Radiation** Amplitude Modulated at Different Frequencies

AM freq. (Hz)	Release of calcium during exposure		Difference in release, paired samples mean ± SEM (n)[a]	P value, for paired samples
	Control ± SEM (n)[a]	Exposed ± SEM (n)[a]		
9	2,750 ± 333 (7)	2,711 ± 343 (7)	− 38 ± 187 (7)	0.844
13	2,696 ± 200 (7)	2,932 ± 243 (7)	236 ± 88 (7)	0.037
16	2,148 ± 192 (7)	3,553 ± 318 (7)	1,405 ± 361 (7)	0.008
18	1,673 ± 129 (7)	1,969 ± 172 (7)	296 ± 176 (7)	0.143
20	1,953 ± 192 (7)	1,609 ± 226 (7)	− 343 ± 155 (7)	0.068
55	1,608 ± 127 (7)	1,713 ± 92 (7)	105 ± 128 (7)	0.445
57.5	2,510 ± 520 (7)	3,140 ± 485 (7)	630 ± 94 (7)	<0.001
60	2,485 ± 282 (7)	3,323 ± 98 (7)	838 ± 288 (7)	0.027
62.5	2,256 ± 221 (6)	2,928 ± 96 (6)	592 ± 317 (6)	0.121
65	2,357 ± 141 (7)	2,457 ± 154 (7)	101 ± 116 (7)	0.420

*IMR-32, from ATCC.
**SAR of 0.05 W/kg.
[a]Mean counts per minute ± standard error of the mean (number of samples).

Blackman et al. [1979, 1980a,b, 1981, 1985a]. The initial work with cell culture preparations [Dutta et al., 1984] used a higher carrier frequency, 915 MHz, and a higher SAR, 0.05 W/kg. These results show that 147 MHz carrier waves, at 0.05 W/kg, can induce increased efflux of calcium ions from mouse-hamster hybrid and human cell culture lines. Furthermore, the results demonstrate the same unusual response pattern, namely, two regions of strongly positive effects surrounded by regions of either negative effects or marginal effects (i.e., 0.010 W/kg produced an result with a P value of 0.066, which does not meet the $P < .05$ criterion for a statistically significant difference between exposed and control). This P value may indicate that the particular SAR is located in the transition region between effect and no effect. No studies have been conducted to determine whether there is a reciprocity between SAR and exposure duration.

The responses of brain tissue in previous reports, and the nervous system-derived cell culture preparations here, are similar in carrier frequency, modulation frequency, and SAR. Thus the results with the avian and cat brain tissue preparation can be generalized to other in vitro biological systems, including cells of human origin. Furthermore, particular ELF modulation ranges show positive effects whereas others do not. The positive responses at 13 and 16 Hz but not at 9, 18, or 20 Hz indicate a frequency window noted by others with chick brain tissue. However, the positive responses at 57.5 and 60 Hz, but not at 55, 62.5, or 65 Hz, show a very narrow frequency response in the frequency region of electric power transmission. It should be noted that the half width is narrower for the cell culture preparation than that reported by Bawin et al. [1975] for the brain tissue preparation. The only other similar response with central nervous system (CNS) samples at a power line modulation frequency was noted by Blackman et al. [1985a], who demonstrated sensitivity of the chick brain preparation to 50 Hz modulation of a 50 MHz field, within a narrow power density region. The reason for this sensitivity is unknown. Although the effective frequencies of ELF fields alone have been shown to be influenced by the local geomagnetic field (LGF) [Blackman et al., 1985b], there is no

information on the role the LGF might play in modulated RF radiation results, because the demodulation site and process are not understood.

The final conclusion from this study is that cell lines derived from tumors of the CNS, neuroblastomas, respond to modulated RF fields in a manner identical to the normal, forebrain-tissue preparations from newborn chicks and from felines. This indicates that the response is not due exclusively to the transformed state of the cells. Furthermore, cells of non-CNS origin (e.g., human nonneuronal cancer cells and fibroblasts) did not show a similar response to the fields (unpublished pilot data). Thus cells of CNS origin may respond to the modulated RF fields in a very specific manner. However, this result cannot be generalized without qualification because of the small number of cell types tested.

ACKNOWLEDGMENTS

The authors wish to acknowledge support from the U.S. Environmental Protection Agency (Cooperative Agreement No. CR-812100) and from the U.S. Department of Energy (Interagency Agreement No. DE-AI06-87RL11374 to U.S. EPA).

The research described in this article has been reviewed by the Health Effects Research Laboratory, U.S. Environmental Protection Agency, and approved for publication. Approval does not signify that the contents necessarily reflect the views and policies of the Agency, nor does mention of trade names or commercial products constitute endorsement or recommendation for use.

REFERENCES

Bawin SM, Adey WR, Sabbot IM (1978): Ionic factors in release of $^{45}Ca^{2+}$ from chicken cerebral tissue by electromagnetic fields. Proc Natl Acad Sci USA 75:6314–6318.

Bawin SM, Kaczmarek LK, Adey WR (1975): Effects of modulated VHF fields on the central nervous system. Ann NY Acad Sci 247:74–81.

Blackman CF, Benane SG, Elder JA, House DE, Lampe JA, Faulk JM (1980a): Induction of calcium-ion efflux from brain tissue by radiofrequency radiation: Effect of sample number and modulation frequency on the power-density window. Bioelectromagnetics 1:35–43.

Blackman CF, Benane SG, House DE, Joines WT (1985a): Effects of ELF (1–120 Hz) and modulated (50 Hz) RF fields on the efflux of calcium ions from brain tissue in vitro. Bioelectromagnetics 6:1–11.

Blackman CF, Benane SG, Joines WT, Hollis MA, House DE (1980b): Calcium-ion efflux from brain tissue: Power-density versus internal field-intensity dependencies at 50-MHz RF radiation. Bioelectromagnetics 1:277–283.

Blackman CF, Benane SG, Rabinowitz JR, House DE, Joines WT (1985b): A role for the magnetic field in the radiation-induced efflux of calcium ions from brain tissue in vitro. Bioelectromagnetics 6:327–337.

Blackman CF, Elder JA, Weil CM, Benane SG, Eichinger DC (1979): Induction of calcium-ion efflux from brain tissue by radiofrequency radiation: Effects of modulation frequency and field strength. Radio Sci 14(6S):93–98.

Blackman CF, Joines WT, Elder JA (1981): Calcium-ion efflux in brain tissue by radiofrequency radiation. In Illinger KH (ed): "Biological Effects of Nonionizing Radiation." Washington, DC: American Chemical Society, pp 299–314.

Dutta SK, Subramoniam A, Ghosh B, Parshad R (1984): Microwave radiation-induced calcium ion efflux from human neuroblastoma cells in culture. Bioelectromagnetics 5:71–78.

Prof. Jerabek

E47

Journal of Cellular Biochemistry 51:410–416 (1993)

Biological Effects of Electromagnetic Fields

W. Ross Adey

Pettis Memorial VA Medical Center and University School of Medicine, Loma Linda, California 92357

Abstract Life on earth has evolved in a sea of natural electromagnetic (EM) fields. Over the past century, this natural environment has sharply changed with introduction of a vast and growing spectrum of man-made EM fields. From models based on equilibrium thermodynamics and thermal effects, these fields were initially considered too weak to interact with biomolecular systems, and thus incapable of influencing physiological functions. Laboratory studies have tested a spectrum of EM fields for bioeffects at cell and molecular levels, focusing on exposures at athermal levels. A clear emergent conclusion is that many observed interactions are not based on tissue heating. Modulation of cell surface chemical events by weak EM fields indicates a major amplification of initial weak triggers associated with binding of hormones, antibodies, and neurotransmitters to their specific binding sites. Calcium ions play a key role in this amplification. These studies support new concepts of communication between cells across the barriers of cell membranes; and point with increasing certainty to an essential physical organization in living matter, at a far finer level than the structural and functional image defined in the chemistry of molecules. New collaborations between physical and biological scientists define common goals, seeking solutions to the physical nature of matter through a strong focus on biological matter. The evidence indicates mediation by highly nonlinear, nonequilibrium processes at critical steps in signal coupling across cell membranes. There is increasing evidence that these events relate to quantum states and resonant responses in biomolecular systems, and not to equilibrium thermodynamics associated with thermal energy exchanges and tissue heating.

Key words: cell membrane, electromagnetic fields, cooperative processes, nonequilibrium thermodynamics, free radicals, athermal interactions

In cellular aggregates that form tissues of higher animals, cells are separated by narrow fluid channels that take on special importance in signaling from cell to cell. These channels act as windows on the electrochemical world surrounding each cell. Hormones, antibodies, neurotransmitters and chemical cancer promoters, for example, move along them to reach binding sites on cell membrane receptors [Adey, 1992a]. These narrow fluid "gutters," typically not more than 150 Å wide, are also preferred pathways for intrinsic and environmental electromagnetic (EM) fields, since they offer a much lower electrical impedance than cell membranes. Although this intercellular space (ICS) forms only about 10 percent of the conducting cross section of typical tissue, it carries at least 90 percent of any imposed or intrinsic current, *directing it along cell membrane surfaces.*

Received October 14, 1992; accepted October 22, 1992.

Address reprint requests to Dr. W.R. Adey, Research Service (151), VA Medical Center, 11201 Benton Street, Loma Linda, CA 92357.

Numerous stranded protein molecules protrude from within the cell into this narrow ICS. Their glycoprotein tips form the *glycocalyx*, which senses chemical and electrical signals in surrounding fluid. Their highly negatively charged tips form receptor sites for hormones, antibodies, neurotransmitters, and for many metabolic agents, including cancer promoters. These charged terminals form an anatomical substrate for the first detection of weak electrochemical oscillations in pericellular fluid, including field potentials arising in activity of adjacent cells or as tissue components of environmental fields.

OBSERVED SENSITIVITIES TO IMPOSED EM FIELDS

As a perspective on the biological significance of this cell-surface current flow, there is evidence from a number of studies that extremely low frequency (ELF) fields in the range 0–100 Hz and radiofrequency (RF) fields amplitude-modulated in this same ELF range, producing tissue gradients in the range 10^{-7}–10^{-1} V/cm, are involved in essential physiological functions

in marine vertebrates, birds, and mammals [see Adey, 1981, for review]. In vitro studies have reported similar sensitivities for cerebral Ca^{2+} efflux, and in a wide spectrum of calcium-dependent processes that involve cell membrane functions, including bone-growth, modulation of intercellular communication mechanisms that regulate cell growth, reduction of cell-mediated cytolytic immune responses, and modulation of intracellular enzymes that are molecular markers of signals arising at cell membranes and then coupled to the cell interior.

The steady *membrane potential* characteristic of most cells is approximately 0.1 V in the resting state. Since this potential exists across the 40 Å of the very thin plasma membrane, it creates an enormous electric barrier of 10^5 V/cm, many orders of magnitude greater than these intrinsic and imposed electric oscillations in fluid surrounding cells. Nevertheless, these sensitivities have been confirmed for many cell types, including lymphocytes, ovary cells, bone cells, fibroblasts, cartilage cells, and nerve cells [Adey, 1992a].

These observations have been viewed cautiously by many biologists as beyond the realm of a possible physical reality. However, it is necessary to view them in the context of cooperative processes and associated nonlinear electrodynamics at cell membranes, revealed with imposed EM fields. As discussed below, these phenomena are in the realm of nonequilibrium thermodynamics, and are thus far removed from traditional equilibrium models of cellular excitation based on depolarization of the membrane potential and on associated massive changes in ionic equilibria across the cell membrane.

PRINCIPAL AREAS OF RECENT RESEARCH IN BIOELECTROMAGNETICS

The main endeavors in this field have focused on limited but widely separated areas of biology and medicine. In many respects, they form an hierarchical sequence: (1) coupling mechanisms between fields and tissues at the cellular level [Adey, 1990, 1992a; Hoth and Penner, 1992; Luben, 1991; Moolenaar et al., 1986]; (2) field effects on embryonic and fetal development [Delgado et al., 1982; McGivern et al., 1990]; (3) modulation of central nervous and neuroendocrine functions [Lerchl et al., 1990; Reiter, 1992; Wilson and Anderson, 1990]; (4) modification of immune functions [Byus et al., 1984; Lyle et al., 1983, 1988]; (5) regulation of cell growth, and EM field action in tumor promotion [Wilson et al., 1990]; (6) modulation of gene expression [Goodman and Henderson, 1988; Phillips et al., 1992]; and (7) from pioneering therapeutic applications in healing ununited fractures, there is a vista of much broader future therapies that may involve joint use of pharmacological agents and EM fields, each tailored for optimal dosage in these specific applications [Mir et al., 1992; Weaver, 1992].

Research in tumorigenesis now emphasizes *epigenetic* mechanisms, focusing on dysfunctions at cell membranes, rather than on damage to DNA in cell nuclei [Pitot and Dragan, 1991; Yamasaki, 1991]. Steps in tumor formation are described in the *initiation–promotion–progression* model [Weinstein, 1988]. *Initiation* typically involves a single event, damaging nuclear DNA, as through action of ionizing radiation or chemicals. Tumor formation does not occur unless there is subsequent, repeated intermittent exposures to *promoters*, with many known to act at cell membranes. There is minimal evidence that EM fields act as initiators. Current and planned research is directed to possible promoter actions of EM fields at cell membranes, acting either alone or together with chemical agents [Adey, 1990b, 1991, 1992b].

THE TRANSDUCTIVE STEP; EM FIELD DETECTION IN BIOMOLECULAR SYSTEMS

As evidence has mounted confirming occurrence of bioeffects of EM fields that are not only dwarfed by much larger intrinsic bioelectric processes, but may also be substantially below the level of tissue thermal noise, there is a mainstream of theoretical and experimental studies seeking the first transductive steps.

CYCLOTRON RESONANCE AND CA COORDINATION COMPOUND MODELS OF LOW-FREQUENCY EM FIELD SENSITIVITIES

In a cyclotron oscillator, charged particles are exposed to a static magnetic field and to an oscillating magnetic field at right angles to one another. The particles will move in circular orbits at right angles to the two imposed fields when the frequency of the imposed oscillating field matches the particle gyrofrequency, determined by its mass, charge, and the intensity of the static magnetic field.

Free (unhydrated) Ca ions in the earth's geomagnetic field would exhibit cyclotron resonance frequencies around 10 Hz, with cyclotron

currents as much as five orders of magnitude greater than the Faraday currents [Polk, 1984]. Liboff [1985] hypothesized that EM fields close to cyclotron frequencies may couple to ionic species, transferring energy selectively to these ions. Criticism of this model has been directed at its requirements for ions to be stripped of hydration shells that would presumably alter gyrofrequencies, and to the presumed direction of ion motion in the magnetic field.

Lednev [1991] has proposed a quite different explanation of the same experimental conditions. Considering an ion inside a Ca-binding protein as a charged oscillator, a shift in the probability of an ion transition between different states of vibrational energy occurs when there is a combination of static and oscillating magnetic fields. This in turn affects the interaction of the ion with surrounding ligands. This effect is maximal when the frequency of the alternating field is equal to the cyclotron frequency of this ion or to some of its harmonics or subharmonics.

These models do not address the question of transductive coupling of these weak EM fields at energy levels substantially below the thermal energy of living tissues. Answers to that important question are currently sought in EM field interactions with free radicals.

A POSSIBLE ROLE FOR FREE RADICALS

McLauchlan [1992] has proposed a role for chemically reactive free radicals at 50 and 60 Hz electric power frequencies. In McLauchlan's model, very low static magnetic fields cause triplet pairs to break and form singlets. But as the field is increased, typically to a level of about 8 mT, two of the three triplet states become entirely decoupled from the singlet state. Thus, at this field level two-thirds of the radical pairs may not react as they would in a weaker field, "an enormous effect of a small magnetic field on a chemical reaction. *and the effect begins at the lowest applied field strength, even at levels below thermal (kT) noise*. . . . The all-important interaction has an energy very much less than the thermal energy of the system, and is effective exclusively through its influence on the kinetics; this is counter-intuitive to most scientists." The effect is quite general and does not depend on any specific chemical identity of the radicals.

Addition of an oscillating field to this system introduces intensity *windows* that cause triplets to return to singlet states that react with one another. The major effect of the field is to remove degeneracies of sublevels of the triplet pair, whose energies are equal in zero field, but differ progressively in an increasing field as a Zeeman splitting effect.

COOPERATIVE MODELS OF FREE RADICAL BEHAVIOR IN EM FIELD BIOEFFECTS

Research at the other extreme in the EM spectrum also support concepts of free radical interactions. There may be special significance to biomolecular interactions with millimeter wave EM fields. At frequencies within the range 10–1,000 GHz, resonant vibrational or rotational interactions, not seen at lower frequencies, may occur with molecules or portions of molecules [Illinger, 1981]. Biomolecular and cell research in this spectral region has been meager. Studies in solutions of DNA and of growth effects in bacteria have yielded conflicting results that may relate to extreme technical difficulties not encountered at lower frequencies. There are major problems in the engineering of suitable exposure systems, in ensuring biocompatible exposure devices, and in evaluation of experimental data for physical and biological artifacts [see Adey, 1990a, for review].

Studies of yeast cell growth by a team of German scientists over the past 15 years using athermal millimeter wave fields [Grundler and Keilmann, 1978; Grundler and Kaiser, 1992] have shown that growth appears finely "*tuned*" to applied field frequencies around 42 GHz, with successive peaks and troughs at intervals of about 10 MHz. In recent studies, they noted that the sharpness of the tuning increases as the intensity of the imposed field decreases; but the tuning peak occurs at the same frequency when the field intensity is progressively reduced. Moreover, clear responses occur with incident fields as weak as 5 picowatts/cm^2.

In a recent synthesis emphasizing nonthermal interactions of EM fields with cellular systems, Grundler et al. [1992] present models of the sequence of EM field transductive coupling, based on magnetic field-dependent chemical reactions, including cytochrome-catalyzed reactions that involve transient radical pairs, and production of free radicals, such as reactive oxygen or nitric oxide, leading to further highly cooperative amplification step. Based on Frohlich's [1986] model of interactions between an imposed field and high-frequency (10^{12} Hz) intracellular van der Pol oscillators, they con-

clude that "imposed fields can be active even at intensities near zero." In other words, a threshold might not exist in such a system.

DETERMINATION OF THE ROLE OF IRON-CONTAINING MOLECULES IN SENSITIVITIES TO EM FIELDS

There is a wealth of evidence that iron-containing molecules are widespread in the chemistry of cellular transductive mechanisms. They include transferrins with specific receptors on cell surfaces, heme-containing G proteins that couple receptors to enzymes at cell membranes, and cytochrome P-450 enzymes that are key elements in cellular respiration. Transferrin mechanisms are sensitive to 60-Hz EM fields [Phillips, 1986]. These iron atoms are not arranged in ferromagnetic configurations and are too scattered to form magnetic dipoles. Nonetheless, future research may focus on their interactions with biomolecules that exhibit paramagnetic properties.

Neuromelanin exhibits paramagnetism, due to the presence of large numbers of unpaired electrons, qualifying this molecule as a stable free radical. It is suspected of a role in Parkinson's disease. These molecules influence proton relaxation times in NMR studies. Although shortened T1 relaxation time in these studies were attributed to paramagnetism of melanin free radicals, it has now been shown that this shortening requires interactions of paramagnetic ferric iron with melanin [Tosk et al., 1992]. Future developments may allow MRI studies of nigrostriatal regions of the brain in Parkinson's disease, based on compromised status of neuromelanin and ferric iron.

BIOPHYSICAL MODELS OF TRANSMEMBRANE SIGNALS; INWARD SIGNALING ALONG CELL MEMBRANE RECEPTOR PROTEINS

McConnell [1975] noted that intrusion of a protein strand into an artificial phospholipid bilayer induces coherent states between charges on tails of adjoining phospholipid molecules, with establishment of energetic domains determined by joint states of intramembranous proteins and surrounding phospholipid molecules. Resulting states of dielectric strain in these lipoprotein interactions may determine optical properties within their cooperative domains. As in fiberoptic systems, these optical properties may depend on states of membrane excitation, and may determine stability of *dark soliton* propagation as a means of transmembrane signaling [Christiansen, 1989].

These dark solitons suggest analogies with the sharp changes in optical properties of living vertebrate and invertebrate axons accompanying polarizing currents [Tobias and Solomon, 1950], and with the highly cooperative movements of about 18 Å reported with laser interferometry at the axon surface within 1 ms of excitation [Hill et al., 1977]. A sensitivity of the traveling waves of the Belousov-Zhabotinski chemical reaction to weak electric fields with reversal and splitting has been noted [Sevcikova et al., 1992] and also ascribed to possible solitonic phenomena.

POSSIBLE ROLE OF HIGHLY COOPERATIVE ELECTRON TRANSFER IN PROTEINS AS A BASIS FOR EM FIELD INTERACTIONS

In 1966, pioneering studies by Chance [DeVault and Chance, 1966] disclosed the physical nature of first steps in activation of cytochrome *c*-bacteriochlorophyll complex by millisecond electron transfer. Since the transfer was temperature-independent from 120K to 4K, they deduced that the reaction proceeded through a quantum mechanical tunneling mechanism, perhaps taking place over distances as large as 30 Å. Their studies coincided with Mitchell's development of his Nobel award winning chemiosmotic model, which proposed that key electron-transfer steps of respiration operated across the full 35 Å width of the cell membrane.

Extension of these early concepts by Moser et al. [1992] has suggested options for much further research on detection and coupling of EM fields at cell membranes. They found that a variation of 20 Å in the distance between donors and acceptors in protein changes the electron-transfer rate by 10^{12}-fold. In the time domain, there is also a strong dependence on distance. Thus, in considering electron transfer across the full thickness of the cell membrane, with edge-to-edge distances between 25 and 35 Å, the optimal electron transfer rate is pushed into time scales of seconds and days, respectively.

Here, protein behaves like an organic glass, presenting a uniform electronic barrier to electron tunneling and a uniform nuclear characteristic frequency. Using this technique to study biological membranes, it would be sufficient to select distance, free energy and reorganizational energy, in order to define rate and directional specificity of biological electron transfer, thus

meeting physiological requirements in a wide range of cytochrome systems.

INWARD SIGNALING ALONG CELL MEMBRANE RECEPTOR PROTEINS

In their simplest forms, membrane receptor proteins appear to cross the plasma membrane only once. In a second group, the strand crosses the membrane seven times or more. The most striking feature of these proteins is in the structure of the extremely short chain of 23 amino acids that lies within the cell membrane at each consecutive membrane crossing. These short segments are composed of *hydrophobic* amino acids (and therefore nonconducting), in contrast to the hundreds of *hydrophilic* amino acids forming the rest of the strand inside and outside the membrane.

Is there evidence that this transmembrane movement of ions is mediated by these receptor protein segments, despite their hydrophobicity and their location in this highly hydrophobic environment? Ullrich et al. [1985] concluded that a hydrophobic segment as short as 23 amino acids is probably too short to be involved in conformation changes; and that its hydrophobic character makes unlikely its participation in either ionic or proton movement by coulombic forces.

Direct measurement of receptor-mediated inward Ca currents in epidermal cells [Moolenaar et al., 1986] and mast cells [Hoth and Penner, 1992] indicates that it is not voltage-activated and would thus be consistent with ion translocation by molecular vibrational modes. Binding of the epidermal growth factor (EGF) to its specific receptor is followed by a fourfold increase in intracellular Ca within 30 sec. All of this increment is derived from extracellular sources, and there is no change in membrane potential. In mast cells, it shows a characteristic inward rectification. For mast cells, Hoth and Penner have proposed that this may be the mechanism by which electrically nonexcitable cells maintain raised intracellular Ca^{2+} stores after receptor stimulation.

EFFECTS OF EM FIELDS ON RECEPTOR-G PROTEIN COUPLING

As a representative model of receptor coupling to intracellular enzymes, Luben [1991] has examined EM field effects on coupling of the parathyroid hormone (PTH) receptor to adenylate cyclase via a G protein. Osteoblasts exposed to a 72-Hz pulsed magnetic field for as little as 10 min show a persistent desensitization to the effects of PTH on adenylate cyclase. This does not result from decreased total adenylate cyclase levels, nor from reduced numbers of hormone receptor sites, nor reduced affinity of the hormone for the receptor, nor from reduced fractional occupancy of the receptor by the hormone.

Rather, the ability of bound hormone-receptor complex to activate G protein alpha-subunits is impaired by this treatment of osteoblasts with a pulsed magnetic field; and in consequence of this desensitization of the PTH receptor, there is increased collagen synthesis by osteoblasts and decreased bone resorption by osteoclasts. Luben has identified potential clues to this EMF-induced desensitization. Using monoclonal antibodies specific for the PTH receptor, exposure to the pulsed field changes certain PTH receptor determinants similar to changes induced by PTH analogs. These determinants modified by the EM field appear homologous to the signal-transduction domains of other G protein-linked receptors, viz., the transmembrane helices denoted as 5, 6, and 7 attached to intracellular loops 2 and 3. These are known sites of interaction of G proteins in rhodopsin and the adrenergic receptors.

FLUORESCENCE SPECTROMETRY AND MICROSCOPY OF INTRACELLULAR CA FLUXES INDUCED BY EM FIELDS

A first indication of the nonequilibrium character of tissue interactions with EM fields came from studies of cerebral Ca efflux. Frequency and amplitude *windows* were observed at low-frequency field frequencies, typically centered around 16 Hz [Bawin et al., 1975; Bawin and Adey, 1976; Blackman et al., 1979]. Ion-sensitive fluophores display the spatiotemporal distribution of Ca^{2+} in single cells and in domains of cultured cells. In confluent cell cultures, aggregate levels of intracellular Ca^{2+} may rise over large domains of the culture while simultaneously decreasing in others [Tsien, 1986].

Such highly cooperative behavior over many hundreds of neighboring cells may be mediated by a wavelike pattern of diffusion of ATP, rapidly released into the intercellular medium in the absence of gap-junction communication and detected by cell-surface purinergic receptors [Osipchuk and Cahalan, 1992]. It is likely to be a manifestation of an important modulating be-

havior within tissue [see Adey, 1992c]. Initial fluorescence microscopy studies with EM fields have measured Ca uptake as an aggregate behavior in cultures of lymphocytes and other cells as a function of field frequency and intensity [Walleczek, 1992].

DISCUSSION

There is a reasonable prospect that bioelectromagnetics may emerge as a separate biological discipline, having developed unique tools and experimental approaches in a search for essential order in living systems. Future research on submolecular transductive coupling will be diversified and increasingly dependent on new technologies, such as high-resolution magnetic resonance spectroscopy and electro-optical techniques. These approaches may answer such challenging problems as structural modifications during receptor–ligand binding, vibration modes in cell membrane lipoprotein domains during excitation [Christiansen et al., 1992], and possible coherent millimeter wave emissions accompanying enzyme action.

In little more than a century, our biological vista has moved from organs to tissues, to cells, and most recently to the molecules that are the exquisite fabric of living systems. There is now a new frontier, more difficult to understand, but of vastly greater significance. It is at the atomic level that physical processes, rather than chemical reactions in the fabric of molecules, appear to shape the transfer of energy and the flow of signals in living systems [Trullinger, 1978].

ACKNOWLEDGMENTS

I gratefully acknowledge support from the US Department of Energy, the US Environmental Protection Agency, the US Bureau of Devices and Radiological Health (FDA), the US Office of Naval Research, the US Department of Veterans Affairs, and the Southern California Edison Company for support of our research.

REFERENCES

Adey WR (1981): Tissue interactions with non-ionizing electromagnetic fields. Physiol Rev 61:435–514.

Adey WR (1990a): Electromagnetic fields and the essence of living systems. In Andersen CB (ed): "Modern Radio Science." Oxford: University Press. pp 1–37.

Adey WR (1990b): Joint actions of environmental nonionizing electromagnetic fields and chemical pollution in cancer promotion. Environ Health Perspectives 86:297–305.

Adey WR (1992a): Collective properties of cell membranes. In Norden B, Ramel C (eds): "Interaction Mechanisms of Low-Level Electromagnetic Fields in Living Systems." Oxford: University Press. pp 47–77.

Adey WR (1992b): ELF magnetic fields and promotion of cancer: experimental studies. In Norden B, Ramel C (eds): "Interaction Mechanisms of Low-Level Electromagnetic Fields in Living Systems." Oxford: University Press. pp 23–46.

Adey WR (1992c): Electromagnetic technology and the future of bioelectromagnetics. Plenary Lecture. Proc. First World Congress of Electricity and Magnetism in Biology and Medicine. Buena Vista, Florida. 31 pp.

Bawin SM, Adey WR (1976): Sensitivity of calcium binding in cerebral tissue to weak electric fields oscillating at low frequency. Proc Natl Acad Sci USA 73:1999–2003.

Bawin SM, Kaczmarek LK, Adey WR (1975): Effects of modulated VHF fields on the central nervous system. Ann NY Acad Sci 247:74–81.

Blackman CF, Elder JA, Weil CM, Benane SG, Eichinger DC, House DE (1979): Induction of calcium ion efflux from brain tissue by radio frequency radiation. Radio Sci 14:93–98.

Byus CV, Lundak RL, Fletcher RM, Adey WR (1984): Alterations in protein kinase activity following exposure of cultured lymphocytes to modulated microwave fields. Bioelectromagnetics 5:34–51.

Christiansen PL (1989): Shocking optical solitons. Nature 339:17–20.

Christiansen PL, Eilbeck JC, Enol'skii VZ, Gaididel JB (1992): On ultrasonic Davydov solitons and the Henon-Heiles system. Phys Lett A 166:129–134.

Delgado JMR, Leal J, Monteagudo JL, Garcia MG (1982): Embryological changes induced by weak, extremely low frequency electromagnetic fields. J Anat 134:553–551.

Devault D, Chance B (1966): Studies of photosynthesis using a pulsed laser. I. Temperature dependence of cytochrome oxidation rate in chromatium. Evidence for tunneling. Biophys J 6:825–847.

Frohlich H (1986): Coherent excitation in active biological systems. In Gutmann F, Keyzer H (eds): "Modern Bioelectrochemistry." Plenum: New York. pp 241–261.

Goodman R, Henderson AS (1988): Exposure of salivary glands to low-frequency electromagnetic fields alters polypeptide synthesis. Proc Natl Acad Sci USA 85:3928–3932.

Grundler W, Keilmann F (1978): Nonthermal effects of millimeter microwaves on yeast growth. Z Naturforsch 33C:15–22.

Grundler W, Kaiser F (1992): Experimental evidence for coherent excitations correlated with cell growth. Nanobiology 1:163–176.

Grundler W, Kaiser F, Keilmann F, Walleczek J (1992): Mechanics of electromagnetic interaction with cellular systems. Naturwissenschaften (in press).

Hill BC, Schubert ED, Nokes MA, Michelson RP (1977): Laser interferometer measurements of changes in crayfish axon diameter concurrent with axon potential. Science 196:426–428.

Illinger KH (ed) (1981): "Biological Effects of Nonionizing Radiation." American Chemical Society Symposium Series No. 157. Washington DC: American Chemical Society.

Lednev VV (1991): Possible mechanisms for the influence of eak magnetic fields on biological systems. Bioelectromagnetics 12:71–76.

Lerchl A, Nonaka KO, Reiter RJ (1990): Pineal gland "magnetosensitivity" is a consequence of induced electric currents (eddy currents). J Pineal Res 10:109–116.

Liboff AR (1985): Cyclotron reonance in membrane transport. In Chiabrerra A, Nicolini C, Schwan HP, (eds): "Interactions Between Electromagnetic Fields and Cells." New York: Plenum Press, pp 281–296.

Luben RA (1991): Effects of low-energy electromagnetic fields (pulsed and DC) on membrane signal transduction processes in biological systems. Health Phys 61:15–28.

Lyle DB, Schechter P, Adey WR, Lundak RL (1983): Supression of T lymphocyte cytotoxicity following exposure to sinusoidally amplitude-modulated fields. Bioelectromagnetics 4:281–292.

Lyle DB, Ayotte RD, Sheppard AR, Adey WR (1988): Suppression of T lymphocyte cytotoxicity following exposure to 60 Hz sinusoidal electric fields. Bioelectromagnetics 9:303–313.

McConnell HM (1975): Coupling between lateral and perpendicular motion in biological membranes. In Schmitt FO, Schneider DM, Crothers DM (eds): "Functional Linkage in Biomolecular Systems." New York: Raven Press, pp 123–131.

McGivern RM, Sokol RZ, Adey WR (1990): Prenatal exposure to a low-frequency electromagnetic field demasculinizes adult scent marking behavior and increases accessory sex organ weight in rats. Teratology 41:1–8.

McLauchlan K (1992): Are environmental magnetic fields dangerous? Phys World pp. 41–45, January.

Mir LM, Domenge C, Belehradek M, Pron G, Poddevin B, Orlowski S, Belehradek J, Schwaab G, Luboinski B, Paoletti C (1992): Electrochemotherapy, a new antitumor treatment using local electric pulses. Proceedings of the First World Congress for Electricity and Magnetism in Biology and Medicine, Buena Vista, Florida, p 19.

Moolenaar WH, Aerts WJ, Tertoolen LGJ, Delast SW (1986): The epidermal growth-factor induced calcium signal in A431 cells. J Biol Chem 261:279–285.

Moser CC, Keske JM, Warncke K, Farid RS, Dutton PL (1992): Nature of biological electron transfer. Nature 355: 796–802.

Osipchuk Y, Cahalan M (1992): Cell-to-cell spread of calcium signals mediated by ATP receptors in mast cells. Nature 359:241–244.

Phillips JL (1986): Transferrin receptors and natural killer cell lysis. A study using Colo 205 cells exposed to 60 Hz electromagnetic fields. Immunol Lett 13:295–299.

Phillips JL, Haggren W, Thomas WJ, Ishida-Jones T, Adey WR (1992): Magnetic field-induced changes in specific gene transcription. Biochim Biophys Acta 1132:140–144.

Pitot HC, Dragan YP (1991): Facts and theories concerning the mechanisms of carcinogenesis. FASEB J 5:2280–2286.

Polk C (1984): Time-varying magnetic fields and DNA synthesis: magnitude of forces due to magnetic fields on surface-bound counterions. Proceedings of the Bioelectromagnetics Society, Sixth Annual Meeting, Atlanta, p 77.

Reiter RJ (1992): Changes in circadian melatonin synthesis in the pineal gland of animals exposed to extremely low frequency electromagnetic radiation: A summary of observations and speculation on their implications. In Moore-Ede MC, Campbell SS, Reiter RJ (eds): "Electromagnetic Fields and Circadian Rhythmicity." Boston: Birkhauser, pp 13–25.

Sevcikova H, Marek M, Muller SC (1992): The reversal and splitting of waves in an excitable medium caused by an electric field. Science 257:951–954.

Tobias JM, Solomon S (1950): Capacity and diameter changes in polarized nereve. J Cell Comp Physiol 35:25–34.

Tosk JM, Holshouser BA, Aloia RC, Hinshaw DB, Hasso AN, MacMurray JP, Will AD, Bozzetti LP (1992): Effects of the interaction between ferric iron and L-DOPA melanin on T1 and T2 relaxation times determined by magnetic resonance imaging. Magnet Resonance Med 26:40–45.

Tsien RY (1986): New tetracarboxylate chelators for fluorescence measurement and photochemical manipulation of cytosolic free calcium concentration. Soc Gen Physiol Ser 40:327–345.

Trullinger SE (1978): Where do we go from here? In Bishop AR, Schneider T (eds): "Solitons and Condensed Matter." Berlin: Springer-Verlag, pp 338–340.

Ullrich A, Coussens L, Hayflick JS, Dull TJ, Gray A, Tam AW, Lee J, Yarden Y, Libermann TA, Schlessinger J, Mayes ELV, Whittle N, Waterfield MD, Seburg PH (1985): Human epidermal growth factor receptor cDNA sequence and aberrant expression of the amplified gene in A431 epidermoid carcinoma cells. Nature 309:428–431.

Walleczek J (1992): Electromagnetic field effects on cells of the immune system: the role of calcium signalling. FASEB J 6:3176–3185.

Weaver J (1992): Electroporation: A dramatic, non-thermal electric field phenomenon. Proceedings of the First World Congress on Electricity and Magnetism in Biology and Medicine, Buena Vista, Florida, p 8.

Weinstein IB (1988): The origins of human cancer: Molecular mechanism of carcinogenesis and their implications for cancer prevention and treatment. Cancer Res 48:4135–4143.

Wilson BW, Anderson LE (1990): Electromagnetic field effects on the pineal gland. In Wilson BW, Stevens RG, Anderson LE (eds): "Extremely Low Frequency Electromagnetic Fields: The Question of Cancer." Columbus, Ohio: Battelle Press, pp 159–186.

Wilson BW, Stevens RG, Anderson LE (eds) (1990): "Extremely Low Frequency Electromagnetic Fields: The Question of Cancer." Columbus, Ohio: Battelle Press.

Yamasaki H (1991): Aberrant expression and function of gap-junctions during carcinogenesis. Environ Health Persp 93:191–197.

Salmon

21

Bioelectromagnetics 1:35–43 (1980)

Induction of Calcium-Ion Efflux From Brain Tissue by Radiofrequency Radiation: Effect of Sample Number and Modulation Frequency on the Power-Density Window

C. F. Blackman, S. G. Benane, J. A. Elder, D. E. House, J. A. Lampe, and J. M. Faulk

Health Effects Research Laboratory, U.S. Environmental Protection Agency, Research Triangle Park, North Carolina

Changes have been found in calcium-ion binding to brain tissue exposed in vitro to a specific power density (0.83 mW/cm^2) of 147-MHz radiation, amplitude modulated by a 16-Hz sine wave. This report replicates and extends this previous work. To define more precisely the range of effective power densities, two different numbers of samples were treated in a Crawford cell. In one series, four brain tissues were exposed at a time; in the other series, four brain tissues plus six dummy loads were exposed together. While the four-sample configuration produced a narrow power-density window, the ten pseudosample configuration resulted in a broader power-density window. The reason for the sample-number dependence is unresolved, but may be due to interactions between samples and field distortions caused by the close spacing. The ten pseudosample configuration was used to test for the presence and range of a power-density window at a sinusoidal modulation frequency of 9 Hz. The response curve at 9 Hz was essentially identical to the results for 16-Hz sinewave modulation.

Key words: calcium ions, brain tissue, radiofrequency radiation, amplitude modulation, power-density window, nonionizing radiation

INTRODUCTION

Bawin et al [1975] reported that a 147-MHz carrier wave, sinusoidally amplitude modulated between 6 and 20 Hz, can enhance the efflux of calcium ions from brain tissue exposed in vitro. We described results [Blackman et al, 1977] consistent with Bawin's report, which revealed an additional and unusual finding: the enhanced efflux of calcium ions occurred only within a narrow range of power densities. At the same time, Bawin et al [1977] reported a similar power-density window with a 450-MHz carrier wave, amplitude modulated at 16 Hz.

Received for review September 24, 1979; revision received January 22, 1980.
Address reprint requests to Dr. Carl Blackman, Experimental Biology Division, Health Effects Research Laboratory, U.S. Environmental Protection Agency, Research Triangle Park, NC 27711.

Salmon

CHAPTER 10

EXPERIMENTAL STUDIES OF ELECTROMAGNETIC FIELD-INDUCED CARCINOGENESIS IN CULTURED MAMMALIAN CELLS

Elizabeth K. Balcer-Kubiczek

INTRODUCTION

The focus of this chapter is on defining the process of neoplastic transformation as it bears on research into the effects of low intensity electric and magnetic fields (EMF). There will be a brief discussion of molecular mechanisms in neoplastic transformation and the use of neoplastic transformation in vitro assays for assessing carcinogenesis. Then the application of these in vitro tests in our laboratory to EMF research will be detailed, and future EMF research directions will be discussed. Some key findings in other systems and issues involved in EMF research have recently been discussed.[1,2,3]

IN VITRO TESTS OF NEOPLASTIC TRANSFORMATION

In the United States, animal models have been used for assessing potential health effects of chemicals, radiation and other agents since 1908. Traditional studies utilizing experimental animals typically involve costly and long-term experiments, and those changes leading to neoplastic development can be elusive and difficult to quantitfy. Apart from the ethical, technical and scientific issues, the routine use of mice, rats, hamsters and larger

On the Nature of Electromagnetic Field Interactions with Biological Systems, edited by Allan H. Frey.

schematic is shown in Figure 10.4. Since a variety of more familiar wave guide or Crawford cell exposure systems are available for in vitro EMF experimentation, the advantage to us of using the less conventional system should be explained. First, it is considered essential to maintain standard conditions of the transformation protocol,[19] so that the results with microwaves would be suitable for comparison with results from transformation studies with well-studied physical agents, such as X-rays. The specific requirements of transformation assay affecting microwave system requirements were the need for self-contained experiments, the use of attached cells in tissue culture flasks, and the need for hours-long exposures of multiple treatment groups, often at different values of the specific absorption rate (SAR). Taken together, these needs were satisfied by requiring simultaneous microwave-irradiation of flasks with cellular monolayers comprising an individual experiment. This, plus the requirements of temperature control, led to our system diagrammatically described in Figure 10.4.

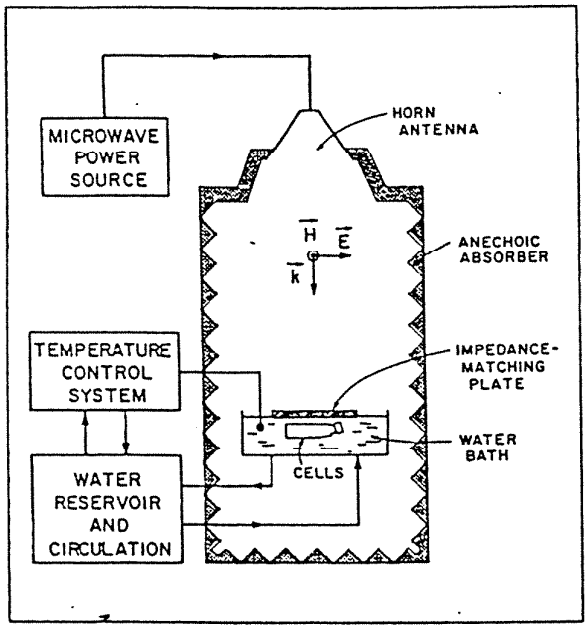

*Fig. 10.4. Microwave exposure system for cellular monolayers[57] used in our transformation studies.[53,54,55] A shielded exposure chamber lined with anechoic material is used for far-field TEM irradiation 2 to 3 m down-range from a standard-gain antenna energized by a Gerling-Moore 3 kW generator operating at 2.45 GHz. A plexiglass water bath, 60 x 60 x 12 cm, is located on a styrofoam support 2.1 m below the antenna. Water is circulated to an external reservoir with temperature control providing steady-state uniformity in the bath to within ± 1°C, with or without field on. In order to increase the maximum SAR for cellular treatments, a 2.45 GHz quarter-wave transformer is placed on the surface of the bath. The transformer plate is 30 x 30 x 1.2 cm, and is supported on four small plastic piers centrally located in the bath. The SAR was calculated using the relation SAR = $C_p \Delta T/\Delta \tau$, where C_p is the specific heat of the exposed sample medium and $\Delta T/\Delta t$ is the rate of temperature increase per unit time. For our system operating at 1 kW forward power, the SAR (W/kg) beneath the quarter wave transformer at the water depth z(cm), can be expressed as SAR = 45 * exp(-0.607z).[57]*

In 1985 we published the first evidence indicative of EMF carcinogenesis at the cellular level.[53] The original purpose of our study was to perform then-novel transformation experiments with C3H/10T1/2 cells to investigate 2.45 GHz microwaves and benzo(α)pyrene [B(α)P], seemingly similar to treatments used by Szmigielski et al[58] in his studies of effects of 2.45 GHz microwaves on chemically-induced or spontaneous neoplasms in mice. In view of negative results on C3H/10T1/2 cell transformation after 24 hours of simultaneous exposure to various doses of B(α)P and to microwaves,[53] we initiated a new protocol in which 10T1/2 cells were given combined microwave and X-ray exposures, followed by a chronic treatment with 0 or 0.1 μg TPA/ml.[53] The positive results of the latter study, showing the enhancement of transformation by combined treatments with EMF relative to treatments without EMF, led us to suggest the need for tumor promoters like TPA in order to develop neoplastic transformation from exposure to EMF.

The above notions were subsequently tested in two studies, whose design followed a classical initiation/promotion protocol in the C3H/10T1/2 assay.[28] In the first series of experiments,[54,55] the effect of 2.45 GHz microwaves was measured by comparing the number of transformants induced by a single free-field microwave radiation lasting 24 hours with and without subsequent

treatment with TPA at 0.1 μg/ml starting immediately at the end of EMF exposure (see Table 10.1 for the results). Two other arms were added to test microwaves for activity as a cocarcinogen with X-rays given *before* or *after* the exposure to microwaves. X-rays alone, at the same doses as in the combination with microwaves, served as a positive control.

To summarize, the important results were

1. There was never any transforming activity of microwaves without postculturing with TPA (Table 10.1).[54,55]
2. When followed by TPA treatment, microwaves were additive rather than synergistic with X-ray-induced transformation, indicating that microwaves and X-rays act on different primary targets.[53,54,55]
3. Transformation frequency measured in microwave exposures combined with TPA were dependent on the specific absorption rate (SAR).[55] The data on dose response curve resulting from microwave exposure followed by TPA are shown in Table 10.1 and plotted in Figure 10.5.

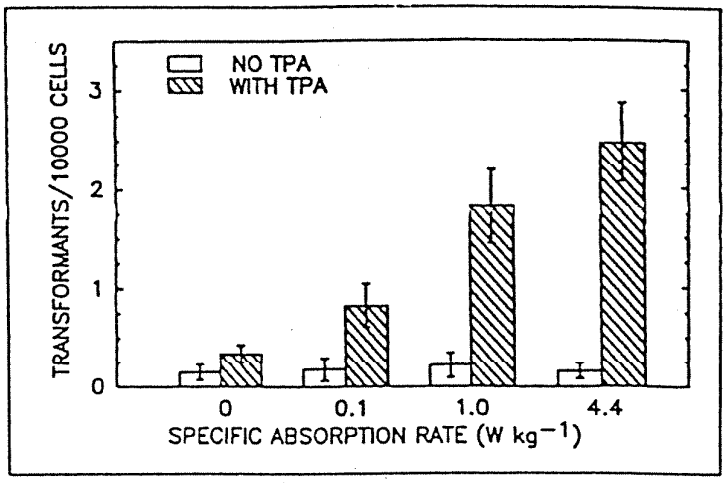

Fig. 10.5. Dose-response relationship for induction of neoplastic transformation in C3H/10T1/2 cells by a 24-h exposure to 2.45 GHz microwaves at the specific absorption rate indicated on the abscissa with or without TPA post-treatment for 8 weeks (data from Balcer-Kubiczek and Harrison.[55]

The experimental strategy in the above studies on the effects of microwaves has currently been applied to investigation of the effects of 60-Hz magnetic fields in the C3H/10T1/2 assay (24 h exposure, 37°C, magnetic flux density, B = 2 G = 200 μT). For a brief review of current literature on experimental studies of 60-Hz magnetic field using in vivo and in vitro assays see Frey,[3] Stuchly et al[61] and Cain et al.[62]

Our system for 60-Hz magnetic field exposure follows a standard design (Balcer-Kubiczek, Davis and Harrison, manuscript in preparation). Briefly, cellular monolayers are exposed in tissue flasks placed in the center of solenoids (38.7 m long, 7.5 cm in diameter) such that the cell attachment plane is parallel to the field lines. The solenoids are wound on thin-walled plexiglas with a clear internal diameter sufficient to accommodate tissue culture flasks. In present experiments, two of these solenoids are placed parallel to each in a circulating temperature-controlled water bath. The control and 200 μT solenoid are 30 cm apart. The control is a bifilar wound solenoid energized at the same level as the 200 μT solenoid. Consequently, control cells experience zero magnetic field, but are subject to the same level of possible artifactual disturbances, such as the geomagnetic field, local acoustic noise and convective heating as field-exposed cells. The maximum background field in our exposure facility, obtained by activating all the power supplies in our laboratory, is 0.1 μT but typical levels are less than 0.01 μT. The magnetic flux density inside a solenoid was determined from a well-known relationship, $B = \mu \cdot n \cdot I$, where I is the current through the solenoid and n is the number of turns per length of the solenoid. The relative permeability of the materials inside the solenoid is indistinguishable from unity. Our solenoids (199 turns, 1.59 mH, 1.76 Ω) provide a flux density of 643 μT at a current of 1 A.

The data from three of our transformation experiments completed to date are shown in Figure 10.6. Analysis of the data in Figure 10.6 with a paired comparisons tests[53] indicated significant differences: B-field + TPA vs. B-field alone ($p = 0.02$) or B-field

+ TPA vs. no B-field + TPA ($p = 0.05$). Because of limited group sizes (< 200 dishes per condition) and one value of magnetic field examined, it remains uncertain whether magnetic field alone can transform the cells; negative in vivo results on co-carcinogenesis from pulsed magnetic fields have recently been reported.[61,63] Future dose-response transformation experiments may elucidate the nature of response to 60-Hz magnetic field.[2,3]

Our EMF dose-response data in terms of SAR for neoplastic effects[55] provides evidence that the effect on tumor induction and development observed in a mouse skin model[58] may operate at the cell level. The mouse data of Szmigielski et al[58] are also consistent with a general picture emerging from our in vitro data in that 2.45 GHz microwaves and, possibly, 60-Hz magnetic fields, seem to act as an initiator or carcinogen, rather than as a promoter of malignant transformation. It is recognized however that the latter interpretation of this and other EMF in vivo results is frequently given.[2,61,62,64,65] In the 1982 experiments by Szmigielski et al[58] the identifiable promoter of chemical carcinogenesis was chronic skin irritation;[1,22,27,28] B(α)P in acetone was routinely painted on a mouse skin, following daily microwave exposures. In later experiments designed along the same lines, Szmigielski et al[66] confirmed their earlier results for two other carcinogens, diethylnitrosoamine and methylcholanthrene. Neither of these experiments investigated the effect of microwave exposure alone followed by chemical promotion, without intervening cocarcinogen treatment.

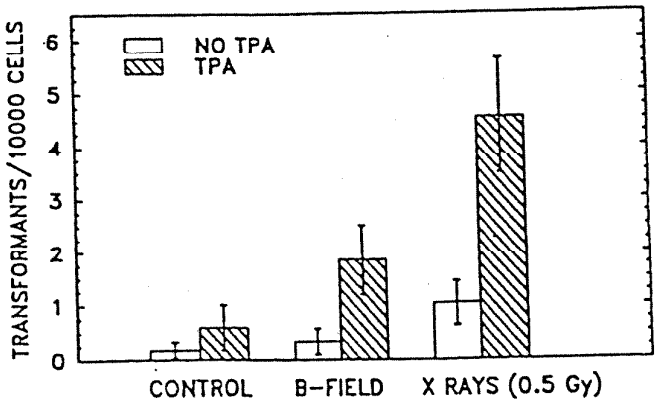

Fig. 10.6. Induction of neoplastic transformation in C3H/10T1/2 cells by 24 h exposure to 60-Hz magnetic field (2 G = 200 μT) with or without TPA post-

The above results are not intended to provide a definite explanation of how electromagnetic fields contribute to neoplastic transformation in vitro. Nevertheless, they offer a framework for thinking about the process and for designing new experiments that may yield additional definition and clarity. Progress in EMF research has led to a number of postulated mechanisms of action such as EMFs may induce nuclear effects via the direct transductive coupling at the cell plasma membrane; for a brief review see Adey,[64] Goldberg and Creasy,[1] Frey[3] and references in Cain et al,[62] Svedenstål and Holmberg[63] and Byus et al.[65] Studies of TPA effects in vitro suggests that the cell membrane is also the major target of the action of TPA.[30,32,67] Since a recent study has identified membrane damage as a critical lesion that is involved in apoptosis,[68] it would be attractive to hypothesize that early events following the cell exposure to EMFs include apoptosis, and that critical lesion(s) blocked by TPA occur soon after EMF stimulation. Thus, an important element of our design of transformation experiments could be that EMF-exposed cells were immediately plated in medium containing TPA.

Experimental data from EMF research supporting the hypothesis that both electromagnetic fields and TPA act at the cell membrane include the synergistic action of imposed EMFs and TPA. The enhancement of EMF-effects by TPA has been demonstrated not only by our neoplastic transformation studies[54,55] but also for diverse endpoints, including increased membrane-bound ornithine decarboxylase (ODC) activity.[63,69] Several indirect lines of evidence from molecular carcinogenesis research indicate that aberrations in ODC regulation are associated with neoplastic transformation, including the stepwise increase of ODC activity during progression of neoplastic development in human malignancies, in mouse skin and in transformable cells (for a brief review see Auvinen et al[70] and references in Moshier et al[52] and Byus et al[65]). A paper by Moshier et al,[52] as recent as June 1993, reported

neoplastic transformation of mouse embryo-derived cells engineered to overexpress ODC. In the context of much discussed EMF activity in terms of promotion, recall that immortalized mouse embryo-derived fibroblasts represent advanced stages of neoplastic progression. The authors' interpretation of their results[52] is that genetic alterations acquired by a mouse cell during the process of immortalization apparently contribute to ODC-induced instabilities and that both changes are needed to fully transform the cell; the interaction between neoplastic and aging processes is also observed in higher organisms, including humans.[71] It has also been shown that ODC overexpression is not sufficient for neoplastic transformation of normal diploid cells and for tumor development in transgenic mice that aberrantly express a human ODC gene.[72] Thus, although the connections can be made between the increase in ODC activity and neoplastic transformation, and between the increase in ODC activity and EMF exposure, these correlations do not present an airtight case that EMFs act as a promoter.

A wide array of tools is now available to screen for EMF induced biological effects and the challenge is to weave these established and new techniques into the fabric of EMF research. Rodent cell assays of neoplastic transformation have made a significant contribution to understanding of radiation and chemical carcinogenesis and to assessing the carcinogenic potential of these agents, but we feel their potential has not been exploited to the full in EMF research. The transformation studies with these physical agents justify the assumption that the response of mouse embryonic cells to EMF can be viewed as a representative example of corresponding responses that can occur in adult tissues and at the whole model-organism level. Despite the recent advances in cell culture research, the next generation of transformation assays based on normal human organ-derived cells is far in the future. The present urgent task remains to reliably establish correlations between transformation response, a dramatic unequivocal phenotype in rodent cells, and physical parameters of EMF exposure. In the case of power frequency magnetic fields, the effects of temporal patterns, flux density and modification of these effects by TPA require further studies. Also, the effects of EMF frequency and other exposure parameters require further studies, since neoplastic effects can critically depend on these parameters. As has been done in radiobiological research into the effects of ionizing radiation, in addition to establishing dose-response relationships, an effort should be made to correlate transformation induction with other end points measured in the same cell system, including apoptosis and other EMF-induced changes in cell behavior. For example, it is well-established by transformation studies that a potentially transformed viable cell is isolated from normal cells at very early stages of transformation; as the result, more than 90% of transformed foci are found near or at the edge of a petri dish (Fig. 10.2). A new quantitative technique for measuring motion of anchorage-dependent cells, such as C3H/10T1/2 cells, has recently become available.[73,74]

Despite sluggish progress, advances have been made in the development of high-resolution genetic linkage maps for the mouse.[75] These maps offer real prospects for identifying the function of mouse genes, which could in turn make transformation studies more biologically driven. While the main focus of the human genome project is looking for disease genes, innovations stemming from the mouse genome project may lead to isolation of genes associated with immortalization and neoplastic transformation of rodent cells by ionizing radiation and nonionizing electromagnetic fields. Powerful approaches in cancer research have been identification of chromosomal regions that undergo genetic changes, such as deletions, mitotic recombination or chromosomal loss during tumor initiation and promotion as well as the development of genetic markers, such as microsatellites, that can be assayed by polymerase chain reaction. Genome-wide studies have been carried out in human preneoplastic tissues and tumors, but they have not yet become common in cultured rodent cells or in the mouse. With availability of mouse genome maps, this situation is likely to

Salmon

similar to that caused by increased temperature, but without elevated temperature. Although details of the mechanism of interaction of EM fields with cells remain unknown, the induction of the stress response appears to be an appropriate cellular response to a stimulus that is not normally part of its environment, and this may well provide a clue to the mechanisms involved.

We thank the NCI, the US Department of Energy and the Heineman Foundation for their support.

References:
1. S. Kwee and P. Raskmark: Changes in cell proliferation due to environmental non-ionizing radiation, 1. ELF electromagnetic fields. *Bioelectrochem. Bioenerg.* 36 (1995) 109.
2. K. V. Steffensen, P. Raskmark and G. F. Pedersen: FDTD calculations of the EM-field distribution in a microtiter suspension well. *Proceedings of the 244 COST meeting on "Biological effects relevant to amplitude modulated RF fields"*. Kuopio, 1995.
3. S. Kwee and P. Raskmark: The minimizing effect of electromagnetic noise on the changes in cell proliferation caused by ELF electromagnetic fields. *Proceedings of the 3rd International Congress of the European Bioelectromagnetics Association.* Nancy 1996.

MS-20-4 1997

THE BIOLOGICAL EFFECTS OF MICROWAVE RADIATION. S. Kwee[1] and P. Raskmark[2]. [1]Institute of Medical Biochemistry, University of Aarhus, DK-8000 Aarhus C, Denmark. [2]Institute of Communication Technology, Aalborg University, DK-9220 Aalborg Ø, Denmark.

In recent times the use of mobile telephones has accelerated, resulting in an increasing exposure of the environment to weak radiofrequency (RF) fields, transmitted from these devices.

In previous work we showed that cell growth is affected by exposure to weak electromagnetic (ELF) fields[1]. Consequently the next thing to investigate was, if EM fields generated by microwave radiation, would have a similar effect on cell proliferation.

The field was generated by signal simulation of the Global System for Mobile communications (GSM) of 960 MHz. Cell cultures, growing in microtiter plates, were exposed in a specially constructed chamber, a Transverse Electromagnetic (TEM) cell. The Specific Absorption Rate (SAR) values for each cell well were calculated for this exposure system[2].

Experiments were performed on cell cultures of transformed human epithelial amnion cells (AMA), which were exposed in the TEM cell to 960 MHz microwave fields at 3 different power levels. The cells, growing in microtiter plates in monolayer cultures, were exposed for 20, 30 or 40 min respectively. Cell proliferation was determined immediately before exposure and again after a 24 hours' growth period. It was found that cell growth in the exposed cells differed from that in the control and sham exposed cells and a decrease in cell growth was seen. Cell proliferation during the period following exposure not only varied with the various SAR levels, but also with the length of exposure time. On the other hand repeated periods of exposure did not seem to change the effects. There was a general linear correlation between power level and growth changes.

However, the exposure time required to obtain the maximum effect was not the same for the various power levels. It turned out that at low power level the maximum effect was first reached after a longer exposure time than at higher power level. A similar phenomenon was registered in our studies on ELF electromagnetic fields[3]. Here we found that there was a linear correlation between the length of exposure time to obtain maximum effect and the field strength. The explanation could be found in terms of "window" effects or adaptation.

MS-20-5

USE OF NON-MAMMALIAN MODEL SYSTEMS TO INVESTIGATE MECHANISMS MEDIATING BIOLOGICAL INTERACTIONS WITH ELECTROMAGNETIC FIELDS. D.M. Binninger. Department of Biological Sciences, Florida Atlantic University, Boca Raton, Florida 33431, USA.

The question of whether power frequency (60 Hz) electromagnetic fields (EMF) present a health risk to humans remains highly controversial. While a variety of biological responses to EMF under laboratory conditions have been reported, the molecular mechanisms that mediate these phenomena remain elusive. Insight into the biochemical and genetic mechanisms that transduce EMF into biologically responsive signals is critical for clarifying the putative role of EMF in the development of certain human cancers.

The yeast *Saccharomyces cerevisiae* is an ideal model organism for studying molecular mechanisms of eukaryotic gene expression. This single-celled fungus is highly amenable to traditional genetic techniques. Additionally, recombinant DNA techniques are available for yeast which are not yet technically feasible with more complex cells, especially those of humans. While completion of the Human Genome Project remains at least 5-10 years away, the DNA sequence of the entire yeast genome is now available. Thus, experimental approaches can be designed using yeast which are not available for the other model organisms typically used in EMF studies.

Has studying yeast actually contributed to our understanding of cancer in humans? An unexpected outcome of cloning human genes has been the discovery that many cancer-related genes are very similar in all eukaryotes—from yeast to humans. Numerous human genes involved in regulating cell growth and are defective in human cancers were first identified as CDC (cell division control) genes in yeast. First identified in genetic studies using yeast, molecular clones of the yeast genes were then used to identify the homologous genes in humans. There is an ever-increasing list of human cancer genes that have structural and functional homologies in yeast.

"Resonance Effects"
(Rd)

Nanobiology (1992) *1*, 163–176

Experimental Evidence for Coherent Excitations Correlated with Cell Growth

W. GRUNDLER[1] AND F. KAISER[2]

[1]*Institut für Biophysikalische Strahlenforschung, GSF mbH, D-8042 Neuherberg, Germany*
[2]*Institut für Angewandte Physik—Theorie, Technische Hochschule, D-6100 Darmstadt, Germany*

Two decades ago it was proposed by H. Fröhlich that electric vibrations with frequencies in the GHz region should be excited coherently in active biological materials through metabolic processes. Excitations of the proposed type could have important biological consequences as they would lead to long-range interactions of, for example, biomolecules. Verification of the theoretical conjecture posed considerable experimental difficulties. Biological investigations must be performed using high accuracy in physical parameters, especially in terms of frequencies and field intensities. In our experiment we have controlled these parameters by using a new precision irradiation chamber, which has a fixed well-defined intensity distribution, and attenuation that extends over nine decades. Irradiation experiments with growing yeast cells (microscopically observed for two generations) generated the following results: (1) the cell growth rate depends on frequency and either increases or decreases by 10%–20%, (2) the overall frequency dependence shows a resonance-like structure and (3) the shape of the resonance curve can be changed by the use of radiation of different intensities. These observations, along with those of others also showing a non-linear response, may be explained in a general sense by the theory of non-linear dynamics. As a hypothesis to adapt this theory to our results, we suggest that only non-linear self-sustained oscillators can respond in the way we have experimentally observed. If this hypothesis is true, then in our yeast system there may indeed be one or more active internal oscillators that are normally coupled to cell growth in an unknown manner, but which are interfered with by an external electromagnetic field.

Keywords: *Microwave, resonance, low level bioeffects.*

INTRODUCTION: THEORETICAL CONSIDERATIONS AND FORMER RESULTS

As the active subunits of biological systems, living cells exhibit a high degree of information processing and communication as well with neighbour cells as with the cell-internal subunits enclosed by the plasma membrane. In this context, the information is usually described from many different viewpoints: ion fluxes, chemical gradients, protein channel openings, conformational changes of biomolecules, etc. However, the cytoplasm within living cells is now appreciated to be close to the 'solid state' due to an extensive cytoskeletal structure, and ordered water-

embedding membranes and organelles (Hameroff, 1987). These highly ordered structures are mostly charged, polarized and of dynamic nature. They may be the candidates for oscillators proposed theoretically by bioenergetic models capable of supporting cooperativity and dynamic information processing.

Over the past two decades one of the most remarkable models for cooperative functions in biological systems has been proposed by the concept of coherent excitations (Fröhlich, 1968, 1986). It provides mechanisms for long-range order and cooperativity, characteristic parameters useful for biomolecular communication and information processing. In short, one of two possible types of Fröhlich's coherence is based on an ensemble of oscillating dipoles (i.e. biomolecules or cellular structures) excited to a collective, coherent vibration of the whole system provided the energy flux density S through the system is greater than a critical value S_0 ($S > S_0$). The necessary energy supply is proposed to be delivered by metabolic processes. The collective vibration of the system is characterized by one (or a few) modes possibly influencing molecular conformational stages or stimulating long-range interaction with other molecules or structures and, by this way, steering biochemical reactions. This idea, applied primarily to biological membranes as the possible oscillator, leads to electric vibrations with frequencies of the order of $10^{11}-10^{12}$ Hz. The given frequency range is to be considered as a very rough order of magnitude (Fröhlich, 1978).

In order to find an experimental evidence of this proposed conjecture, in principle, two approaches may be applied. (1) If vibrational states with these frequencies are strongly excited by metabolic processes, then corresponding Raman lines (Brillouin scattering) should be found when the system is metabolically active. (2) An alternative approach would be to attempt to interfere with the biological processes by exciting the systems from outside.

Approach (2) has been chosen by us in testing the proposed existence of actively oscillating 'receptors', by analysing the influence of millimetre microwave (40 GHz) radiation on cell growth in three experimental series, performed with a step-like improvement of the applied techniques. In a first experimental series, we analysed the growth behaviour of yeast cultures in aqueous suspension by monitoring the visible light extinction. We found an exponential growth rate reproducible within ± 4% limits. When the cultures were irradiated by continuous wave microwave fields of a few mW per cm^2, the growth rate either stayed constant or was considerably enhanced or reduced depending on the frequency around 42 GHz. A spectral fine structure with a width of the order of 10 MHz was observed. Careful temperature monitoring excludes a trivial thermal origin of this effect (Grundler *et al.*, 1977; Grundler & Keilmann, 1978). Repetition of this experiment has confirmed that the growth of aqueous yeast cultures is indeed affected by weak microwave radiation in a frequency-selective manner (Grundler *et al.*, 1983; Grundler & Keilmann, 1983). To exclude any possible influence of uncontrolled experimental parameters, many improvements were added in these studies. These include refined frequency stabilization, refined power recording, impedance matching elements, two geometrically different antenna structures and two recording photometers. Laser thermometry was employed to locate any hot spots (Keilmann, 1983). The results of this study using two different types of antennae and described above are shown in Figure 1. These data prove that the microwave irradiation leads to fairly reproducible effects, increasing or decreasing the growth rate by up to about 10%, depending on the frequency of irradiation.

The results, however, are obtained as an average reaction of nearly 10^6 cells. No exact measurement can be made of the power actually applied or of the time during which a cell is affected by irradiation. To overcome these disadvantages inherent in the photometer experiment, a new method was developed for studying microscopically the kinetics of single cell growth during the influence of microwave radiation.

Each cell develops into a microcolony of eight cells. To apply the radiation the microwaves are guided through a sapphire plate (multimode chamber) on to which the cells are spread in a monolayer. The data obtained from this second experimental series with frequencies in the 41 780 MHz resonance (Figure 1) again prove the existence of a microwave effect on the growth on yeast cells (Grundler *et al.*, 1988, 1989).

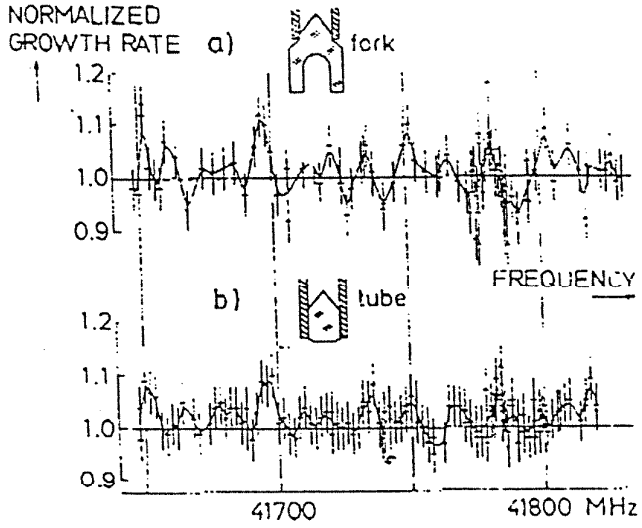

FIGURE 1. Normalized growth rate of yeast cultures versus microwave irradiation frequency using (a) fork-shaped or (b) tubular antennae. The curves were obtained by single three-point smoothing.

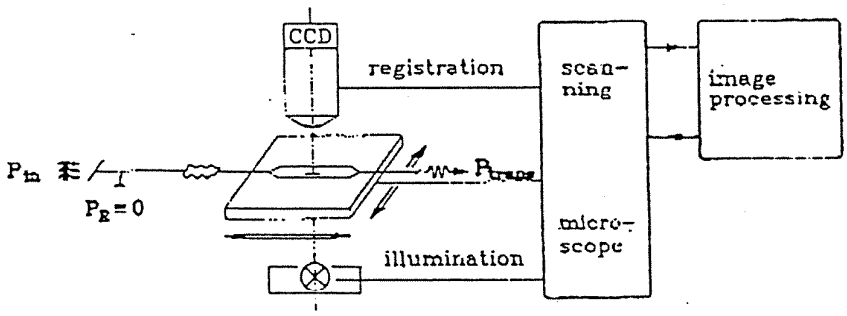

FIGURE 2. Schematic drawing of the experimental set-up for observation of kinetics of single cell growth.

Due to difficulties in reproduction of the observed cells reactions further improvements seem to be necessary, since, apart from highly stabilized frequencies, the theory demands a knowledge of the intensity for the irradiation of every single cell and a definable orientation of the biological object in respect to the field.

Then due to the frame of the theoretical concept outlined above, resonantly applied external microwave radiation should function as a trigger for the system's transition from the less ordered ($S < S_0$) to the highly ordered state ($S > S_0$). Extended theoretical studies of the non-linear dynamical behaviour of this phase transitions demonstrate their high sensitivity to slight changes of the external physical parameters (Kaiser, 1984, 1988).

How we meet these requirements experimentally and what the first observations are will be treated in this paper.

METHOD: IRRADIATION PROCEDURE AND SINGLE CELL OBSERVATION

Long time frequency stability (± 10 kHz) can be achieved even in the GHz region by using high quality, commercially available equipment and the usual stabilization procedures (phase

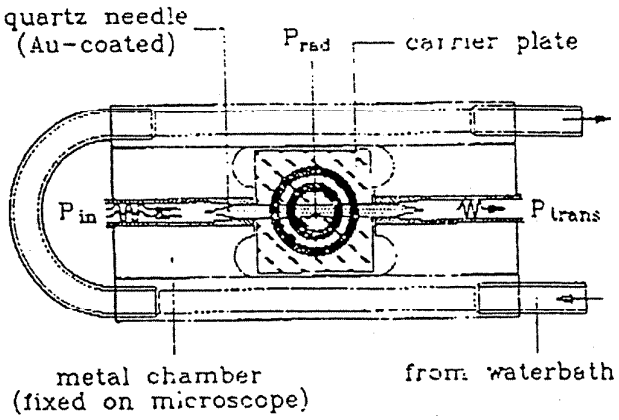

FIGURE 3. Thermostatted irradiation chamber (top view) and the removable dielectric (quartz needle and carrier plates).

lock technique). Short wavelength radiation, however, creates great difficulties in defining the intensity qualitatively for an irradiated single cell, for instance, as the reacting biological unit. Figure 2 demonstrates schematically the experimental set-up developed by us for this purpose.

The irradiation chamber, coupled by a flexible waveguide with a standardized millimetre wave set-up (Grundler *et al.*, 1983), is mounted on the stage of a scanning microscope. Between the fixed illumination and registration systems the movable stage enables the observation of individual cells (40 at maximum) by the use of a CCD camera. The pictures of the selected cells and their progenies are stored by an image processing system at fixed time intervals (e.g. 7·5 min) over an observation period of about three cell cycles.

Irradiation System

The incoming radiation is guided through the thermostatted chamber by means of a tapered quartz needle broadened by transparent quartz plates (carrier plates) on both sides (Figure 3). The quartz needle is part of the microwave circuit, in fact it is the dielectric in a dielectric-filled metal waveguide. The needle is mostly covered with gold to confine the microwaves, except at the ends and within a radiating slot (0·4 mm × 1·7 mm). A similar but broader opening is provided at the opposite surface to allow microscopic viewing, but this is covered with a fine metallic mesh structure which completely (−50 dB) suppresses leakage of microwaves.

The yeast cells are fixed to the lower surface of a thin transparent agar layer (0·2 mm) filling the inner part of the smaller plastic ring (shown as dark rings in Figure 3). The agar layer and the cells now rest on the quartz needle and the carrier plates. To apply the radiation, the microwaves are guided through the gold-coated quartz needle and radiated out of the slot on which the cells are spread in a monolayer.

To quantitatively determine the intensity distribution, the three quantities P_{in}, P_{trans} and P_{rad} can be measured. The 1·70 mm half wavelength slot delivers a frequency-dependent radiating power resonance around 43 GHz. If using frequencies between 41 and 42 GHz, a negligible variation of intensity with frequency can be guaranteed.

In this set-up the microwave field in the radiating slot can be expected to be monomodal. This was experimentally tested as shown in Figure 4. The electric field is polarized and oscillates in the y direction only, surrounded by the magnetic field in the $x-z$ plane. The intensity radiated out is proved to be a $\sin^2$ distribution. These data (Figure 4) correspond to a fixed frequency (41 652 MHz) and a constant input power of 30 mW. In order to test both the linearity of the waveguide system and the accuracy of the experimental irradiation entities, the input power

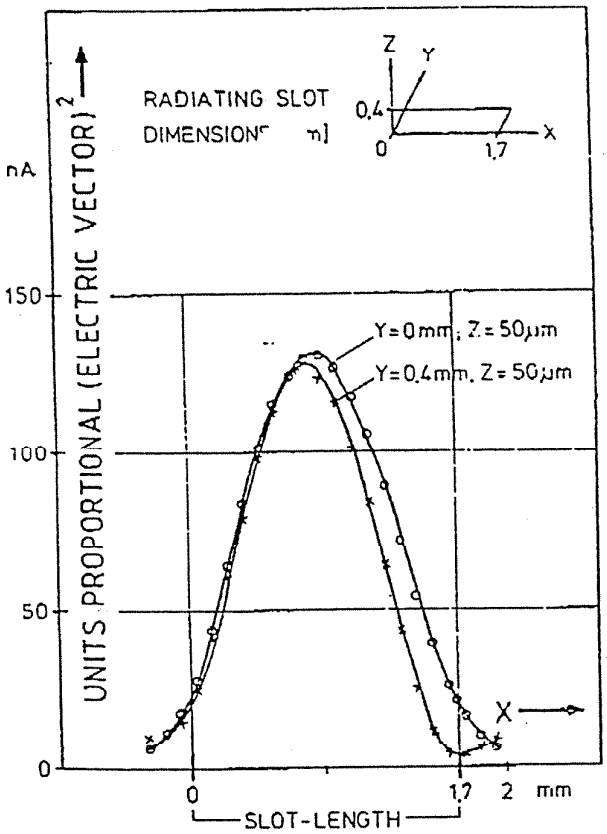

FIGURE 4. Intensity distribution of a radiating slot (1·7 mm long) measured at the long boundaries.

was systematically varied and the corresponding P_{trans} and P_{rad} values registered using standard adaption and attenuation procedures (Figure 5).

By resetting (open triangles in Figure 5) and reproduction (open squares in Figure 5) experiments, the relative accuracy was experimentally proved to amount to a factor of ± 2 due to a slightly changed geometrical coupling when the quartz needle is repositioned for a new experiment. Using high accuracy attenuators the applied energy flux densities can be varied over nine decades within an accuracy of ± 5 on an absolute scale.

Observation of Growth

For our experiments diploid yeast cells (*Saccharomyces cerevisiae*) were obtained from a stock culture of stationary state cells on solid nutrient agar (20 g l^{-1} glucose, 20 g l^{-1} Bacto agar, 5 g l^{-1} yeast extract; 4°C) and suspended in phosphate buffer. A synchronized subpopulation (early G_1 phase) was selected by volume sedimentation and used for a series of experiments. For every experiment 10 µl of a medium suspension containing 4×10^6 cells ml^{-1} was used in the cell chamber (Grundler *et al.*, 1988).

In order to run an experiment, about 20 cells were selected for observation. By the use of prescreening programs three quantities could be defined for every start cell and stored in a data file:

(1) the (x,y) coordinates, corresponding to the intensity individually achieved by a single cell;
(2) the orientation of the cell's main axis to the E vector direction;
(3) the cell area, which is proportional to the cell volume defining the individual state of the cell in G_1 phase.

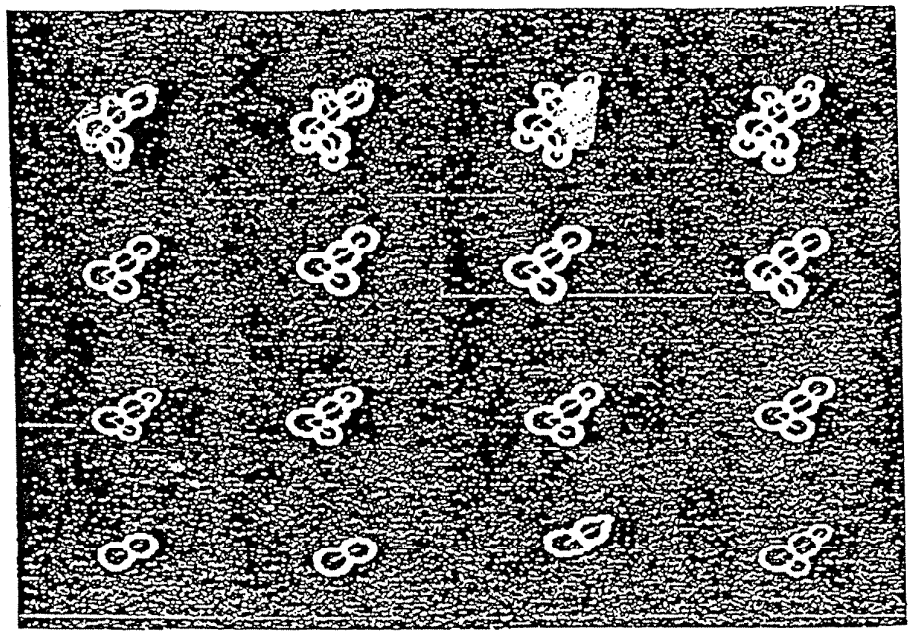

FIGURE 6. The second half of a processed set of 32 pictures describing a single cell kinetic from a double cell to an eight cell colony. (Numbers correspond to registration intervals; generations are indicated by colours, the degree of relationship by bars.)

EXPERIMENTAL RESULTS

Microwave radiation responses of cells stirred in suspension suggest both a short radiation time or an intensity much lower than some mW per cm^2 sufficient for causing growth effects (Keilmann, 1983). In addition, the theoretically proposed trigger function of microwaves can be performed by very low intensities (Kaiser, 1988). Finally, biological effects caused by frequencies lower than 100 Hz have been shown to be induced by extremely low electrical field strengths (Nair *et al.*, 1989). These suggestions have brought us to the application of very low mean intensities (P = 1 nW cm^{-2}) as the mean of the slot $\sin^2$ distribution, corresponding to a mean specific absorption rate of $\overline{SAR}$ = 0·04 μW g^{-1}) when reproducing the most pronounced resonance around 41 696 MHz (Figure 1) measured on cells in suspension.

We conducted a series of 37 growth experiments, 27 with and 10 without microwave radiation. Figure 7 gives several examples of the resulting distribution of cell cycle times as computed by the image processing programs.

In these runs the control experiments resulted in the narrowest distributions. The effect of irradiation can be seen in Figure 7 to be an asymmetric deformation of the distribution. Any broadening must mean that not all cells respond in the same way. In particular, radiation induced reduction of growth velocity is significantly pronounced. Partly, a doubling of cell cycle time can be observed (Figure 7), a 100% effect for a single cell.

For further evaluations we disregard this effect and concentrate on the shift of the distribution by calculating the average cycle time t_{av} in each distribution. By taking the inverse of t_{av} we obtain the average growth rate t_{av}^{-1}, which we further normalize to the mean value obtained in the control runs. Figure 8 shows the resulting normalized growth rate for different frequencies.

The data obtained from the new experimental set-up (determining absolutely the intensity within a factor of ± 5 for a single cell), again prove the existence of a microwave effect on the growth of yeast cells. Significant growth rate values are found well outside the scatter of

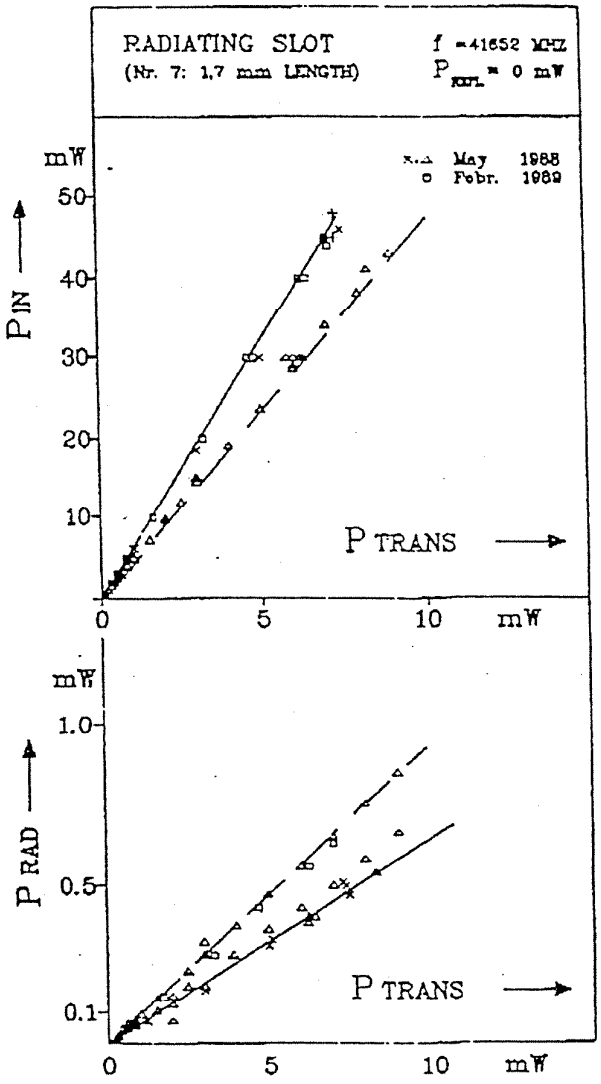

FIGURE 5. Power emitted by radiating slot dependent on the incident and transmitted power of the irradiation chamber.

After switching on c.w. radiation, the pictures of the selected cell ensemble are recorded by a CCD camera every 7·5 min over a time period of 10 h corresponding the lag phase and two cell cycle times.

The cells can easily be discerned by pattern-recognizing programs. The appearance of budding can be determined with high resolution. This budding coincides with the transition of the cell from the G_1 to the S phase. Therefore, by defining the cell cycle time as the time between consecutive budding our method allows us to determine the cell cycles for each of the cells individually (Figure 6).

The evaluation of experimental data for all cells observed thus yields the distribution of cell cycle times, either separately for the first generation (= first-to-second budding), for the second generation or for all generations together.

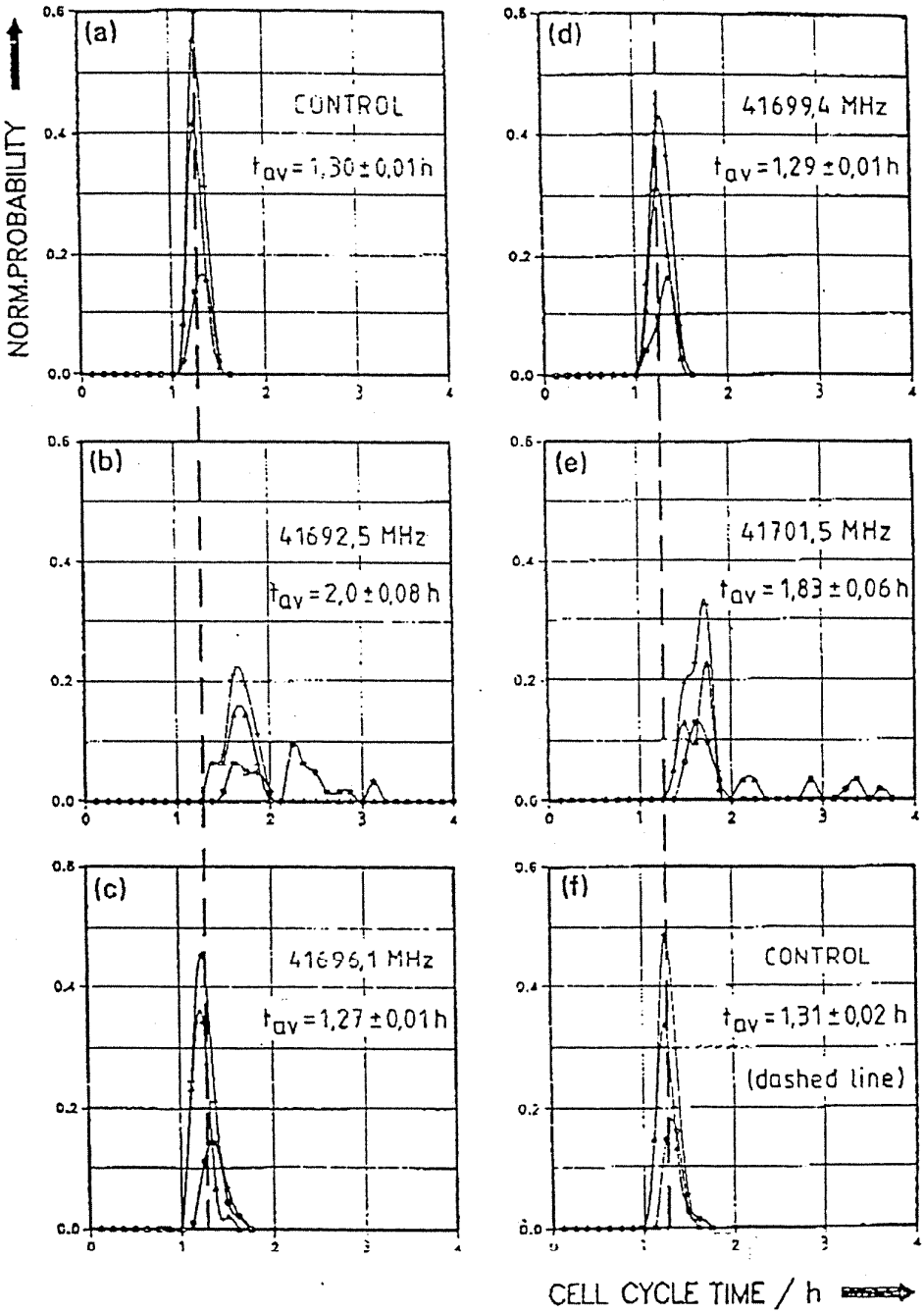

FIGURE 7. Normalized distribution of cell cycle times of growing single yeast cells for two generations (○, first; ▲ second) and for all together (×). (a) and (f) Results for cells without irradiation. (b)–(e) Irradiated with different frequencies. Intensity: 1 nW cm^{-2} (0.04 μW g^{-1}). Modulation: 8 kHz, square wave. Dashed line: mean value of all control distributions.

control runs (±3%). In particular, at frequencies inducing a shortened cell cycle time the overall effect is established to the greatest degree. Between these minima the normalized growth rate values measured vary around one. Nevertheless, the maximum value can be observed at 41 696

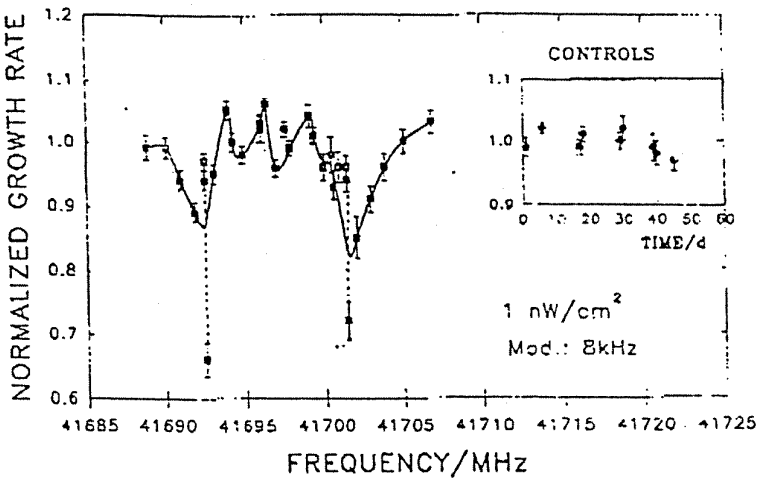

FIGURE 8. Normalized growth rate of population obtained by averaging over individually determined cell cycle times in dependence on frequencies around 41 696 MHz ($\bar{P}_{mod}$ = 1 nW cm^{-2}, f_{Mod} = 8 kHz, square wave).

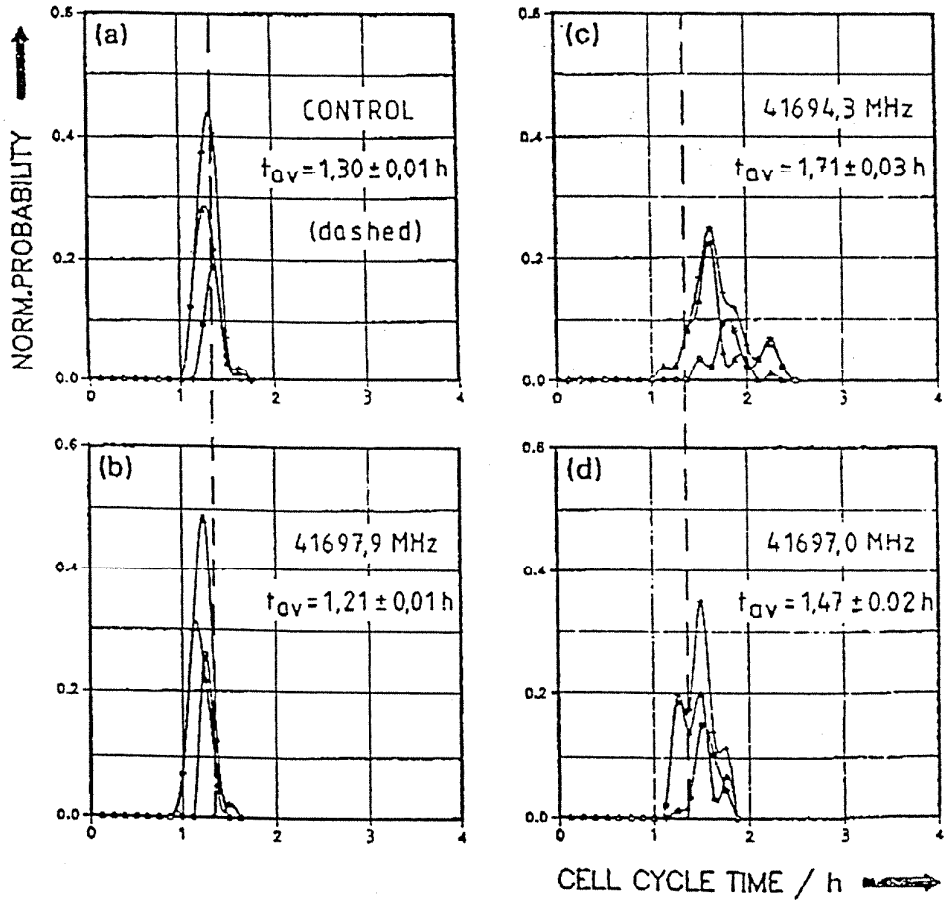

FIGURE 9. Normalized distribution of cell cycle times of growing yeast cells for two different generations (○, first; ▲, second) and for all together (×). (a) Results for cells without radiation. (b)–(d) irradiated with different frequencies. Intensity: 5 pW cm^{-2} (0.2 nW g^{-1}). Modulation: 8 kHz, square wave. Dashed line: mean value of all control distributions.

MHz. For testing the intensity dependence of the growth response on intensity of 5 pW cm^{-2} ($\overline{SAR}$=0.2 nW g^{-1}) was chosen for a further long series of 33 runs. In Figure 9 the rough experimental data indicate once again a frequency-dependent cell growth effect in spite of this extremely low intensity applied. Summarizing the results of this second series, the normalized growth rates of these three runs (Figure 9) together with the other ones demonstrate the dependence on frequency (Figure 10). Once again, a resonance like structure can be observed around 41 696 MHz, as already measured on cells in suspension (Figure 1). At the frequency position characterized by the most pronounced negative effects a special sensitivity can be observed, indicated by effects partly of different signs.

In comparing both resonance curves measured by the use of intensities, roughly distinct by a factor of 200, we can summarize our main experimental findings as follows.

(1) The resonance frequency remains at the same position when the external applied intensity is changed.
(2) There is a clear indication of strong negative effects at both sides of the resonance frequency, though extremely low intensities are active.
(3) A narrowing of the resonance is observed when radiation of lower intensity (some orders of magnitude) is applied.

DISCUSSION

With respect to the results of the irradiation experiments it is clearly demonstrated that a fast oscillating, very weak outer field is influencing biological reactions of cells by changing their growth velocity. In spite of our assumption of a cell to be a black box, due to the lack of knowledge about the biomolecular reaction involved, we have to take into account an 'internal' oscillator (the cell itself or parts of the cell or of its environment) coupling with

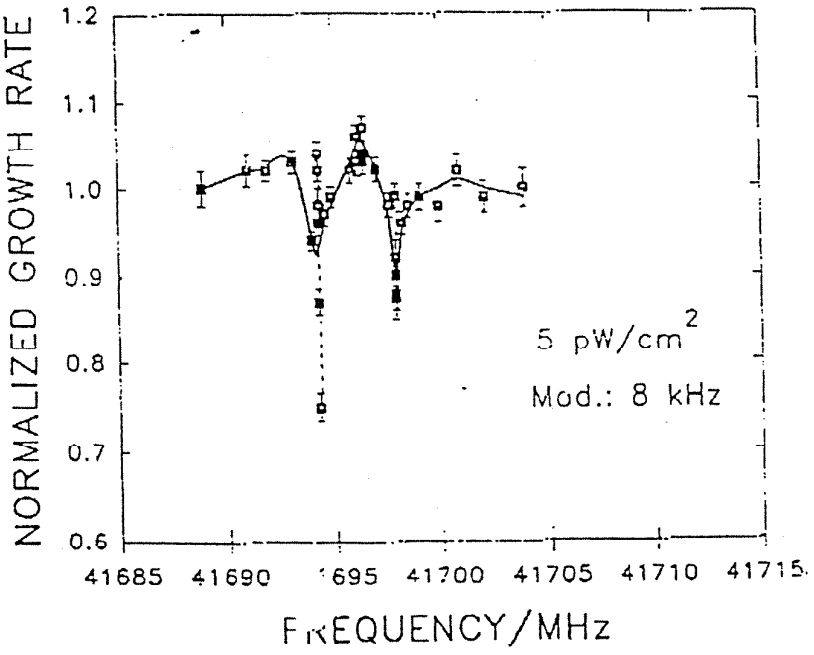

FIGURE 10. Normalized growth rate of population obtained by averaging over individually determined cell cycle times in dependence on frequencies around 41 696 MHz ($\bar{P}_{mod.}$ = 5 pW cm^{-2}, $f_{Mod.}$ = 8 kHz, square wave).

'he outer field. Models seeking to explain such a bioactive field–cell interaction mechanism must take into account the highly non-linear properties of living systems. Apart from non-linearity, such an oscillator must be dissipative. Consequently the question arises now as to whether the energy dissipation is internally compensated or not, i.e. whether we are dealing with a self-sustained or a non-self-sustained internal oscillatory system. This distinction can be clarified by the analysis of experimental results in comparison with theoretical considerations.

From a rather fundamental point of view, Fröhlich has promoted the ideas that coherent states can be established in active biological systems (Fröhlich, 1968, 1984). Possible types of coherent excitations are (1) highly polar metastable states and (2) coherent vibrations as a realization of self-sustained oscillators. The establishment of the latter type is possible if the rate of energy flux through the system is beyond a certain threshold ($S \geq S_0$).

The possible excitation of coherent vibrations has been demonstrated with some simple physical model calculations (Fröhlich, 1968; Kaiser, 1979, 1988). The coherent vibrations include a very large frequency range from slow chemical or electrical oscillations to oscillations beyond the GHz range in membranes and proteins. The interaction of these non-linear coherent vibrations (for instance of limit-cycle type) with external fields creates a rich variety of non-linear responses (Kaiser, 1988). In particular, those processes or mechanism not explained by direct high intensity processes or by heating, e.g. non-thermal effects in irradiated biosystems, reveal a new interpretation.

In the realm of these theoretical considerations the sharp resonance peaks (Q value, $\Delta f/f \approx 10^{-4}$) in the frequency response relating to extremely frequency-sensitive processes, as found in our experiments, can be explained very consistently. The existence of sharp resonances is thus confirmed by both a very general theoretical concept and by the results of two different experimental methods (Grundler *et al.*, 1983). The biological responses found experimentally and their quantified dependence on different physical parameters may strongly increase the acceptance level of the validity of the theoretical concept. In this context, the evidence for the existence of self-sustained oscillators as specific coherent excitations is enhanced.

As a theoretical example of an internal system disturbed from outside and fitting the characteristic model behaviour, a limit-cycle oscillator (Van der Pol type) has been intensively studied (Kaiser, 1983, 1984). Its simplified resonance diagram (1/1 resonance, schematically) is demonstrated in Figure 11, indicating the system's response as a function of the external frequency and the external amplitude, with which the outer field entrains the internal oscillator. For a high external amplitude a broad response curve is to be expected; for a low external amplitude a smaller frequency region is relevant. It should be noticed that in this model even intensities near to zero can be active. This resonance curve is characteristic of a disturbed oscillator where a phase-locked or synchronized behaviour is displayed for certain λ and F_1 regions. Quantitatively we have observed the same behaviour by applying different external intensities to our yeast cells when registering their growth response.

Figure 12 shows the most important experimental results on a frequency scale listing the resonance positions and the resonance width (due to the minima positions) for the different intensities used. The position of the resonance frequency is not changed for any of the intensities applied, indicating that in every case an oscillator with nearly the same resonance frequency has been disturbed. The intensity dependent resonance width is clearly demonstrated when comparing the frequency differences correlated to the minima positions caused by different intensities. Such an experimentally documented response indicates that an internal oscillator is involved as a coupling system between the external field and the biological response.

Finally, the experimental data should be analysed with respect to the fundamental question of whether a self-sustained or a non-self-sustained system is involved. As theoretical model representatives of a non-self-sustained system and of a self-sustained system, a physical pendulum with small deviations and a Van der Pol oscillator may be used (Kaiser, 1988). With respect to Fröhlich's coherence the latter selection may be adequate since Fröhlich's long-range coherent oscillation model is a self-sustained oscillator related to a generalized Van der Pol oscillator. The results of the theoretical treatment of these two oscillating systems with respect to their

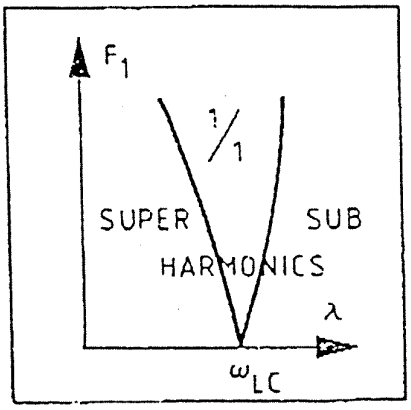

FIGURE 11. Schematic resonance diagram of a limit cycle oscillator. F_1, external field amplitude; λ, external field frequency.

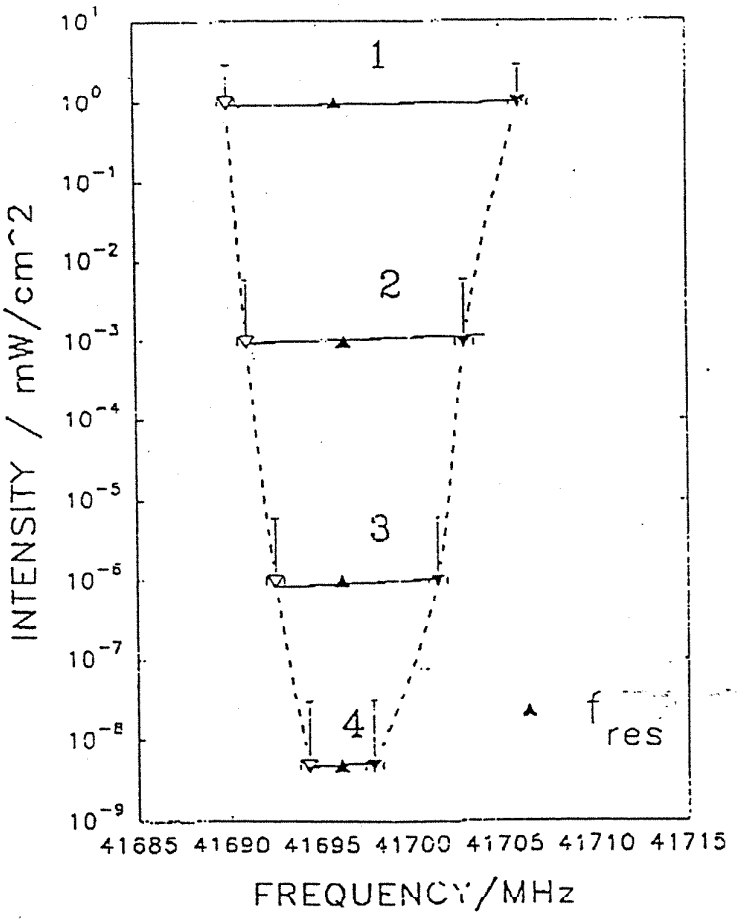

FIGURE 12. Experimental results: resonance frequency positions and resonance width for growth responses to microwave radiation of different intensities. (1) Cells in suspension, 10 mW cm^{-2} and lower. (2) Single cells in monolayer, around 1 μW cm^{-2}. (3) Single cells in monolayer, around 1 nW cm^{-2}. (4) Single cells in monolayer, around 5 pW cm^{-2}.

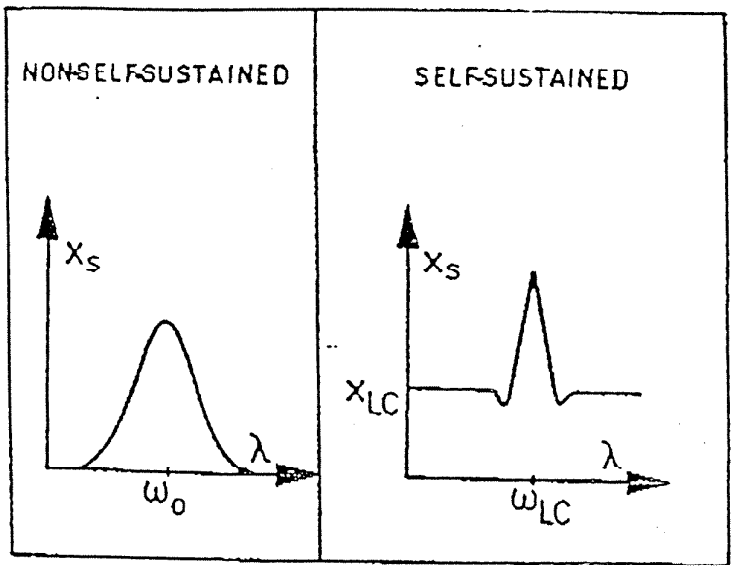

FIGURE 13. Schematic view of the steady state amplitude X_S of a non-self-sustained and a self-sustained oscillator. The oscillators are driven by $F_1\cos\lambda t$ (subscript S = steady state, subscript LC = limit-cycle).

response to external disturbances are schematically summarized in Figure 13. For the non-self-sustained (passive) oscillator, the resulting internal frequency is always λ (i.e. the external frequency). The system oscillates with the driver frequency and with an amplitude that is directly proportional to the external field amplitude. The behaviour changes drastically in the self-sustained (active) case. Assuming a stable limit cycle with amplitude X_{LC} and frequency ω_{LC} for $F_1(t) = 0$, for a certain range of frequency the internal oscillation becomes entrained. One finds the following transitions: the internal frequency ω_{LC} with internal amplitude X_{LC} is synchronized to λ (sharp resonance peak). Then the reversed situation occurs. The important point is that the internal amplitude is reduced with respect to the undisturbed amplitude X_{LC}, just before the external frequency enters the entrainment region.

The biological response observed (Figures 8 and 10) has some similarity with the behaviour of the active, self-sustained system. Provided the amplitude of the unknown oscillator coupled to the external field is proportional to the biological response observed, the strong reduction of the normalized growth rate on both sides of the resonance curves provides strong evidence that the oscillator involved must be self-sustained.

ACKNOWLEDGEMENTS

This study was supported by the Deutsche Forschungsgemeinschaft and the Stiftung zur Förderung der Erfahrensheilkunde im Stifterverband für die Deutsche Wissenschaft. The authors are indebted to Chenghe Xu (Beijing) and Baoming Wang (Teijing) for analysing microwave irradiation chambers. The technical assistance of I. Zimmermann, O. Lock, L. Mindl and K. W. Kussmaul is gratefully acknowledged.

EFERENCES

FRÖHLICH, H. (1968) Long range coherence and energy storage in biological systems. *International Journal of Quantum Chemistry* 2, 641.

FRÖHLICH, H. (1978) Coherent electric vibrations in biological systems and the cancer problem. *IEEE Transactions on Microwave Theory and Technologie* MTT-26 No. 8, pp. 613–617.

FRÖHLICH, H. (1984) In *Nonlinear Electrodynamics in Biological Systems* (ADEY, W.R. & LAWRENCE, A.F., Eds) Plenum, New York, pp. 491–496.

FRÖHLICH, H. (1986) Coherent excitation in active biological systems, in *Modern Bioelectrochemistry* (GUTMANN, F. & KEYZER, H., Eds) Plenum, New York, pp. 241–261.

GRUNDLER, W., KEILMANN, F. & FRÖHLICH, H. (1977) Resonant growth rate response of yeast cells irradiated by weak microwaves. *Physics Letters A* 62, 463.

GRUNDLER, W. & KEILMANN, F. (1978) Nonthermal effect of millimeter microwaves on yeast growth. *Zietschrift für Naturforschung* 33c, 15–22.

GRUNDLER, W., KEILMANN, F., PUTTERLIK, V., SANTO, L., STRUBE, D. & ZIMMERMANN, I. (1983) Nonthermal resonant effects of 42 GHz microwaves on the growth of yeast cultures, in *Coherent Excitations in Biological Systems* (FRÖHLICH, H. & KREMER, F., Eds) Springer, Berlin, pp. 21–37.

GRUNDLER, W. & KEILMANN, F. (1983) Sharp resonances in yeast prove nonthermal sensitivity to microwaves. *Physical Review Letters* 51(13), 1214–1216.

GRUNDLER, W., JENTZSCH, U., KEILMANN, F. & PUTTERLIK, V. (1988) Resonant cellular effects of low intensity microwaves, in *Biological coherence and response to external stimuli* (FRÖHLICH, H., Ed.) Springer, Heidelberg, pp. 65–85.

GRUNDLER, W. & KEILMANN, F. (1989) Resonant microwave effect on locally fixed yeast microcolonies. *Zietschrift für Naturforschung* 44c, 863–866.

HAMEROFF, S. R. (1987) *Ultimate Computing: Biomolecular Consciousness and Nanotechnology*. North-Holland, Amsterdam.

KAISER, F. (1979) Boltzmann equation approach to Fröhlich's vibrational model. *Zeitschrift für Naturforschung* 34a, 134.

KAISER, F. (1983) in *Biological Effects and Dosimetry of Nonionizing Radiation*. Plenum, New York, pp. 251–282.

KAISER, F. (1984) Entrainment-quasiperiodicity-chaos-collapse, bifurcation routes of externally driven self-sustained oscillating systems, in *Nonlinear Electrodynamics in Biological Systems*. (ADEY, W.R. & LAWRENCE, A.F., Eds) Plenum, New York, pp. 393–412.

KAISER, F. (1981) Theory of nonlinear excitations, in *Biological Coherence and Response to External Stimuli*. (FRÖHLICH, H., Ed.) Springer, Heidelberg, pp. 24–48.

KEILMANN, F. (1983) Experimental RF and MW resonant nonthermal effects, in *Biological Effects and Dosimetry of Nonionizing Radiation* (GRANDOLFO, M., MICHAELSON, S.M. & RINDI, A., Eds) Plenum, New York, pp. 283–297.

NAIR, I., MORGAN, G. & FLORIG, H.K. (1989) *Biological Effects of Power Frequency Electric and Magnetic Fields*. Office of Technology Assessment, Washington, DC.

Salmon Divide.

E167

Bioelectromagnetics 17:312–321 (1996)

Resonance Effect of Millimeter Waves in the Power Range From 10^{-19} to 3×10^{-3} W/cm^2 on *Escherichia coli* Cells at Different Concentrations

I.Y. Belyaev, V.S. Shcheglov, Y.D. Alipov, and V.A. Polunin

SRC Vidguk, Moscow Engineering Physics Institute, Moscow, Russia

The effect of millimeter waves (MMWs) on the genome conformational state (GCS) of *E. coli* AB1157 cells was studied by the method of anomalous viscosity time dependencies (AVTD) in the frequency range of 51.64–51.85 GHz. The 51.755 GHz resonance frequency of the cell reaction to MMWs did not depend on power density (PD) in the range from 10^{-19} to 3×10^{-3} W/cm^2. The half-width of the resonant reaction of cells showed a sigmoid dependence on PD, changing from 3 MHz to 100 MHz. The PD dependence of the half-width had the same shape for different concentrations of exposed cells (4×10^7 and 4×10^8 cells/ml), whereas the magnitude of the 51.755 GHz resonance effect differed significantly and depended on the PD of MMW exposure. Sharp narrowing of the 51.755 GHz resonance in the PD range from 10^{-4} to 10^{-7} W/cm^2 was followed by an emergence of new resonance frequencies. The PD dependence of the MMW effect at one of these resonance frequencies (51.674 GHz) differed markedly from the corresponding dependence at the 51.755 GHz resonance, the power window occurring in the range from 10^{-16} to 10^{-8} W/cm^2. The results obtained were explained in the framework of a model of electron-conformational interactions. The frequency-time parameters of this model appeared to be in good agreement with experimental data.

Key words: low-intensity microwaves, genome conformation, viscosity, electron-conformational interaction model, half-width of resonance

INTRODUCTION

The biological effect of millimeter waves (MMWs) or electromagnetic fields (EMFs) of extremely high frequency has been discussed for more than 20 years [Webb and Booth, 1971; Vilenskaya et al., 1972; Devyatkov, 1973; Gründler et al., 1988]. However, the mechanism of these effects has yet to be elucidated. Moreover, some biological effects of MMWs have been questioned due to poor reproducibility [Motzkin et al., 1983; Gandhi, 1983]. One reason for poor reproducibility may be that the effects of low-intensity MMWs are dependent on numerous genetic, physiological, and physical parameters that are not always reproduced in different laboratories. For instance, the MMW effect on *Escherichia coli* cells is dependent on the growth stage of the bacterial culture [Belyaev et al., 1993a], on the cell concentration and the magnitude of the static magnetic field during exposure [Belyaev et al., 1994a], on the MMW polarization [Belyaev et al., 1992b,c], and on the time between microwave exposure and registration of the effect [Belyaev et al., 1994a].

It has been previously established that nonthermal MMWs influenced the genome conformational state (GCS) of *E. coli* cells [Belyaev et al., 1992a] and thymocytes of rats [Belyaev and Kravchenko, 1994]. This effect was dependent on the frequency and polarization of the MMWs. To account for these data, it has been proposed that a set of resonance frequencies is determined by a genome structure and that an effective polarization is determined by a helicity of DNA sequences that interact efficiently with MMWs [Belyaev et al., 1992b,c]. This assumption was further supported by the finding that the induction of approximately one single-strand DNA break per genome of *E. coli* cell by means of irradiation with X-rays eliminated the difference in biological effect of left- and right-handed circularly polarized MMW [Belyaev et al., 1992d].

Received for review March 21, 1995; revision received December 1, 1995.

Address reprint requests to Dr. I.Y. Belyaev, Department of Radiobiology, Stockholm University, S-106 91, Stockholm, Sweden.

Two physical mechanisms have been proposed in support of the idea that the natural resonance frequencies of MMW interaction with living cells are determined by the genome structure. The first model describes the oscillations in the regulatory DNA sequences that control elementary genetic processes of transcription, replication, recombination, and repair [Arinichev et al., 1993]. The second model considers the natural mechanical and acoustic oscillations in the domains of supercoiling [Belyaev et al., 1993b]. This latter model is related to the model of direct excitations in DNA that was developed previously [Davis et al., 1986]. Based on these models, the relationship between the resonance frequencies, the mass of the nucleoid, and the genome length was obtained. The predicted theoretical dependence of resonance frequencies on the length of the genome was supported in experiments where the length of the bacterial genome was changed by inserting DNA of different prophages into an *E. coli* chromosome [Belyaev et al., 1993b].

If a resonance frequency is determined by the genome structure only, then it would be insensitive to power density (PD). In this study, we examined the PD dependence of the resonance frequency of a 10 min MMW effect within the range from 10^{-19} to 3×10^{-4} W/cm^2.

We have previously established that reduction of the PD from 10^{-4} to 10^{-14} W/cm^2 resulted in a significant narrowing of the resonance response of *E. coli* cells to MMW exposure [Belyaev et al., 1992d]. Similar results have been obtained with yeast cells [Gründler, 1992] and thymocytes of rats [Belyaev and Kravchenko, 1994]. In this study, we examined the PD dependence of resonance half-width down to the minimal value of 10^{-19} W/cm^2, where a MMW effect was previously observed [Belyaev et al., 1994a]. Because the magnitude of the resonant reaction of cells to MMWs appears to be dependent on the concentration of exposed cells [Belyaev et al., 1994a], the PD dependence of the resonant MMW effect on *E. coli* cells at different concentrations was also investigated. The MMW effects were examined by using the method of anomalous viscosity time dependencies (AVTD). A correlation of the AVTD measurements with the GCS changes was examined and discussed previously [Belyaev et al., 1992a,d, 1993a]. In this study, we provided new evidence for such correlation by using ethidium bromide, which is known as a specific intercalating drug for DNA [Cook and Brazell, 1976].

MATERIALS AND METHODS

E. coli K12 AB1157 cells were grown in 100 ml of Luria broth (Difco; tryptone 10 g/liter, yeast extract 5 g/liter, NaCl 10 g/liter) for 20 h, as previously described [Belyaev et al., 1993b]. Under these conditions, the cells reached a concentration of about 10^9 colony-forming units/ml and an optical density of 0.85–1.05, which corresponded to the early stationary phase of bacterial growth [Belyaev et al., 1993a].

The experimental unit for cell exposure to MMW (Fig. 1) has already been described [Belyaev et al., 1992a, 1994a]. Voltage standing wave ratio (VSWR) in the waveguide system was measured by means of a measuring instrument at 1 mW incident power. The VSWR did not exceed 1.4 in different points of the waveguide system. The reflected power was less than 10% at the studied frequency range. The MMW frequency was measured by using two frequency converters and a frequency meter. The frequency deviation was not more than 1 MHz. The output power was measured by a wattmeter in the range of from 6×10^{-7} to 6×10^{-2} W. All of the MMW devices were made in the former USSR. Average PD at the exposure site was calculated by dividing the output power by the projected area of the horn at the surface of the Petri dish. A PD of less than 10^{-7} W/cm^2 was obtained by means of four metallic flap attenuators, which were calibrated in the range from 6×10^{-7} to 6×10^{-2} W. Each of them reduced the MMW intensity by 40–50 dB. Attenuators were calibrated in the frequency range of 51.6–51.9 GHz. Additional adjustment of the PD was also carried out by changing the oscillator output level with a maximum attenuation of 30 dB. In some experiments, the last flap attenuator in the waveguide system was replaced by a carbon attenuator. This attenuator was made by inserting a carbon-containing absorber into the waveguide segment. It reduced the MMW intensity by 40 dB. We did not observe significant differences in results for the different types of attenuator.

The local distribution of PD on the surface of a styrofoam plate between the horn and the exposed Petri dish was measured at 100 μW/cm^2, as previously described [Belyaev et al., 1992a]. The maximum deviation of local PD on this surface did not exceed 5 dB. A frequency change of a few GHz could lead to a marked shift of PD minima and maxima, including changing an increase to a decrease or vice versa. But frequency changes of ±150 MHz around the 51.755 GHz frequency did not lead to significant changes in the pattern of PD distribution. The PD value, which was averaged over the whole surface under irradiation, did not change for different frequencies if the output level was the same.

Cells were exposed in Petri dishes (50 mm in diameter). Each dish contained 3.5 ml of a cell suspension. The suspension temperature was measured by a microthermocouple with a 0.1 °C accuracy. The average heating of the cell suspension did not depend on the MMW frequency in the frequency range under study. No heating was measurable when the PD was less than

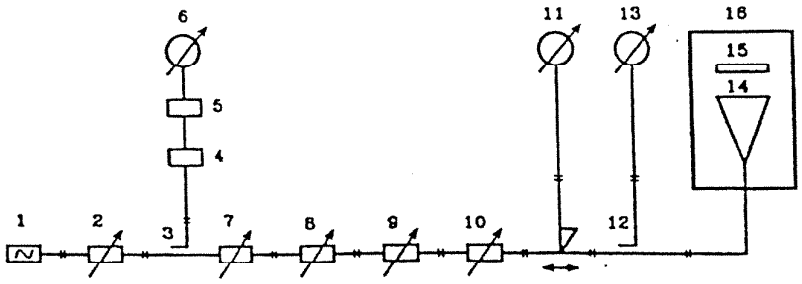

Fig. 1. Block diagram for the millimeter wave (MMW) irradiation of cells. 1, a backward wave tube of oscillator; 2, an internal attenuator of the oscillator; 3,12, directional couplers to separate about of 10% of the output power for measurements: 4,5, frequency converters; 6, frequency meter; 7–10, calibrated flap attenuators; 11, measuring instrument for the voltage standing wave ratio (VSWR) measurements in a waveguide system; 13, wattmeter with an accuracy of measurements better than 10%; 14, pyramidal horn with dimensions of 40 × 50 mm²; 15, Petri dish (50 mm in diameter) with a cell suspension; 16, chamber for irradiation.

10^{-4} W/cm². The Petri dishes were closed during exposure and the prelysis incubation. The cells were exposed in a special chamber that was shielded by carbon-containing tissue and aluminum foil. In each experiment, the sham exposure was carried out while the oscillator was working at the resonance frequency and while the MMW radiation was maximally attenuated by all attenuators down to PD < 10^{-21} W/cm². Our exposure system was clamped well to avoid mechanical vibrations.

Before exposure, the cells were diluted to a concentration of 4×10^7 or 4×10^8 cells/ml, as previously described [Belyaev et al., 1994a]. Incubation of cells after dilution was not less than 30 min. Cells were exposed in Petri dishes for 10 min and incubated for 120 min before lysis, as previously described [Belyaev et al., 1994a]. It has been shown previously that a weak change in the static magnetic field could affect the GCS of *E. coli* cells [Belyaev et al., 1994b]. In this study, we controlled the static magnetic field, as described previously [Belyaev et al., 1993a]. This field was 48 ± 5 μT in the places of growth, exposure, and incubation of cells.

The cells were lysed, and the GCS changes were measured in lysates by using the method of AVTD, as previously described [Belyaev et al., 1992a]. Briefly, this method is based on the radial migration of large DNA-protein complexes in the high-gradient hydrodynamic field of a rotary viscometer. Radial migration of molecular complexes toward the rotating rotor causes anomalous changes of viscosity that can be registered by measuring the rotor rotation period as a function of time. This AVTD depends strongly on the conformational state of the genome, which, in turn, is dependent on DNA parameters such as molecular weight, micromedium, and the number of proteins bound to the DNA. Each AVTD curve is a set of 30–50 experimental points (period of rotation vs. time of measurement) that were recorded by an IBM PC. The AVTDs were measured at a shear rate of 5.6 s^{-1} and at a shear stress of 0.007 N/m².

The maximum period of rotation (T_{max}) corresponds to maximum viscosity and has previously been shown to be the most sensitive AVTD parameter. The significance of differences between mean values in irradiated samples ($T_{max\ irr}$) and control samples ($T_{max\ con}$) was evaluated with Student's t test in each experiment. Maximum relative viscosity (η) was used to determine the MMW effect on the GCS: $\eta = (T_{max\ irr})/(T_{max\ con})$. Results were considered as significantly different at $P < .05$. Each version of the experiment included not less than three measurements, which were compared to corresponding variants of intact and sham-exposed cells by using Student's t test. Comparison of control with sham control revealed no significant differences. We performed some experiments blind. An independent observer analyzed the data without any knowledge of which sets of samples were exposed. Both kinds of experiments, blind and ordinary, resulted in the same data.

RESULTS

Figure 2 presents three frequency dependencies of the MMW effect on the GCS of *E. coli* AB1157 cells that were exposed at a concentration of 4×10^7 cells/ml. In summary, 19 experiments were performed. In these experiments, the PD changed in the range from 10^{-19} W/cm² to 3×10^{-3} W/cm². In each experiment, the frequency dependence of the effect showed a resonance nature and fitted well to a Gaussian distribution with a significance level of $P < 5 \times 10^{-4}$ to .05. The center frequency of the resonance did not depend on PD and was 51.755 ± .001 GHz (Table 1). A study of the MMW effect on cells that were exposed at a concentration of 4×10^8 cells/ml revealed similar regularities: 1) a statistically significant

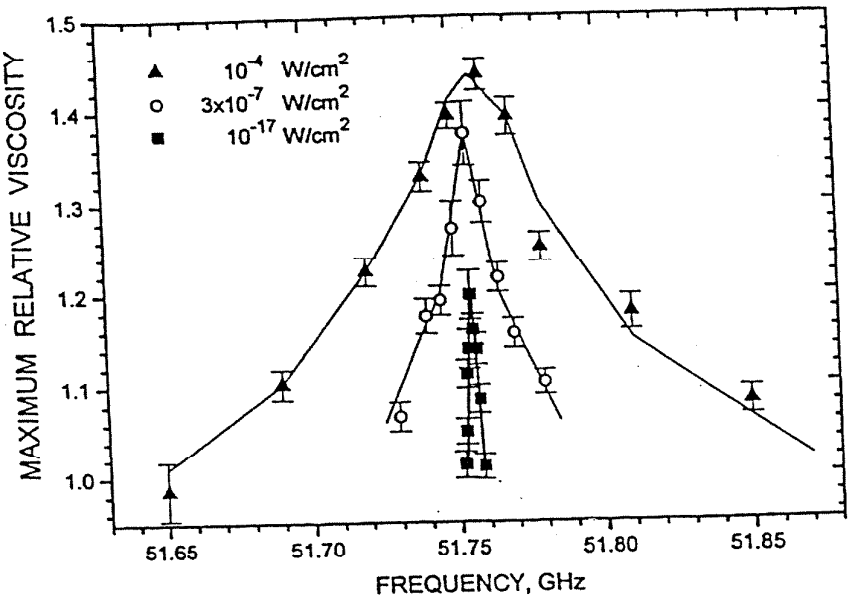

Fig. 2. Dependencies of maximal relative viscosity of cell lysates on frequency of cell exposure to MMWs at different power densities (10^{-4} W/cm², 3×10^{-7} W/cm², and 10^{-17} W/cm²).

TABLE 1. Resonance Frequencies of Millimeter Wave Effect on the Genome Conformational State of *E. coli* Cells at Different Power Densities and Cell Concentrations During Exposure*

Power density (W/cm²)	Cell concentration during exposure: 4×10^7 cells/ml	4×10^8 cells/ml
10^{-19}	—	51.755 ± .001
10^{-18}	51.755 ± .001	51.755 ± .001
10^{-16}	51.755 ± .001	51.755 ± .001
10^{-17}	51.755 ± .001	—
10^{-16}	51.755 ± .001	51.755 ± .001
10^{-15}	51.755 ± .001	—
10^{-14}	51.755 ± .002	—
10^{-13}	51.756 ± .002	—
10^{-10}	51.755 ± .002	51.755 ± .002
10^{-10}	51.754 ± .002	—
10^{-10}	51.753 ± .002	—
10^{-10}	51.76 ± .01	—
10^{-8}	51.755 ± .004	—
10^{-7}	51.756 ± .002	—
3×10^{-7}	51.755 ± .005	—
10^{-6}	51.756 ± .002	51.755 ± .005
10^{-5}	51.755 ± .005	51.755 ± .005
10^{-4}	51.76 ± .01	51.76 ± .02
5×10^{-4}	51.76 ± .01	51.76 ± .01
5×10^{-4}	—	51.76 ± .01
3×10^{-3}	51.76 ± .01	—

*The uncertainty in frequency shown reflects the steps used in changing frequency in each experiment.

approximation of frequency dependence by the Gaussian distribution and 2) stability of the 51.755 ± .001 GHz resonance frequency at different PDs.

Thus, the resonance frequency of 51.755 GHz did not depend on PD for both cell concentrations during exposure. At the same time, the half-width of the resonance (width at half-maximum of the effect) displayed a strong PD dependence in both cases. It can be seen in Figure 3 that this dependence had the same shape for both cell concentrations. Specific features of this dependence were: 1) very weak growth, which was close to a plateau of about 3–4 MHz in the range from 10^{-19} to 10^{-15} W/cm²; 2) weak growth in the range from 10^{-15} to 10^{-7} W/cm²; and 3) a sharp increase in half-width up to about 100 MHz in the range from 10^{-7} to 10^{-4} W/cm².

The minimum half-widths of the resonance MMW effect were determined in our experiments as 3.1 ± .1 MHz at PD = 10^{-18} W/cm² for the 4×10^7 cells/ml concentration during exposure and 3.0 ± .5 MHz at PD = 10^{-19} W/cm² for the 4×10^8 cell/ml concentration. Unlike the half-width of the resonance, the dependence of the magnitude of the resonance effect on PD showed a considerable difference from one concentration of exposed cells to another (Fig. 4). The relative MMW effect, in which each exposed culture was normalized to its own control at each concentration, was greater at higher concentrations of cells than at lower concentrations. At both concentrations, the PD dependence of the effect had a plateau region. This plateau was reached at quite

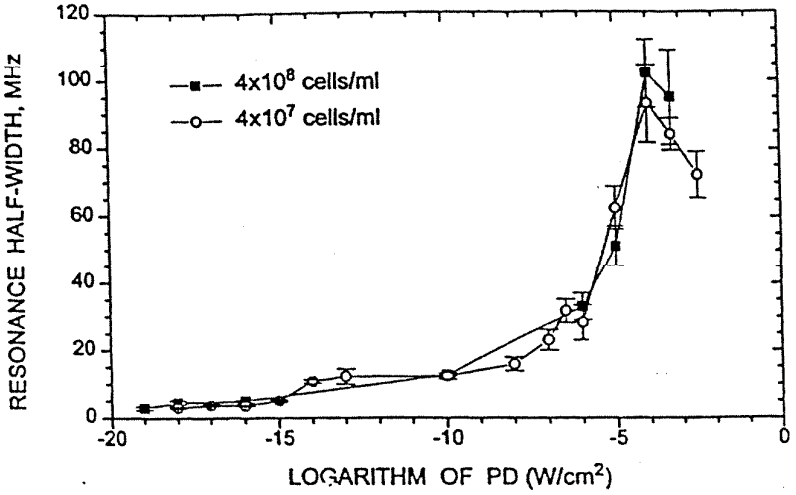

Fig. 3. Dependence of half-width of the 51.755 GHz resonance effect on power density of cell exposure at different concentrations (4×10^8 cells/ml and 4×10^7 cells/ml).

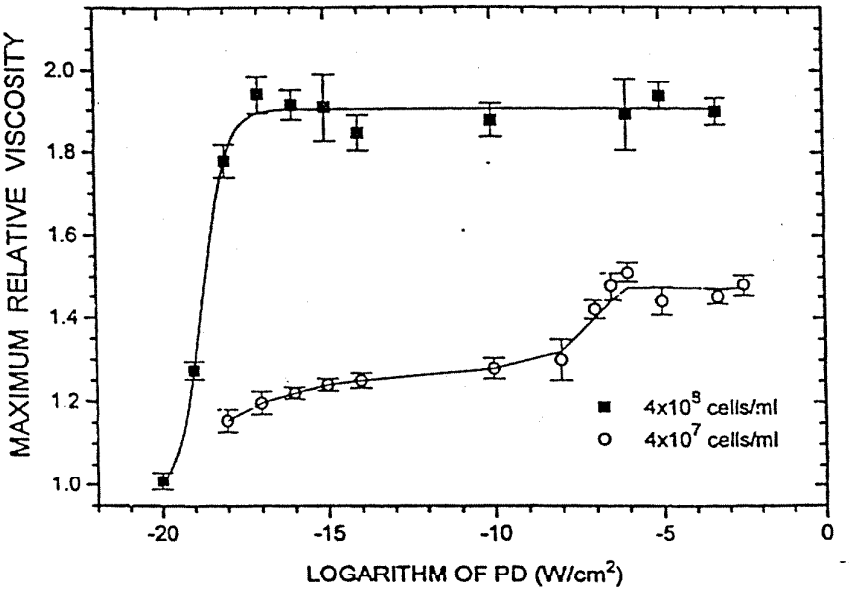

Fig. 4. Power density dependencies of maximal relative viscosity after exposure of *E. coli* cells to MMWs with 51.755 GHz frequency at different cell concentrations (4×10^8 cells/ml and 4×10^7 cells/ml). Lysis was performed at the concentration of 4×10^7 cells/ml.

different PDs: 1) 10^{-6} W/cm² if cells were exposed at a concentration of 4×10^7 cells/ml and 2) 10^{-17} W/cm² for a concentration of 4×10^8 cells/ml.

We studied the frequency dependence of the MMW effect at 10^{-10} W/cm² within the frequency range of 51.65–51.85 GHz. In this range, the resonance response with a half-width of about 100 MHz was observed at 10^{-4} to 10^{-3} W/cm². Four sharp resonances were detected at PD = 10^{-10} W/cm²: 51.674 ± .003, 51.755 ± .001, 51.805 ± .002, and 51.835 ± .005 GHz (Fig. 5). Each resonance was reproduced in two to four independent experiments. Half-widths of these four

sonances were about 10 MHz and could not be distinguished within the error of measurements.

It was established in preliminary experiments that MMWs at 51.674 GHz and a PD of 3×10^{-3} to 10^{-4} W/cm^2 did not produce significant effects on the GCS of *E. coli* cells. At the same time, MMWs of the same frequency caused an approximately 30% increase in the AVTD peaks when cells were exposed at 10^{-10} W/cm^2 (Fig. 5). This dependence of the MMW effect on the power density was different from one that was obtained previously when exposing the cells to MMWs at the 51.755 GHz resonance frequency (Fig. 4). In this connection, we studied the dependence of MMW effect at the 51.674 GHz frequency on PD in more detail. This dependence, averaged over three independent experiments, had the shape of a "window" in the PD range from 10^{-16} to 10^{-8} W/cm^2 (Fig. 6). Such a dependence cannot be explained by a thermal effect of MMWs. We investigated the frequency dependence of effects in the frequency range of 51.664–51.688 GHz in five experiments. The 51.674 GHz resonance frequency was found to be independent of PD in the range from 10^{-18} to 10^{-8} W/cm^2 within the 3 MHz error. No fine structure in the resonance dependence of the MMW effect at 3×10^{-3} and 10^{-4} W/cm^2 PDs was detected in the frequency range of 51.805–51.830 GHz.

Figures 2–6 show that the exposure of cells to MMWs resulted in an increase of the maximum relative viscosity in lysates. The same effect was observed if the cell lysates were treated with ethidium bromide during lysis (Fig. 7). This antitumour drug is known to be a very specific intercalating agent for DNA. In three independent experiments, ethidium bromide in a concentration of 3–10 μg/ml increased the maximum relative viscosity by 60–80% ($P < 5 \times 10^{-3}$). A concentration dependence obtained had a maximum around a concentration of 5 μg/ml. At this concentration, a maximum relaxation of a nucleoid has been observed under the influence of ethidium bromide [Synzynys et al., 1986]. Ethidium bromide changes the behavior of large DNA-protein complexes due to changes in a conformation of DNA that is supercoiled in cells and cell lysates [Cook and Brazell, 1976]. The data with ethidium bromide provide new evidence of the correlation of AVTD measurements with changes in conformation of the genome structures.

DISCUSSION

In our laboratory, the MMW effect on the GCS of *E. coli* K12 AB1157 cells has been investigated for 8 years. We established the experimental conditions that were critical for reproducibility of the resonance reaction of cells to low-intensity MMWs. The existence of a reproducible and stable effect is a principal reason for studying the mechanisms of the resonance MMW bioaction. Among other things, it is important to know the dependence of resonance frequency and half-width of the resonance on PD. Our

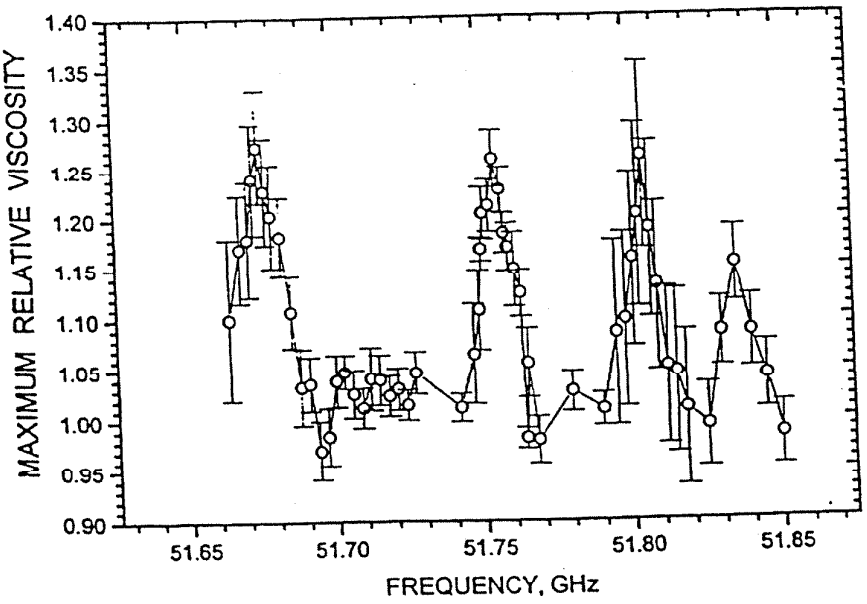

Fig. 5. Frequency dependence of MMW effect at the 10^{-10} W/cm^2 power density. Concentration was 4×10^7 cells/ml during exposure.

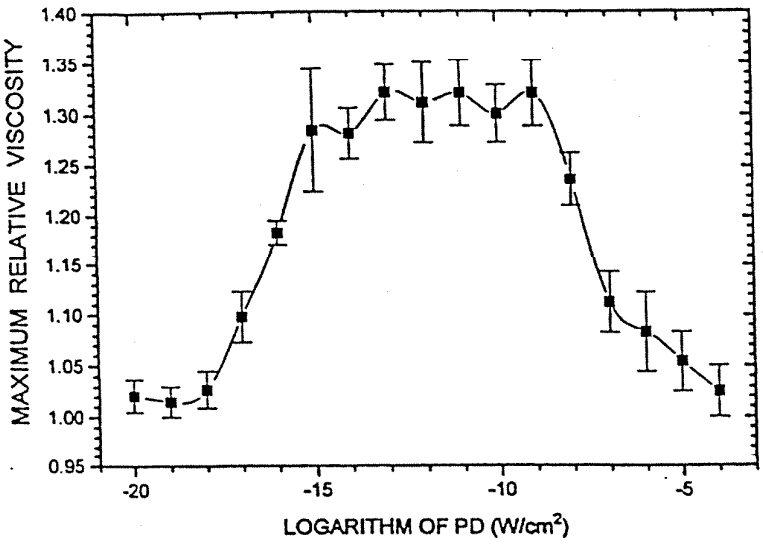

Fig. 6. Power density dependence of maximal relative viscosity in cell lysates after *E. coli* cell exposure to MMWs at the 51.674 GHz frequency. Cell concentration during exposure was 4×10^7 cells/ml.

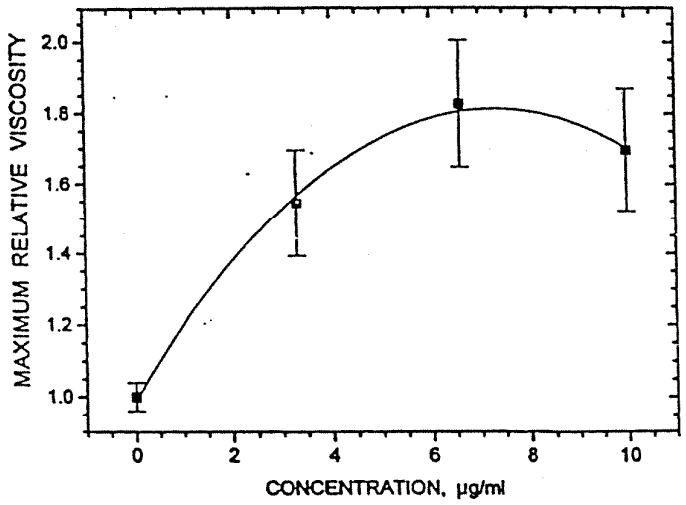

Fig. 7. Dependence of the maximum relative viscosity on the concentration of ethidium bromide during lysis of cells. Ethidium bromide was added at the beginning of lysis.

previous results have revealed the power dependence of the 51.755 GHz resonance half-width [Belyaev et al., 1992d]. Similar findings were reported for yeast cells [Gründler, 1992] and thymocytes of rats [Belyaev and Kravchenko, 1994]. The purpose of the present work was to study this dependence in the broad PD range from 10^{-19} to 3×10^{-3} W/cm². In this range, a stable resonance reaction of cells to MMWs with a resonance frequency of 51.755 GHz was registered. The resonance frequency did not change within the accuracy of our measurements. The previous calculations indicated that only a quantum-mechanical approach could be valid at PD < 10^{-15} W/cm² [Belyaev et al., 1994a]. This approach to the MMW bioaction was introduced by Frölich [1968] and was developed later in studies by other authors [Didenko et al., 1983; Sitko and Sugakov, 1984; Keilmann, 1986; Arinichev et al., 1993].

The results of the present work could be explained in the framework of the model of electron-conformational interaction (ECI), which has been previously described [Chernavskaya and Chernavskii, 1977; Didenko et al., 1983]. A short description of this model is given below for comparison to experimental data. The ECI model is characterized by three frequency-time parameters: frequency of elastic oscillations, which determines the energy of an electron transition from an initial (|i>) to an excited (|i*>) state (from 10^{10} to 10^{11} Hz); time of electron tunneling from one quasiequilibrium excited state (|i*>) to another one (|f*>; from 10^{-6} to 10^{-7} s); and time of slow electron-conformational change of the macromolecule's ionic frame (from 10^{-2} to 10^{-3} s).

Based on earlier observations, chromosomal DNA can be regarded as a specific cellular target for MMW bioaction, and the DNA parameters can determine an effective MMW frequency and polarization [Belyaev et al., 1992d, 1993b]. It can be assumed that the ionic framework of the DNA-protein complex forms an asymmetric multiplex potential, which is partially presented in Figure 8. In the first stage of interaction, a DNA macromolecule resonantly absorbs a MMW photon, resulting in an electron transition from the initial state, |i>, to the quasiequilibrium state, |i*>. Then, the electron tunnels to another quasiequilibrium state, |f*>. The time of this tunneling determines the half-width of the resonance transition. Electron tunneling to |f*> induces an electron-conformational transition, which involves rearrangement of the ionic frame in a segment of the DNA-protein complex.

The final effect of this electron-conformational interaction is deformation of the macromolecule frame. This conformational rearrangement is caused by migration of electron density along the macromolecule and can be regarded as excitation of long-wave phonons. The system of electron and macromolecule deformation appears to be similar to a polaron. The electron-conformational transition provides a time of from 10^{-2} to 10^{-3} s for changing the ability of the corresponding DNA sequence to bind proteins and metallic ions, which have a significant influence on electron-conformational interaction. If the DNA sequences that control the conformation of the domains of supercoiling are rearranged, then one would expect the GCS changes. The likely candidates for this interaction in *E. coli* cells are repeated extragenic palindromes (REPs), which contain the binding sites for DNA gyrases [Krawiec and Riley, 1990]. These enzymes are located at the attachment sites for supercoiled domains at the cellular membranes and are supposed to control the supercoiling of a nucleoid. It is important that REPs alternate in a left-to-right orientation. These alternations may be responsible for the previously observed difference in the effects of left- and right-handed circularly polarized MMWs at the same resonance frequency [Belyaev et al., 1992b,c].

The frequencies of elastic oscillations in the ECI model are of the same order of magnitude as the MMW frequencies. The lifetime of an electron in the excited state |i*> can be assessed from the resonance half-width. The PD dependence of the 51.755 GHz resonance half-width has a minimum of about 3 MHz at a PD of 10^{-18} W/cm^2 (Fig. 3), wherein the interaction must be assessed by a quantum-mechanical approach [Belyaev et al., 1994a]. A very similar half-width of the resonance of about 3 MHz was obtained previously in investigation of the MMW effect on conformation of hemoglobin in vitro [Didenko et al., 1983]. This effect was also explained in the framework of the ECI model. In the case of a quantum interaction, the lifetime is inversely proportional to the half-width of the energy levels; therefore, it can be estimated as 3×10^{-7} s. This estimate is in good agreement with the time of electron tunneling in the ECI model as well as with the lifetime of excited electrons in solids and semiconductors [Kittel, 1978].

Based on the experimental data, the minimal energy requirement for induction of the GCS changes in *E. coli* cells can be estimated. A statistically significant and reproducible effect was observed when cells at both concentrations were exposed to MMWs with PD = 10^{-18} W/cm^2 for 10 min. Thus, the minimum density of the absorbed energy was determined in our experiments to be at least from 10^{-16} to 10^{-15} J/cm^2. It follows from the ECI model that, during the rearrangement of the macromolecule frame (from 10^{-2} to 10^{-3} s), the system absorbs this minimum energy for 10 min at a PD of about 10^{-13} W/cm^2. At higher PD values, the half-width of the resonance is expected to increase, because it is determined by the overall lifetime of an electron in the |i*> and |f*> levels. Actually, an approximately twofold increase of half-width from 5 to 12 MHz is observed at a PD of about 10^{-13} W/cm^2 (Fig. 3) when exposing the cells at the 4×10^7 cells/ml concentration.

A more dramatic increase of the 51.755 GHz resonance half-width occurred in the range from 10^{-7} to 10^{-4} W/cm^2. A simple explanation of this increase seems to be an additive superposition of the resonances registered in the frequency range of 51.65–51.85 GHz at the lower PD (Fig. 5). However, the results obtained did not support this explanation, because: 1) no fine structure of the frequency dependence was observed for the broadest 51.755 GHz resonances at PD of from 10^{-3} to 10^{-4} W/cm^2 in the region of the resonance frequencies 51.674, 51.805, and 51.835 GHz; and 2) the resonance MMW effect at 51.674 GHz was significant at low intensities and practically disappeared at higher PDs (Fig. 6), whereas the MMW effect should be increased due to superposition of the resonances.

Thus, we assume that a broad resonance is formed by a mechanism other than additive superposition of several sharp resonances. One possibility is that MMW radiation with subthermal intensity induces effective rearrangement of levels in an electron subsystem of DNA. This rearrangement may take place in a magnetic field (Zeeman effect) or in an electric field (Stark effect) of MMW radiation. One cannot exclude the possibility that the effective rearrangement is induced by MMW-induced heating.

Let us note that excited levels li*+> (51.835 GHz) and li*–> (51.674 GHz) are symmetrically situated with respect to the central stable level li*> (51.755 GHz; see Fig. 8). It seems that this fact fits well with the spin models that were suggested previously [Sitko and Sugakov, 1984; Keilmann, 1986]. According to our preliminary data, left-handed circularly polarized MMWs were effective at all three resonances, and right polarization was not effective. In contrast, left-handed polarized MMWs at 10^{-10} W/cm^2 were ineffective at the 51.805 GHz resonance frequency, whereas right polarization affected the cells. The potential dependence of unstable resonance frequencies on static fields is under investigation now.

The present work provides further support for the existence of cooperativity in the resonance reaction of cells to MMWs. The dependence of an EMF effect on the concentration of exposed cells implies an interaction of the cells that is presumably of an electromagnetic nature [Belyaev et al., 1994a]. In the context of the ECI model, secondary radiation is formed during radiative electron transitions in the course of rearrangement of the ionic frame. A possible frequency range of this secondary radiation of the cooperative resonance reaction of cells to weak EMFs was discussed elsewhere [Belyaev et al., 1994a]. The detailed dependence of resonance MMW effect on the concentration of the exposed cells will be described in a separate paper.

Although the resonance effect on the GCS strongly depended on the concentration of exposed cells, the half-width of 51.755 GHz resonance proved to be independent of concentration within a broad range of PD. This data suggests a subcellular structure for resonance interaction of cells with MMWs at a stable frequency. This fact is also in agreement with the previous experimental evidence for the role of DNA as a target of the resonance influence of MMWs on cells [Belyaev et al., 1992d, 1993b]. The possible dependence of half-width at unstable resonance frequencies on the cell concentration during exposure is currently under investigation. The present investigation supports a window dependence of resonance MMW effect on power density in the nonthermal PD range, which has been previously established [Devyatkov, 1973; Gründler et al., 1988].

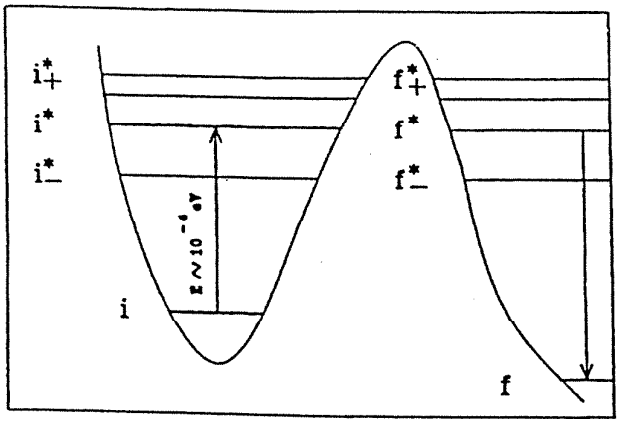

Fig. 8. A part of multiplex asymmetric potential in which the electron-conformational interactions can be directly induced in DNA-protein complex by means of resonance MMW absorption. The vertical axis represents energy, and the horizontal axis represents interparticle distance; neither is drawn to scale. See Discussion text for details.

CONCLUSIONS

The 51.755 GHz resonance effect of MMWs on *E. coli* cells was shown in the range from 10^{-19} to 3×10^{-3} W/cm^2. The half-width of the resonance showed a sigmoid dependence on PD, changing from 3 MHz to 100 MHz. The resonance half-width was the same for different concentrations of exposed cells, whereas the magnitude of the 51.755 GHz resonance effect varied by two to four times. A splitting of the 51.755 GHz resonance into four resonances was observed as the PD decreased from 10^{-4} to 10^{-7} W/cm^2. The PD dependence of the MMW effect at one of these resonance frequencies (51.674 GHz) differed markedly from the corresponding dependence at the 51.755 GHz resonance and had a power window in the range from 10^{-16} to 10^{-8} W/cm^2. The frequency-time parameters of a model of electron-conformational interactions were in agreement with experimental data.

ACKNOWLEDGMENTS

These studies were supported in part by grant J20100 from the International Science Foundation and the Russian Government and grant 95-04-12038a from the Russian Foundation for Fundamental Research.

REFERENCES

Arinichev AD, Belyaev IY, Samedov VV, Sitko SP (1993): The physical model of determining the electromagnetic characteristic frequencies of living cells by DNA structure. Second

International Scientific Meeting "Microwaves in Medicine. 1993." Rome: University of Rome, pp 305–307.

Belyaev IY, Kravchenko VG (1994): Resonance effect of low-intensity millimeter waves on the chromatin conformational state of rat thymocytes. Z Naturforsch 49:352–358.

Belyaev IY, Alipov YD, Shcheglov VS, Lystsov VN (1992a): Resonance effect of microwaves on the genome conformational state of *E. coli* cells. Z Naturforsch 47:621–627.

Belyaev IY, Shcheglov VS, Alipov YD (1992b): Selection rules on helicity during discrete transitions of the genome conformational state in intact and X-rayed cells of E. coli in millimeter range of electromagnetic field. In Allen MJ, Cleary SF, Sowers AE, Shillady DD (eds): "Charge and Field Effects in Biosystems—3." Berlin: Birkhauser, pp 115–126.

Belyaev IY, Shcheglov VS, Alipov YD (1992c): Existence of selection rules on helicity during discrete transitions of the genome conformational state of *E. coli* cells exposed to low-level millimeter radiation. Bioelectrochem Bioenerg 27:405–411.

Belyaev IY, Alipov YD, Shcheglov VS (1992d): Chromosome DNA as a target of resonant interaction between *Escherichia coli* cells and low-intensity millimeter waves. Electromagnetobiology 11:97–108.

Belyaev IY, Shcheglov VS, Alipov YD, Radko SP (1993a): Regularities of separate and combined effects of circularly polarized millimeter waves on *E. coli* cells at different phases of culture growth. Bioelectrochem Bioenerg 31:49–63.

Belyaev IY, Alipov YD, Polunin VA, Shcheglov VS (1993b): Evidence for dependence of resonant frequency of millimeter wave interaction with *Escherichia coli* K12 cells on haploid genome length. Electromagnetobiology 12:39–49.

Belyaev IY, Alipov YD, Shcheglov VS, Polunin VA, Aizenberg OA (1994a): Cooperative response of *Escherichia coli* cells to the resonance effect of millimeter waves at super low intensity. Electromagnetobiology 13:53–66.

Belyaev IY, Matronchik AY, Alipov YD (1994b): The effect of weak static and alternating magnetic fields on the genome conformational state of *E. coli* cells: The evidence for model of phase modulation of high frequency oscillations. In Allen MJ (ed): "Charge and Field Effects in Biosystems—4." Singapore: World Scientific, pp 174–184.

Chernavskaya NM, Chernavskii DS (1977): "Tunnel Effect of Electrons in Photosynthesis." Moscow: MGU.

Cook PR, Brazell IA (1976): Detection and repair of single-strand breaks in nuclear DNA. Nature 263:679–682.

Davis CC, Edvards GS, Swicord ML, Sagripanti J, Saffer J (1986): Direct excitation of internal modes of DNA by microwaves. Bioelectrochem Bioenerg 16:63–76.

Devyatkov ND (1973): Influence of electromagnetic radiation of millimeter range on biological objects. Usp Fiz Nauk 116:453–454.

Didenko NP, Zelentsov VI, Cha VA (1983): Conformational changes in biomolecules induced by electromagnetic radiation. In Devyatkov ND (ed): "Effects of Nonthermal Millimeter Waves on Biological Objects." Moscow: IRE AN SSSR, pp 63–77.

Frölich H (1968): Long range coherence and energy storage in biological systems. Int J Quant Chem 2:641–652.

Gandhi OP (1983): Some basic properties of biological tissues for potential biomedical applications of millimeter waves. J Microwave Power 18:295–304.

Gründler W (1992): Intensity- and frequency-dependent effects of microwaves on cell growth rates. Bioelectrochem Bioenerg 27:361–365.

Gründler W, Jentzsch V, Keilmann F, Putterlik V (1988): Resonant cellular effects of low intensity microwaves. In Frölich H (ed): "Biological Coherence and Response to External Stimuli." Berlin: Springer-Verlag, pp 65–85.

Keilmann F (1986): Triplet-selective chemistry: A possible cause of biological microwave sensitivity. Z Naturforsch 41:795–798.

Kittel C (1978): "Introduction to Solid State Physics." Moscow: Nauka.

Krawiec S, Riley M (1990): Organization of the bacterial chromosome. Microbiol Rev 54:502–539.

Motzkin SM, Benes L, Block N, Israel B, May N, Kuriyel J, Birenbaum L, Rosenthal S, Han Q (1983): Effects of low-level millimeter waves on cellular and subcellular systems. In Frölich H, Kremer F (eds): "Coherent Excitations in Biological Systems." Berlin: Springer- Verlag, pp 47–57.

Sitko SP, Sugakov VI (1984): Rol spinovyh sostoyanii belkovyh molekul (in Russian). Dokl Acad Nauk USSR 6A:63–65.

Vilenskaya RL, Smolyanskaya AZ, Adamenko VG, Buldasheva ZN, Gelvitch EA, Golant MB, Goldgaber DY (1972): Induction of the lethal colicin synthesis in *E. coli* K12 C600 (E1) by means the millimeter radiation. Bull Eksperim Biol Med 4:52–54.

Webb SJ, Booth AD (1971): Microwave absorption by normal and tumor cells. Science 174:72–74.

epidemiologic study of radio transmission and cancer that we know of*, in Honolulu (10), found a relative risk of leukemia of 1.56 (99 percent CI 0.86–2.63) in census tracts with broadcasting antennae, within the context of an overall raised cancer risk in these census tracts (relative risk = 1.36, 99 percent CI 1.25–1.48). Interpretation of that study was complicated both by the ecologic nature of the design and the problem of potential confounding. We are aware of no other epidemiologic (2, 11) evidence to suggest an increased risk of leukemia from non-ionizing radiation in the radiofrequency range. The existence of biologically significant athermal effects of radiofrequency radiation in animal and in vitro experiments is a subject of research and controversy, and evidence at present is not sufficient to support a leukemogenic effect (4, 12), especially at the low field strengths to which people who reside near radio transmitters are exposed. We can consider three options. First, the apparent decline in risk may be a chance finding although statistically significant at the conventional 5 percent level. Second, there may be a shallow decline in risk with distance from the transmitters, but this does not necessarily imply any causal link with radiofrequency transmission and may reflect the geographic distribution of other unmeasured sociodemographic or environmental factors. Third, if there were a true association with radio transmission, the lack of replication of the pattern and magnitude of excesses near Sutton Coldfield may indicate that a simple radial decline exposure model is not sufficient (1). The results, at most, give no more than very weak support to the Sutton Coldfield findings.

ADDENDUM

* We have subsequently become aware of a paper about to be published in which the authors found an excess of childhood leukemia near TV towers in Sydney, Australia (13).

ACKNOWLEDGMENTS

The Small Area Health Statistics Unit is funded by grants from the Department of Health, Department of the Environment, Health and Safety Executive, Scottish Office Home and Health Department, Welsh Office, and Northern Ireland Department of Health and Social Services.

The authors thank the Office of Population Censuses and Surveys (now the Office of National Statistics) and the Information and Statistics Division of the Scottish Health Service, who made the postcoded cancer data available for use.

REFERENCES

1. Dolk H, Shaddick G, Walls P, et al. Cancer incidence near radio and television transmitters in Great Britain. I. Sutton Coldfield transmitter. Am J Epidemiol 1997;145:1–9.
2. World Health Organization. Electromagnetic fields (300 Hz to 300 GHz). Environmental Health Criteria 137. Geneva: World Health Organization, 1993.
3. Department of Health. Report on health and social subjects, no. 42. Guidelines for the evaluation of chemicals for carcinogenicity. Committee on Carcinogenicity of Chemicals in Food, Consumer Products and the Environment. London: HMSO, 1991.
4. Michaelson SM, Elson EC. Interaction of nonmodulated and pulsemodulated radiofrequency fields with living matter: experimental results. In: Polk C, Postow E, eds. Handbook of biological effects of electromagnetic fields. 2nd ed. Boca Raton, FL: CRC Press, 1996:441–540.
5. Stone RA. Investigations of excess environmental risks around putative sources: statistical problems and a proposed test. Stat Med 1988;7:649–60.
6. Hills M. Some comments on methods for investigating disease risk around a point source. In: Elliott P, Cuzick J, English D, et al, eds. Geographical and environmental epidemiology: methods for small area studies. Oxford: Oxford University Press, 1992:231–7.
7. Elliott P, Shaddick G, Kleinschmidt I, et al. Cancer incidence near municipal solid waste incinerators in Great Britain. Br J Cancer 1996;73:702–10.
8. Shaddick G, Elliott P. Use of Stone's method in studies of disease risk around point sources of environmental pollution. Stat Med 1996;15:1927–34.
9. Swerdlow AJ. Cancer incidence data for adults. In: Elliott P, Cuzick J, English D, et al, eds. Geographical and environmental epidemiology: methods for small area studies. Oxford: Oxford University Press, 1992:51–62.
10. Cancer incidence in census tracts with broadcasting towers in Honolulu, Hawaii. Report submitted to the Honolulu City Council. Honolulu, HI: Environmental Epidemiology Program, Hawaii, October 1986.
11. Dennis JA, Muirhead CR, Ennis JR. Human health and exposure to electromagnetic radiation. National Radiation Protection Board report no. NRPB-R241, July 1992.
12. Postow E, Swicord ML. Modulated fields and "window" effects. In: Polk C, Postow E, eds. Handbook of biological effects of electromagnetic fields. 2nd ed. Boca Raton, FL: CRC Press, 1996:541–86.
13. Hocking B, Gordon I, Grain H, et al. Cancer in proximity to TV towers. Med J Aust (in press).

Plastic Divider - Green
"Animal Studies"

"Neurologic"
Disorder

Bioelectromagnetics 15:95–104 (1994)

Microwave Irradiation Affects Radial-Arm Maze Performance in the Rat

Henry Lai, Akira Horita, and Arthur W. Guy

Department of Pharmacology (H.L., A.H.) and the Center for Bioengineering (H.L., A.W.G), University of Washington, Seattle, Washington

After 45 min of exposure to pulsed 2450 MHz microwaves (2 μsec pulses, 500 pps, 1 mW/cm², average whole body SAR 0.6 W/kg), rats showed retarded learning while performing in the radial-arm maze to obtain food rewards, indicating a deficit in spatial "working memory" function. This behavioral deficit was reversed by pretreatment before exposure with the cholinergic agonist physostigmine or the opiate antagonist naltrexone, whereas pretreatment with the peripheral opiate antagonist naloxone methiodide showed no reversal of effect. These data indicate that both cholinergic and endogenous opioid neurotransmitter systems in the brain are involved in the microwave-induced spatial memory deficit. ©1994 Wiley-Liss, Inc.

Key words: microwaves, radial-arm maze, learning, memory, cholinergic systems, endogenous opioids

INTRODUCTION

In previous research, we have found that rats acutely exposed (45 min) to pulsed 2450 MHz microwaves [power density = 1 mW/cm², average whole body specific absorption rate (SAR) = 0.6 W/kg] showed a deficit in learning to perform in the radial-arm maze [Lai et al., 1989]. This behavioral task involves spatial memory functions, i.e., the ability to remember and learn to use spatial cues in the environment. Study of spatial memory functions in rodents has been suggested as a model for the investigation of cognitive and memory functions in humans [Gallagher and Pelleymounter, 1988; Upchurch and Wehner, 1989]. Deficit in memory functions, even transient, can lead to serious detrimental consequences. Thus, it is important to understand further this behavioral effect of microwaves and, especially, the underlying neural mechanisms involved. The present series of experiments was carried out with these goals.

From the data of our research on the effects of low-level microwave irradiation on the neurochemical changes in the brain of the rat, we have hypothesized

Received for review May 10, 1993; revision received June 29, 1993.

Address reprint requests to Dr. Henry Lai, Department of Pharmacology, SJ-30, University of Washington, Seattle, WA 98195

that acute low-level microwave exposure activated endogenous opioids which in turn caused a decrease in cholinergic activity in the hippocampus and frontal cortex [Lai, 1992; Lai et al., 1987a, 1989]. Cholinergic systems are known to play an important role in memory functions and also in performance in the radial-arm maze [cf. Levine, 1988]. It is also well established that radial-arm maze performance involves central, but not peripheral, cholinergic functions [Beatty and Bierley, 1985; Eckerman et al., 1980; Levy et al., 1983; Okaichi and Jarrard, 1982]. In the present research, we investigated whether cholinergic systems and endogenous opioids played a role in the microwave-induced spatial memory deficit in the radial-arm maze. A series of experiments was carried out to study whether pretreatment with the cholinergic agonist physostigmine or the opiate antagonist naltrexone could reverse this behavioral effect of microwaves. In addition, since the origin (peripheral or central) of the endogenous opioid effect was not known, we also studied the effect of pretreatment with the peripheral opiate antagonist naloxone methiodide. If the behavioral effect involves only endogenous opioids inside the central nervous system, treatment with naloxone methiodide would have no significant effect on the microwave-induced spatial memory deficit.

METHODS

Animals

Male Sprague-Dawley rats (250–300 g at the start of an experiment) purchased from Tyler Laboratories (Bellevue, WA) were used in our experiments. During these experiments they were housed in a room adjacent to the microwave exposure room and were maintained on a 12 h light-dark cycle with the light on between 7 AM and 7 PM. The ambient temperature of the experimental environment was 23 °C.

Microwave Exposure

The 2450 MHz cylindrical waveguide exposure system of Guy et al. [1979] was used. The waveguide system consists of eight individual cylindrical exposure tubes connected though a power divider network to a single microwave power source. Each tube consists of a section of circular waveguide constructed of galvanized wire screen in which a circularly polarized TE_{11} mode field configuration is excited. The tube also contains a plastic chamber to house a rat. The floor of the chamber is formed of glass rods, allowing waste to fall through plastic funnels into a collection container outside of the waveguide.

Both experimental and control animals were subjected to either microwave or sham exposure simultaneously. The microwave-exposed rats were irradiated with pulsed (2 μsec pulses, 500 pps), circularly polarized 2450-MHz microwaves at a spatially averaged power density of 1 mW/cm² (average whole body SAR was 0.6 W/kg). Study measuring local SAR in eight regions of the brain of rats exposed in this waveguide system showed that the values vary from 0.5–2.0 W/kg per mW/cm² [Chou et al., 1985].

For sham exposure, animals were placed in similar waveguides for the same period of time and exposure schedule as the microwave-exposed animals, but they did not receive irradiation. All exposures were done between 8–10 AM to control for possible circadian variation in response.

Radial-Arm Maze

A wooden 12
circular center hub
arms 68 cm long.
end of each arm.

Rats were ma
to 90% of ad libitu
ad lib weights, they
for 10 min each in
the maze. This pro
the animals used t
In the next session
receive either micr
ter hub, and allow
wells. All 12 food
12 arm entries or
corded when an an
adjacent room obs
and the performan
maze was cleaned
mal was given 10 c
into an arm during
into an arm was sc

Drug Treatmen

Before expos
ing intraperitoneal
(PH SO) (1 mg/k
methiodide (NMI)
in pyrogen-free ph
experiment consist
SAL, microwave/P
NMI, and sham/N
groups.

Data Analysis

The learning
training session v
errors made by ea
the one-way analy
ment groups was c
considered statisti

RESULTS

Results of th
the different trea

Radial-Arm Maze Training

A wooden 12-arm radial maze was used in this experiment. It consisted of a circular center hub (86 cm in diameter, 20 cm high) surrounded by 12 equally spaced arms (38 cm long, 10 cm wide) with a food wall (2 cm diameter) situated at the end of each arm.

Rats were maintained on a restricted food schedule to reduce their body weight to 90% of ad libitum level before experiment. When the rats reached 90% of their ad lib weights, they were sham-exposed (45 min) in the waveguides and then placed for 10 min each in the maze with pieces of rat chow (0.1 g each) scattered within the maze. This procedure was repeated for 4 more days and was designed to get the animals used to the experimental procedures of exposure and maze running. In the next session (start of learning session), the rats were randomly assigned to receive either microwaves (45 min) or sham exposure and then placed in the center hub, and allowed to explore the maze and obtain food bait placed at the food wells. All 12 food wells were baited. Each rat remained in the maze until it made 12 arm entries or 10 min had elapsed, whichever occurred first. An entry was recorded when an animal placed all four paws inside an arm. An experimenter in the adjacent room observed the performance, using a closed circuit television system, and the performance was also recorded on videotape for detailed data analysis. The maze was cleaned with 2.5% cider vinegar after each training session. Each animal was given 10 consecutive daily training sessions. In data analysis, the first entry into an arm during a training session was scored as a correct choice, whereas a reentry into an arm was scored as an error.

Drug Treatments

Before exposure in each training session, rats were given one of the following intraperitoneal injections: physiological saline (SAL) (1 ml/kg), physostigmine (PHYSO) (1 mg/kg); naltrexone hydrochloride (NAL) (1 mg base/kg); or naloxone methiodide (NMI) (1 mg base/kg). All drugs were dissolved daily before injection in pyrogen-free physiological saline and injected in a volume of 1 ml/kg. Thus, the experiment consisted of the following eight treatment groups: microwave/SAL, sham/SAL, microwave/PHYSO, sham/PHYSO, microwave/NAL, sham/NAL, microwave/NMI, and sham/NMI. There were eight animal subjects in each of these treatment groups.

Data Analysis

The learning curves of the treatment groups (i.e., average errors made in each training session versus training sessions) were analyzed by trend analysis. Total errors made by each treatment group in the ten training sessions were analyzed by the one-way analysis of variance (ANOVA) and the difference between two treatment groups was compared by the Newman-Keuls test. A difference at $P < .05$ was considered statistically significant.

RESULTS

Results of the radial-arm training sessions (errors made) of rats subjected to the different treatments are shown in Figures 1–4. Figure 1 shows the data of

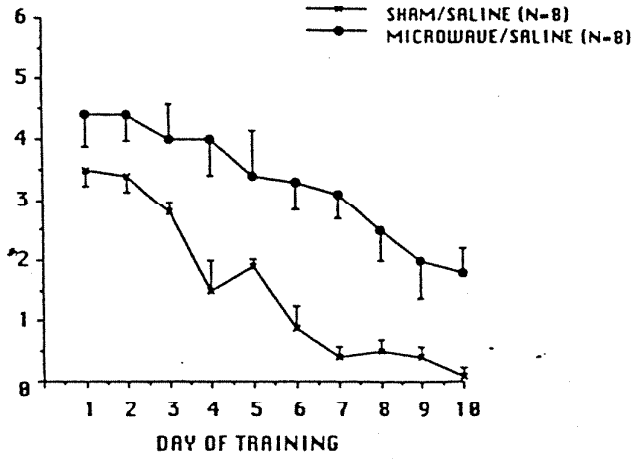

Fig. 1. Performance of the microwave/saline and sham/saline treated rats during the ten training sessions. N = 8 in each group. Treatment effect: F[1,14] = 14.84, $P < .005$; training effect: F[9,63] = 12.67, $P < .005$.

microwave- and sham-exposed animals pretreated with physiological saline before each training session. The trend analysis of the data showed significant treatment (microwave or sham) effect (F[1,14] = 14.82, $P < .005$). The microwave-exposed rats learned significantly slower than the sham-exposed animals (i.e., they made more errors during the training sessions). Pretreatment with physostigmine (Fig. 2) or naltrexone (Fig. 3) attenuated the effects of microwaves. There was no significant difference in performance between the microwave- and sham-exposed animals under these drug-treatment conditions (treatment effect for physostigmine:

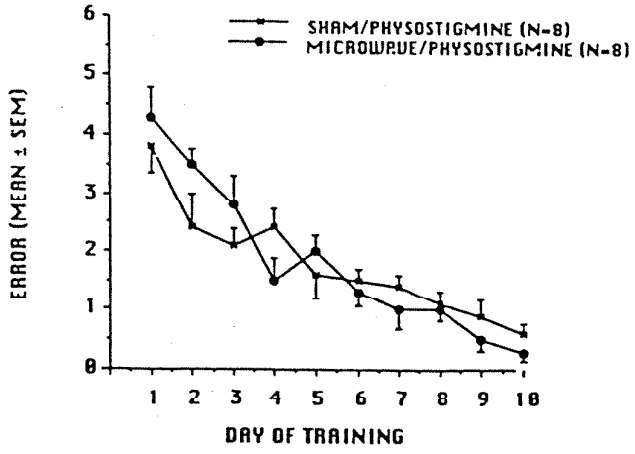

Fig. 2. Performance of the microwave/physostigmine and sham/physostigmine rats during the ten training sessions. N = 8 in each group. Treatment effect: F[1,14] = 1.14, nonsignificant; training effect: F[9,63] = 15.2, $P < .005$.

Fig. 3. Performan
N = 8 for each g
$P < .005$.

F[1,14] = 1.1
However, in
learned signif
$P < .005$).
methiodide

Data fr
ent treatmen
cant treatme

Fig. 4. Performa
rats. N = 8 in ea
$P < .005$.

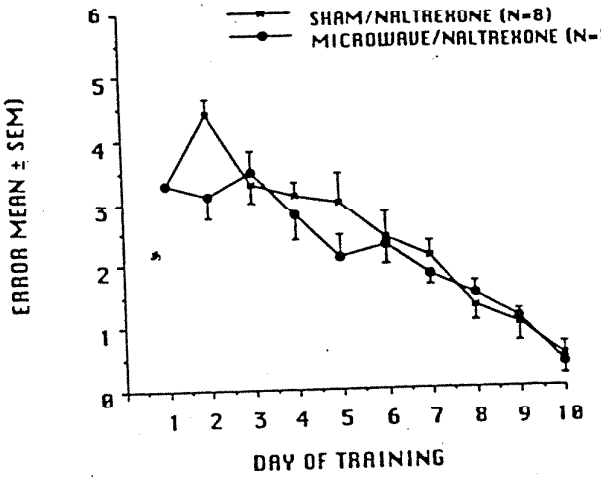

Fig. 3. Performance of the microwave/naltrexone and sham/naltrexone rats during the ten training sessions. N = 8 for each group. Treatment effect: F[1,14] = 2.35, nonsignificant; training effect: F[9,63] = 12.19, $P < .005$.

F[1,14] = 1.14, nonsignificant; and for naltrexone: F[1,14] = 2.35, nonsignificant). However, in rats treated with naloxone methiodide, the microwave-exposed rats learned significantly slower than the sham-exposed animals (Fig. 4) (F[1,14] = 175.4, $P < .005$). Thus, the effect of microwaves was not significantly blocked by naloxone methiodide.

Data from the sum of errors made in the ten training sessions by the different treatment groups are shown in Figure 5. One-way ANOVA showed a significant treatment effect (F[7,56] = 18.99, $P < .005$) and the Newman-Keuls test

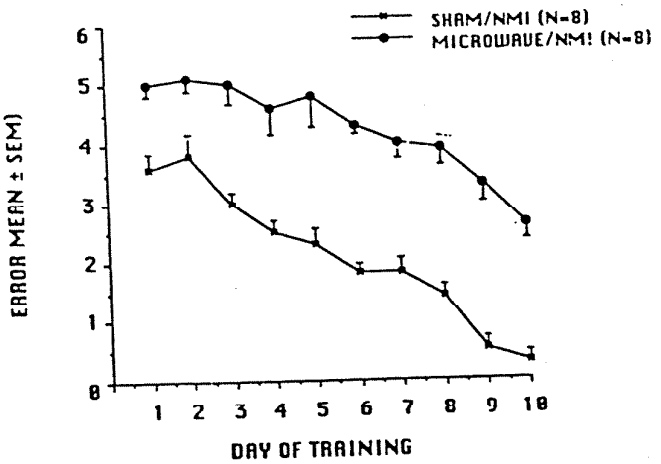

Fig. 4. Performance of the microwave/naloxone methiodide (NMI) and sham/naloxone methiodide treated rats. N = 8 in each group. Treatment effect: F[1,14] = 175.4, $P < .005$; training effect: F[9,63] = 13.9, $P < .005$.

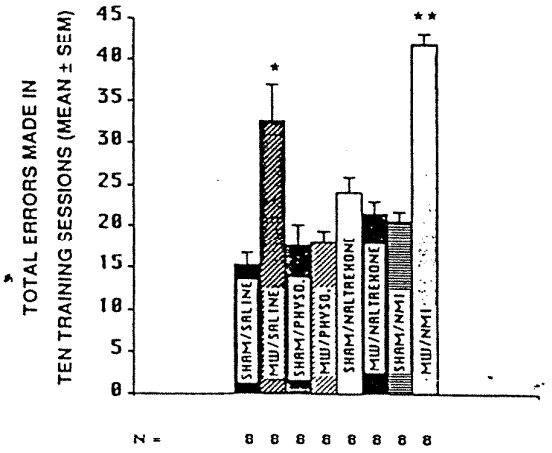

Fig. 5. Total errors made in the ten training sessions of the different treatment groups. *,** indicate difference between the sham/saline vs. microwave/saline groups, and sham/NMI vs. microwave/NMI groups, respectively, at $P < .01$ (Newman-Keuls test). MW, microwave; PHYSO, physostigmine; NMI, naloxone methiodide

comparing treatment groups showed a significant difference between the microwave/saline vs sham/saline ($P < .01$) and microwave/NMI and sham/NMI ($P < .01$) groups, whereas no significant difference was found between the microwave/physostigmine vs. sham/physostigmine and microwave/naltrexone vs. sham/naltrexone groups.

Thus, these data show that the microwave-induced learning deficit in the radial-arm maze was blocked by pretreatment with the cholinergic agonist physostigmine or the opiate antagonist naltrexone, but not by the peripheral opiate antagonist naloxone methiodide.

DISCUSSION

Data from the present experiment indicate that both cholinergic and endogenous opioid neurotransmitter systems within the central nervous system are involved in the microwave-induced deficit in learning in the radial-arm maze. Since the effect is reversed by a cholinergic agonist or an opiate antagonist, these data are in agreement with our hypothesis that low-level microwaves activate endogenous opioids which in turn cause a decrease in cholinergic activity in the brain [Lai, 1992], and the decrease in cholinergic activity is responsible for the behavioral deficit observed. In our experiments, since all the arms of the radial maze were baited, this allowed us to study "working" memory function, a memory function similar to short-term memory. During each training session, the rat has to remember its previous arm choices in order to obtain food from the arms and not to re-enter an arm. Since the pattern of arm choices varies from session to session, the "working" memory is not fixed and changes with each session. Our data imply that acute microwave irradiation affects "working" memory in the rat.

Involvement of central cholinergic systems in the performance in the radial-arm maze is well known [cf. Levin, 1988]. Deficits in maze learning have been reported in animals after disruption of cholinergic functions, for example, after administration of cholinergic antagonists [Okaichi and Jarrard, 1982; Stevens, 1981; Watts et al., 1981; Wirsching et al., 1984], or lesioning of the hippocampal or cortical cholinergic pathways [Altman et al., 1985; Jarrard et al., 1984; Murray and Fibiger, 1985; Olton and Papas, 1979]. Furthermore, similar to our results, deficits in maze performance caused by lesioning of the cholinergic pathways is reversible by treatment with the cholinergic agonist physostigmine [Murray and Fibiger, 1985].

Since endogenous opioids play a modulatory role on the activity of the cholinergic systems in the brain, they have also been implicated in radial-arm maze perfo. nance. However, it seems that whether the endogenous opioid systems in the brain play a role in the performance in the radial-arm maze depends on the complexity of the training and testing procedures used. For example, Beatty [1983] showed that opiate agonists and antagonists had no significant effect on spatial memory of rats performing in an 8-arm radial maze. Gallagher et al. [1983, 1985] also found no significant effect of the opiate antagonist naloxone in the rat on the rate of learning in an 8-arm radial maze. However, they did show in rats, which had been previously trained in the maze, that post-training treatment with opiate antagonists impro ed the rate of learning when these animals were retrained in a similar maze arranged in novel spatial environments. They have further demonstrated that the medial septal areas of the brain mediated the effect of the opiate antagonists [Bostock et al., 1988]. This is significant because the medial septum contains the cholinergic cell bodies which send innervations to the hippocampus. More recently, Canli et al. [1990] reported that the opiate antagonists, naloxone and naltrexone, enhanced the "working" memory component of the performance when a significantly more complex 12-arm radial maze, the type of maze used in our experiments, was used.

In our previous research, we have found in the rat that acute exposure to pulsed low-level microwaves decreased the activity of cholinergic innervations in the hippocampus and frontal cortex. These brain regions receive innervation from cholinergic neurons located in the medial septum/diagonal band of broca and the nucleus basalis magnocellularis, respectively. Moreover, the effect of microwaves on the hippocampal cholinergic innervation was blocked by pretreatment with opiate antagonists, whereas that on the frontal cortex was not [Lai et al., 1987a, 1989]. In the present experiment, we found that treatment with naltrexone completely blocked the maze learning deficit of the microwave-exposed rats. This would imply that reversal of cholinergic activity in the hippocampus alone is sufficient to reverse the behavioral deficit.

The cholinergic systems of the cerebral cortex and hippocampus may play different roles in learning and memory in the radial-arm maze. It is known that the septo-hippocampal and basalis-cortical cholinergic pathways respond differently to learning in the radial-arm maze. For example, Wenk et al. [1984] reported an increase in cholinergic activity in the hippocampus of rats performing in a radial-arm maze, whereas the cortex showed a slight decrease. In other cases, the two cholinergic pathways have been shown to respond at different time courses after radial-arm maze training [Jaffard et al., 1989; Toumane et al., 1988, 1989]. While the role of the hippocampal cholinergic system on radial-arm maze performance is well established, the specific role played by the basalis-cortical cholinergic system

is not entirely clear. Several studies have implied that the cortical cholinergic pathway is not as critical in radial-arm maze performance as the hippocampal system. Becker et al. [1980] showed that lesions of the fimbia-fornix, the pathway of cholinergic innervations to the hippocampus, have a more severe and persistent effect on radial-arm maze "working" memory function than lesioning of the frontal cortex in the rat. Another study [Murray and Fibiger, 1985] has shown that the basalis-cortical cholinergic pathway is not involved in "working" memory in the radial-arm maze, the memory function studied in our experiments. Miyamoto et al. [1987] also reported that lesioning of the septo-hippocampal pathway caused a more severe effect on "working" memory function in the radial-arm maze than lesioning the basalis-cortical pathway in rats. Deyo et al. [1990] showed that decorticated rats can do spatial learning in the radial-arm maze. Oades [1981] also reported no change in "working" memory function after neocortical lesioning in the rat. These reports suggest that the cortical cholinergic systems are less involved in the "working" memory function necessary for radial-arm maze performance. However, it must be pointed out that in other studies, it has been shown that rats with frontal cortical lesions showed specific "working" memory deficit [e.g., Bartus et al., 1985; Poucet, 1990; Walsh et al., 1984].

In addition, in a previous experiment [Lai et al., 1987b], we have found that after ten daily sessions of low-level microwave exposure, the cholinergic response in the hippocampus adapted, i.e., no significant response was observed after further exposure, whereas no adaptation was observed in the cortical cholinergic system. This is also consistent with the interpretation that the hippocampal cholinergic system is mainly responsible for the radial-arm maze learning deficit seen after acute exposure to microwaves, whereas the cortical cholinergic system only plays a minor role or is even not involved, since the microwave-exposed rats also showed a significant gradual improvement in performance with increased training, even though not as fast as the sham-exposed animals [see Fig. 1; Lai et al., 1989].

ACKNOWLEDGMENTS

Research described in this paper was supported by a grant from the National Institute of Environmental Health Sciences (ES-03712). We thank Mrs. Dorothy Pratt for the preparation of the figures and for editing this paper.

REFERENCES

Altman HJ, Crosland RD, Jenden DJ, Berman RF (1985): Further characterizations of the nature of the behavioral and neurochemical effects of lesions to the nucleus basalis of Meynert in the rat. Aging 6:125–130.

Bartus RT, Flicker C, Dean RL, Pontecorvo M, Figueiredo JC, Fisher SK (1985): Selective memory loss following nucleus basalis lesions: Long term behavioral recovery despite persistent cholinergic deficiencies. Pharmacol Biochem Behav 23:125–135.

Beatty WW (1983): Opiate antagonists, morphine, and spatial memory in rats. Pharmacol Biochem Behav 19:397–401.

Beatty WW, Bierley RA (1985): Scopolamine degrades spatial working memory but spares spatial reference memory: Dissimilarity of anticholinergic effect and restriction of distal visual cues. Pharmacol Biochem Behav 23:1–6.

Becker JT, Walker JA, Olton DS (1980): Neuroanatomical bases of spatial memory. Brain Res 200:307–320.

Bostock E, Gallag... tial informati... 102:645–65...

Canli T, Cook RG, ... the radial m...

Chou C..., Guy AW ... MHz microw...

Deyo RA, Panksepp ... maze task. P...

Eckerman DA, Gor ... pentobarbita... Behav 12:59...

Gallagher M, Pelle... decline in th...

Gallagher M, King ... 1:975–97...

Gallagher M, Bost... and aged rats...

Guy AW, Wallace J, ... exposure of ...

Jaffard R, Durkin T, ... systems in m...

Jarrard LE, Kant C, ... ventricular A...

Lai H (1992): Rese... Washington.

Lai H, Horita A, Ch... linergic activ...

Lai H, Horita A, Ch... ampal and f... 27:635–6...

Lai H, Carino MA ... ergic systems...

Levin ED (1988): ... 2:169–175.

Levy A, Kluge PB, ... ropine effects...

Miyamoto M, Kato J ... lesioning of ...

Murray CI, Fibiger ... magnocellula...

Oades RD (1981): T... limbic ventra...

Okaichi H, Jarrard L ... Neural Biol ...

Olton DS, Papas ... 17:667–682.

Poucet B (1990): A ... of the medial...

Stevens R (1981): ... 27:385–386.

Toumane A, Durkin ... tical choliner... discriminatio...

Toumane A, Durkin ... cholinergic ac... maze decreas...

Bostock E, Gallagher M, King RA (1988): Effects of opiate manipulations on retention of novel spatial information: sensitivity of the medial septal area to β-endorphin and naloxone. Behav Neurosci 102:645–652.

Canli T, Cook RG, Miczek KA (1990): Opiate antagonists enhance the working memory of rats in the radial maze. Pharmacol Biochem Behav 36:521–525.

Chou CK, Guy AW, McDougall JA, Lai H (1985): Specific absorption rate in rats exposed to 2450-MHz microwaves under seven exposure conditions. Bioelectromagnetics 6:73–88.

Deyo RA, Panksepp J, Abbott B (1990): Perinatal decortication impairs performance on an 8-arm radial maze task. Physiol Behav 48:55–60.

Eckerman DA, Gordon WA, Edwards JD, McPhail RC, Gage MI (1980): Effects of scopolamine, pentobarbital and amphetamine on radial arm maze performance in the rat. Pharmacol Biochem Behav 12:595–602.

Gallagher M, Pelleymounter MA (1988): Spatial learning deficits in old rats: A model for memory decline in the aged. Neurobiol Aging 9:549–556.

Gallagher M, King RA, Young NB (1983): Opiate antagonists improve spatial memory. Science 221:975–976.

Gallagher M, Bostock E, King R (1985): Effects of opiate antagonists on spatial memory in young and aged rats. Behav Neural Biol 44:374–385.

Guy AW, Wallace J, McDougall JA (1979): Circular polarized 2450-MHz waveguide system for chronic exposure of small animals to microwaves. Radio Sci 14(6S):63–74.

Jaffard R, Durkin T, Toumane A, Marighetto A, Lebrun C (1989): Experimental dissociation of memory systems in mice: Behavioral and neurochemical aspects. Arch Gerontol Geriat Supp 1:55–70.

Jarrard LE, Kant CJ, Meyerhoff JL, Levy D (1984): Behavioral and neurochemical effects of intraventricular AF64A administration in rats. Pharmacol Biochem Behav 21:273–280.

Lai H (1992): Research on the neurological effects of nonionizing radiation at the University of Washington. Bioelectromagnetics 13:513–526.

Lai H, Horita A, Chou CK, Guy AW (1987a): Low-level microwave irradiation affects central cholinergic activity in the rat. J Neurochem 48:40–45.

Lai H, Horita A, Chou CK, Guy AW (1987b): Effects of low-level microwave irradiation on hippocampal and frontal cortical choline uptake are classically conditionable. Pharmacol Biochem Behav 27:635–639.

Lai H, Carino MA, Horita A, Guy AW (1989): Low-level microwave irradiation and central cholinergic systems. Pharmacol Biochem Behav 33:131–138.

Levin ED (1988): Psychopharmacological effects in radial-arm maze. Neurosci Biobehav Rev 12:169–175.

Levy A, Kluge PB, Elsmore TF (1983): Radial-arm maze performance of mice: Acquisition and atropine effects. Behav Neural Biol 39:229–240.

Miyamoto M, Kato J, Narumi S, Nagaoka A (1987): Characterizations of memory impairment following lesioning of the basal forebrain and medial septal nucleus in rats. Brain Res 419:19–31.

Murray CI, Fibiger HC (1985): Learning and memory deficits after lesions of the nucleus basalis magnocellularis: Reversal by physostigmine. Neurosci 14:1025–1032.

Oades RD (1981): Types of memory or attention? Impairments after lesions of the hippocampus and limbic ventral tegmentum. Brain Res Bull 7:221–226.

Okaichi H, Jarrard LE (1982): Scopolamine impaired performance of a place and cue task in rats. Behav Neural Biol 35:319–325.

Olton DS, Papas BS (1979): Spatial memory and hippocampal function. Neurophysiologia 17:667–682.

Poucet B (1990): A further characterization of the spatial problem-solving deficit induced by lesions of the medial frontal cortex in the rat. Behav Brain Res 41:229–237.

Stevens R (1981): Scopolamine impaired spatial maze performance in rats. Physiol Behav 27:385–386.

Toumane A, Durkin T, Marighetto A, Galey D, Jaffard R (1988): Differential hippocampal and cortical cholinergic activity during the acquisition, retention, reversal and extinction of a spatial discrimination in an 8-arm radial maze by mice. Behav Brain Res 30:225–234.

Toumane A, Durkin T, Marighetto A, Jaffard R (1989): The durations of hippocampal and cortical cholinergic activation induced by spatial discrimination testing of mice in an eight-arm radial maze decrease as a function of acquisition. Behav Neural Biol 52:279–284.

Upchurch M, Wehner JM (1989): Inheritance of spatial learning ability in inbred mice: A classical genetic analysis. Behav Neurosci 103:1251–1258.

Walsh TJ, Tilson HA, DeHaven DL, Mailman RB, Fisher A, Hanin I (1984): AF64A, a cholinergic neurotoxin, selectively depletes acetylcholine in hippocampus and cortex, and produces long-term passive avoidance and radial-arm maze deficits in the rat. Brain Res 321:91–102.

Watts J, Stevens R, Robinson C (1981): Effects of scopolamine on radial maze performance in rats. Physiol Behav 26:845–847.

Wenk G, Helper D, Olton D (1984): Behavior alters the uptake of [^{3}H]-choline into the acetylcholinergic neurons of the nucleus basalis magnocellularis and medial septal area. Behav Brain Res 13:129–138.

Wirsching BA, Berringer RJ, Jhamandas K, Boegman RJ, El-Defrawy SR (1984): Differential effects of scopolamine on working and reference memory of rats in the radial maze. Pharmacol Biochem Behav 20:659–662.

Superi
Electr
Induce
Chick

T.A. Litovit

Department
(T.A.L., C.J.
ton Universit

Living c
to-noise
(ELF) e
enous fi
tic... livi
over the
multane
the bioc
cells a-
sugg
cohere
observe
was con
h- elect
c... npar
field), tl
duced t

Key words: n

INTRODUC

The as
ELF electro
nearly a de
considerati
Astumian, J

Received for r

Address reprir
Washington, I

"Circular"
Division

ADIATION RESEARCH 123, 199–202 (1990)

Physiological Changes in Rats after Exposure to Low Levels of Microwaves

S. RAY AND J. BEHARI[1]

School of Environmental Sciences, Jawaharlal Nehru University, New Delhi-110067, India

RAY, S., AND BEHARI, J. Physiological Changes in Rats after Exposure to Low Levels of Microwaves. *Radiat. Res.* 123, 199–202 (1990).

The effects of exposure to sublethal levels of microwaves were studied. Young albino rats of both sexes were exposed for 60 days to 7.5-GHz microwaves (1.0-KHz square wave modulation, average power 0.6 mW/cm^2) for 3 h daily. During and after microwave exposure several physiological parameters were measured in both control and exposed animals. It was found that the animals exposed to microwaves tended to eat and drink less and thus showed a smaller gain in body weight. Some of the hematological parameters and organ weights were also significantly different. It is proposed that a nonspecific stress response due to microwave exposure and mediated through the central nervous system is responsible for the observed physiological changes.

INTRODUCTION

Although the biological effects of microwave radiation have been studied (*1, 2*), there are still insufficient data available to establish any threshold level or dose–effect relationship, because the fundamental nature of these effects, or the basic mechanism of the interaction between microwaves and biological systems, is not well understood.

Studies of the biological effects of microwave radiation can be divided into two categories: short-term exposure at high intensities and long-term exposure at low intensities. The effects of exposure to high intensities are generally attributed to elevated body temperatures, while the thermally translated energy absorbed at lower power densities is generally believed to be dissipated easily by the organism and has little or no lasting effect. Dumanski and Shandala (*3*) and Rudnev *et al.* (*4*) found behavioral and physiological changes in albino rats after chronic microwave irradiation at power densities as low as 0.5 mW/cm^2. The effects they saw included lowered reactivity to electric foot shock, altered levels of cholinesterase and sulfhydryl groups in blood, increased urinary output of 17 ketosteroids, and deficits in performance in the shuttle box. Low-level, short-[illegible] exposure may affect the nervous, hemopoietic, and [illegible]unocompetent cell systems of animals (*5*). More recently, the effect of low-level microwave exposure on reproduction in rats (*6*) and the stress reaction due to total-body exposure (*7*) have been reported. However, to our knowledge data are not available regarding the development of animals exposed to low-level microwave power over a period of months. To bridge this gap, we designed our experiment to use relatively low microwave (7.5 GHz) power density so that the thermoregulatory capacity of the animals is not overridden. The aim of the study was to determine the nature and extent of microwave-induced alterations after irradiation at sublethal levels. A number of measurements including food and water intake, body weight gain, organ weights of the animals, and hematological parameters were made in control and microwave-exposed rats.

MATERIALS AND METHODS

Albino rats 40 days old and weighing approximately 75 g were used for the experiments. The rats were sexed, marked, and kept separately in cages. Experimental animals were exposed to microwaves in the anechoic chamber daily for 3 h each day. During experiments the two groups of animals were treated identically except for microwave exposure to the experimental group. Daily consumption of food and water was recorded for each group. Every 10 days, the body weight of the animals was also recorded. After 60 days, blood was collected from each rat from its marginal eye vein and standard techniques were followed for determination of the different parameters, including hemoglobin (Hb), erythrocyte sedimentation rate, red blood cells, total leukocytes, and differential counts.

The animals were irradiated at a frequency of 7.5 GHz (1 KHz square wave modulation) in a microwave anechoic chamber. The pulses were 0.6 ms wide and had an average power level of 0.6 mW/cm^2. Following the work of Durney *et al.* (*8*), the specific absorption rate (SAR) was 0.0317 W/kg in the far field of standard gain antenna (16-db gain) within the anechoic chamber (Fig. 1). The exposure chamber was a tapered one, specially designed for the frequency range 2.4–10 GHz, and had an inside geometry of 1 m on each side. The inner lining of the chamber was made of a pyramid-shaped absorbing material (40 db). The constraining cage was placed 2 m away from the antenna. The position was determined by the position of the quiet zone within the chamber, which was checked using a specially made dipole probe. The cage was placed symmetrically along the midline of the antenna aperture, which was a pyramidal horn having dimensions 14.2 × 10.8 cm. The antenna was coupled to the Klystron power supply through an isolator. The absolute power calibration was made with an identical antenna of the same aperture which was connected to the power meter through a waveguide to coaxial transition.

Field measurements were performed using the probe as described by Guru.[2] The repeller voltage of the Klystron power supply was adjusted for

[1] To whom correspondence should be addressed.

[2] B. S. Guru, *An Experimental and Theoretical Study on the Interaction of Electromagnetic Fields with Arbitrarily Shaped Biological Bodies*, Ph.D. dissertation, Michigan State University, East Lansing, MI, 1976.

0033-7587/90 $3.00

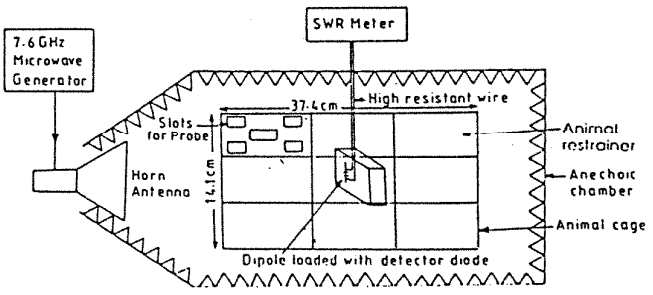

FIG. 1. Schematic diagram of the experimental design for the measurement of field distribution in the animal cage.

maximum available output power and was kept constant throughout the course of the experiment.

The unanesthetized rats were put into separate chambers of the cage. Each chamber had holes at the top for proper ventilation. The dipole probe could be inserted through these holes for field measurements. The cage was made of 0.5-cm-thick acrylic, and the dielectric constant was 2.20. Nine animals (male, female) were irradiated at a time. Using the special dipole probe, the field in each chamber in the presence of the animals was monitored. The power distribution in each animal position is shown in Fig. 2. This gives the average power in the presence of all other animals at their respective positions in the cage. Each animal was kept in a prespecified compartment of the cage throughout the exposure period. Each animal was thus irradiated homogeneously at the same power level. Measurements were made at room temperature (30°C) and corresponding humidity level (60%). After the exposure was over (60 days), the animals were sacrificed and their organ weights determined. The normalized values [(weight of organ/weight of animal) × 100] are presented in Table III. For statistical analysis of the experimental data, mean differences in dependent variables (hematological data and organ weights) were compared using Student's t test. The significance of the hypothesis was tested at the 5% level.

RESULTS

The daily intake of food and water by control and experimental animals (determined individually for nine males and nine females) is shown in Figs. 3 and 4, respectively. The changes in food and water intake as a function of time in the exposed and sham-exposed rats were assessed by an analysis of variance (Table I). Average food and water intake per animal was found to be less in exposed animals compared to the controls. After 50 days of microwave exposure the average daily total (food + water) intake per animal

0.40 0.49 0.44 Six 0.44 0.44	0.49 0.40 0.40 Two 0.44 0.49	0.32 0.32 0.35 Nine 0.40 0.40
0.44 0.44 0.60 Five 0.60 0.54	0.44 0.44 0.6 mW/cm² One 0.40 0.49	0.40 0.44 0.49 Three 0.49 0.32
0.49 0.49 0.44 Eight 0.40 0.49	0.54 0.49 0.54 Four 0.49 0.60	0.49 0.44 0.49 Seven 0.6 0.32

FIG. 2. Field configuration (mW/cm²) inside the animal cage in the presence of the animal due to exposure to microwave radiation.

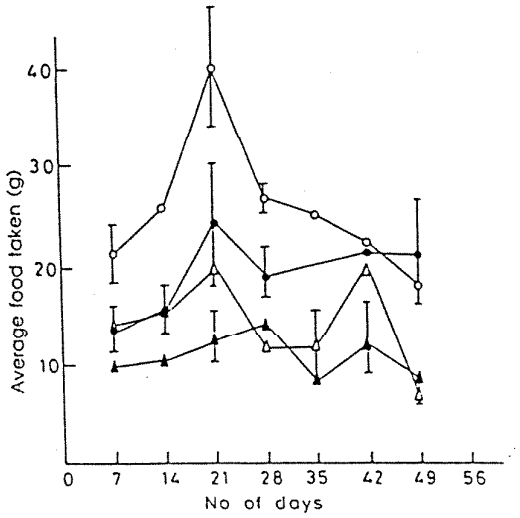

FIG. 3. Effect of exposure of growing albino rats to 7.5-GHz microwaves for 3 h daily on food intake. (○) Control males, (●) exposed males, (△) control females, (▲) exposed females.

was 75.6 ± 8.2 g for control males and 60.5 ± 2.6 g for irradiated males. For female animals the corresponding figures are 53.1 ± 15.0 g for controls and 31 ± 5.0 g for experimental rats. The experimental and control groups also differed in body weight. The relative weight gain in the two groups was less for exposed animals (Fig. 5). The depressed growth rate can be attributed to the microwave exposure.

The hematological responses of the rats after 60 days of exposure are shown in Table II. The RBC and hemoglobin levels did not change significantly. In the differential counting, the percentages of neutrophils, lymphocytes, and monocytes were not significantly different. There was also no variation in the hemoglobin level. The difference in

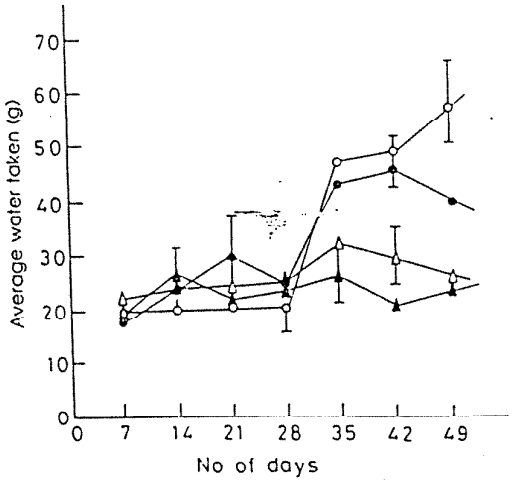

FIG. 4. Effect of exposure of growing albino rats to 7.5-GHz microwaves for 3 h daily on water intake. (○) Control males, (●) exposed males, (△) control females, (▲) exposed females.

TABLE I
An Analysis of Variance Table for Classification

Parameter analyzed	Variation	Degrees of freedom	Sum of squares	Mean squares	F ratio
Food intake by male rats	Within treatments	$k-1=1$	227.15	227.15	6.36
	Between treatments	8	285.95	35.74	
	Total	$nk-1=9$	513.10		
Food intake by female rats	Within treatments	$k-1=1$	25.92	25.92	3.39
	Between treatments	8	61.13	7.64	
	Total	$nk-1=9$	87.05		
Water intake by male rats	Within treatments	$k-1=1$	143.08	143.08	7.11
	Between treatments	4	80.47	20.12	
	Total	$nk-1=5$	223.55		
Water intake by female rats	Within treatments	$k-1=1$	44.56	44.56	63.65
	Between treatments	6	4.20	0.7	
	Total	$nk-1=7$	48.76		

erythrocyte sedimentation rate was not statistically significant.

The normalized organ weights (weights of organ per 100 g of body weight) for irradiated and control rats are shown in Table III. A statistically significant decrease was observed for spleen, kidney, brain, and ovary, with percentage decrements of 21.6 ± 9.0, 13.97 ± 3.2, 15.4 ± 1.1, and 22.0 ± 5.0, respectively. No statistically significant variations were observed for other organs. We observed a slight increase in testicular weight in exposed animals. Since our data for hematological and organ weights for male and female did not vary significantly, they were pooled for statistical analysis.

DISCUSSION

It is concluded that microwave exposure causes differences in food intake during Days 7 to 35; F ratio values are 6.36 and 3.39 for male and female rats, respectively. Thus the effect is more significant statistically for male rats. Similarly, during Days 28 to 49, water intake by the exposed female rats differed significantly from that of control counterparts. During 35–49 days, water intake differed considerably for male rats. The F ratios were 7.11 for males and 63.65 for females. Thus, from Figs. 3–5, we see that microwave exposure lowers the food and water intake and also total food and water consumption in animals of both sexes. The food consumption, defined as grams of food required to produce a gram of body tissue gain, was not significantly influenced by the microwave exposure. However, a depressed growth rate was evident.

The total leukocyte count increased almost 35% in the exposed animals. Although a thermal effect at this lower level (0.6 mW/cm^2) is unlikely, there was an almost twofold increase in the number of eosinophils in irradiated animals. We observed no change in the number of lymphocytes. This suggests that the immunologic responses are likely to have been unchanged, which in turn suggests that the response to infections will remain unchanged for irradiated animals.

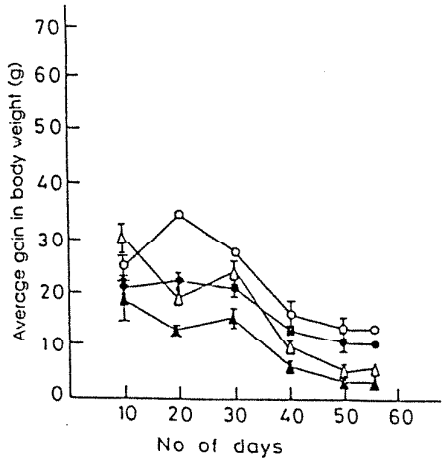

FIG. 5. Effect of exposure of growing albino rats to 7.5-GHz microwaves for 3 h daily on body weight. (○) Control males, (●) exposed males, (△) control females, (▲) exposed females.

TABLE II
Hematological Effects of 60 Days Exposure to Microwaves in Growing Rats

Parameters	Control animals	Experimental animals	
Hemoglobin (g/100 ml)	11.15 ± 0.81	11.35 ± 1.13	NS
Erythrocyte sedimentation rate (mm in first h)	2.28 ± 0.46	1.75 ± 0.45	NS
Total leukocyte count (per μl)	6906 ± 850	9191 ± 1600	S
RBC ($\times 10^6/\mu$l)	4.51 ± 0.99	4.60 ± 0.91	NS
Differential counting			
Neutrophils (%)	15.0 ± 4.0	13.25 ± 3.30	NS
Eosinophils (%)	1.50 ± 1.20	3.75 ± 1.60	S
Lymphocytes (%)	82.1 ± 4.5	81.1 ± 2.90	NS
Monocytes (%)	1.38 ± 0.50	1.9 ± 0.40	NS

Note. Total no. of animals used in the study is 18 for each group. NS, not significant; $P > 0.05$. S, significant; $P < 0.05$.

TABLE III
Normalized Organ Weights for Control and Experimental Animals Exposed to Microwaves

Organ	Organ weight for experimental animals	Organ weight for control animals	
Lungs	0.88 ± 0.17	0.93 ± 0.23	NS
Heart	0.48 ± 0.13	0.57 ± 0.22	NS
Spleen	0.29 ± 0.04	0.37 ± 0.07	S
Testis	1.29 ± 0.20	1.27 ± 0.23	NS
Kidney	0.80 ± 0.10	0.93 ± 0.06	S
Liver	3.77 ± 0.82	3.89 ± 0.39	NS
Skull	7.17 ± 1.08	7.69 ± 1.12	NS
Brain	0.88 ± 0.15	1.04 ± 0.24	S
Ovary	0.051 ± 0.004	0.064 ± 0.009	S

Note. Total no. of animals used in the study is 18 for each group. NS, not significant; $P > 0.05$. S, significant; $P < 0.05$.

However, the change in total leukocyte count may alter the compensatory and homeokinetic mechanisms of the body.

The observation of an increase in testicular weight in exposed males is important in view of the reported effects of microwaves, particularly in reproductive organs and the central nervous system (*9, 10*).

It is highly unlikely that, at the power level used in our experiments, the microwave energy would be converted into thermal energy and raise the body temperature of the treated animals significantly. However, a nonuniform pattern of microwave absorption may occur (*11*). The nonthermal effects of microwaves have been characterized mainly by electrophysiological studies (*12*). On the basis of our observations, we feel that the reduced growth may be caused by some stimulating mechanism of the induced temperature gradient, and we suggest that the localized effect of microwaves on animals needs further study.

Our results are in agreement with published observations of the effects of microwaves on animals (*5, 13, 14*). The outcome of our studies suggests that combined biochemical, physiological, and pathological studies offer the most promise for studies of the effects of microwaves and should provide a more complete data base upon which to judge the physiological responses and therefore exposure standards.

RECEIVED: October 24, 1986; ACCEPTED: February 8, 1990

REFERENCES

1. W. R. ADEY, Tissue interactions with non-ionizing electromagnetic fields. *Physiol. Rev.* 61, 435–514 (1981).
2. P. S. NAWROT, D. I. MCREE, and M. I. CALVIN, Teratogenic, chemical, and histological studies with mice prenatally exposed to 2.45 GHz microwave radiation. *Radiat. Res.* 102, 35–45 (1985).
3. J. D. DUMANSKI and M. G. SHANDALA, The biologic action and hygienic significance of electromagnetic fields of super high and ultra high frequencies in densely populated areas. In *Biologic Effects and Health Hazards of Microwave Radiation*. Polish Medical Publishers, Warsaw, 1974.
4. M. RUDNEV, A. BOKINA, N. EKSLER, and M. NAVAKATIRYAN, The use of evoked potential and behavioral measures in the assessment of environment insecret. In *Multidisciplinary Perspective in Evoked Brain Potential Research* (D. A. Otto, Ed.). Office of Research and Development, U.S. Environmental Protection Agency, Washington, DC, 1978.
5. S. BARANSKI, Effects of chronic microwave irradiation on the performing systems of guinea pigs and rabbits. *Aerospace Med.* 1196–1199 (1971).
6. S. T. LU, N. A. LEBDA, S. J. LU, S. PETTIT, and S. M. MICHAELSON, Effects of microwaves on three different strains of rats. *Radiat. Res.* 110, 173–191 (1987).
7. S. T. LU, S. PETTIT, S. J. LU, and S. M. MICHAELSON, Effects of microwaves on the adrenal cortex. *Radiat. Res.* 107, 234–249 (1986).
8. C. H. DURNEY, M. F. ISKANDER, H. MASSOUDI, and C. C. JOHNSON, An empirical formula for broad band SAR calculations of prolate spheroidal models of humans and animals. *IEEE MTT* 27, 75–78 (1979).
9. S. BARANSKI and P. CZERSKI, in *Biological Effects of Microwaves*, 234. Dowden, Hutchinson & Ross, Stroudsburg, PA, 1976.
10. WHO Report on Environmental Health Criteria No. 16, *Radiofrequency and Microwaves*. WHO, Geneva, 1981.
11. H. N. KRITIKOS and H. P. SCHWAN, Hot spots generated in conducting spheres by electromagnetic waves and biological implications. *IEEE Trans. Bio-Med. Eng. BME* 19, 53–58 (1972).
12. S. M. MICHAELSON, Microwave biological effects. An overview. *IEEE* 68, 40–49 (1980).
13. I. A. KITSOVSKAJA, The effect of centimeter wave of different intensities on the blood of haemopoietic organ of white rats. *Gig. Prof. Zabol* 18(14) (1964). [In Russian]
14. J. A. D'ANDREA, J. R. DEWITT, O. P. GANDHI, S. STENSAAS, L. LORD, and H. C. NIELSON, Behavioural and physiological effects of chronic 2450-MHz microwave irradiation of the rat at 0.5 mW/cm². *Bioelectromagnetics* 7, 45–46 (1986).

Teratogenicity

Green Chemicals

Bioelectromagnetics 18:455–461 (1997)

RF Radiation–Induced Changes in the Prenatal Development of Mice

Ioannis N. Magras[1]* and Thomas D. Xenos[2]

[1]Department of Anatomy, Histology, and Embryology, School of Veterinary Medicine, Aristotle University of Thessaloniki, Thessalonike, Greece
[2]Department of Telecommunications, School of Electrical Engineering and Computer Engineering, Aristotle University of Thessaloniki, Thessaloniki, Greece

The possible effects of radiofrequency (RF) radiation on prenatal development has been investigated in mice. This study consisted of RF level measurements and in vivo experiments at several places around an "antenna park." At these locations RF power densities between 168 nW/cm^2 and 1053 nW/cm^2 were measured. Twelve pairs of mice, divided in two groups, were placed in locations of different power densities and were repeatedly mated five times. One hundred eighteen newborns were collected. They were measured, weighed, and examined macro- and microscopically. A progressive decrease in the number of newborns per dam was observed, which ended in irreversible infertility. The prenatal development of the newborns, however, evaluated by the crown-rump length, the body weight, and the number of the lumbar, sacral, and coccygeal vertebrae, was improved. *Bioelectromagnetics 18:455–461, 1997.* © 1997 Wiley-Liss, Inc.

Key words: RF radiation effects; prenatal development; mice development

Five years ago the "antenna-park of Thessaloniki" progressively developed on the top of the nearby mountain Chortiatis, 1.5 km away from a small village of the same name. Today, almost 100 commercial TV and FM-radio broadcasting transmitters in the VHF and the UHF bands are situated there. The antennas are installed on towers well visible from a large part of the village. Living so close to the antennae and the vast amount of RF power they transmit, which is of the order of 300 kW, the people of the village Chortiatis, anxious for their health, encouraged the author to undertake a research program.

The hypothesis that RF radiation may adversely affect the health of the animal organism is still under consideration in public and scientific forums. One of the critical issues seems to be the RF effects on the reproductive process [Chernoff et al., 1992]. Numerous studies dealing with this subject ended up with seemingly contradictory results. Therefore, an "in vivo" study on experimental animals sensitive to RF radiation, was chosen. Based on the relevant literature, this research investigated RF radiation effects on the reproductive system, particularly on prenatal development. The mouse was selected as the experimental animal, because it is easily manipulated in the environment in which the experiments had to take place. Of course, experimenting at the mountain sites, far from the easily controlled laboratory conditions, might add a certain amount of uncertainty; therefore, these experiments should be considered preliminary.

MATERIALS AND METHODS

We used a total of 36 mice (18 females and 18 males), 2 months old and sexually mature (BALB/c/f breed colony). Breeding colony virgin males and females were obtained from the "Theageneion Anticancer Institute of Thessaloniki." The use of these experimental animals was approved by the Veterinary Service of the Municipality of Thessaloniki, according to the provisions of the laws 1197/81 and 2015/92 and the Presidential Decree 160/91 of the Greek Democracy. Upon arrival, all experimental animals were quarantined for 2 weeks to discover and to allow them to acclimatise the mountain environment, an altitude ranging between 570 (position h) and 730 m (position d) above sea level. All the mice were healthy at the end of this period and showed no signs of illness during

*Correspondence to: Ioannis N. Magras, Department of Anatomy, Histology, and Embryology, School of Veterinary Medicine, Aristotle University of Thessaloniki, 540-06 Thessaloniki, Greece.

Received for review 9 June 1996; revision received 30 January 1997

TABLE 1. Light–Dark Cycle during the Experimental Matings

Gestation	Date	Day		Night	
		Min	Max	Min	Max
1st	25.5–16.6	14.28	14.47	09.13	09.32
2nd	21.6–12.7	14.37	14.48	09.12	09.23
3rd	6.9–29.9	11.54	12.45	11.15	12.06
4th	7.10–28.10	10.45	11.35	12.25	13.15
5th	23.11–13.12	09.34	09.55	14.05	14.26

the course of the study. Tap water and certified feed (Greek Sugar Factory) were freely available.

The mice were maintained under natural lighting, both during the daytime and at the night (Table 1). Twelve Plexiglas cages transparent to RF radiation, were placed at several locations with one female in each cage. Each female was caged with one male for 12 h. Vaginal smears were taken the next morning and successful mating was identified by the presence of sperm. The day on which evidence of mating was observed was considered to be the first day of gestation. The litters were collected in the first 2 h after delivery and were moved to the laboratory for examination. After a period of recovery, the same mating procedure was repeated for each dam. Five experimental pregnancies were carried out in a period of almost 6 months.

The first pregnancy of the experimental animals took place in eight selected positions (a–h, Fig. 1), some close to the "antenna-park" and some near the village of Chortiatis. Then the experimental animals were moved to two positions, because these positions presented almost the same RF radiation levels with those initially selected and the experiment could be managed more effectively. Six dams (labelled as group A), initially placed at positions a, b, c, and d, with their males, were moved to the position d (Refuge of Hypaithrios Life). The other six dams (labelled group B), with their males, initially placed at positions e, f, g, and h were moved to position h (Public Primary School of Chortiatis). These two positions were selected because the most important living conditions, i.e., light, temperature, ventilation, food, etc., were the same.

Finally, all the experimental animals were moved to position i (Laboratory of Anatomy, School of Veterinary Medicine, University of Thessaloniki) about 10 km away from the Mountain Chortiatis, in the city of Thessaloniki, for the fifth pregnancy. This relocation was done to seek an indication of a possible reversibility of the observed phenomena. In fact, we wanted to repeat the experiment in an environment almost free of RF. An extra group of six couples of mice were mated once and used as controls in the laboratory (posi-

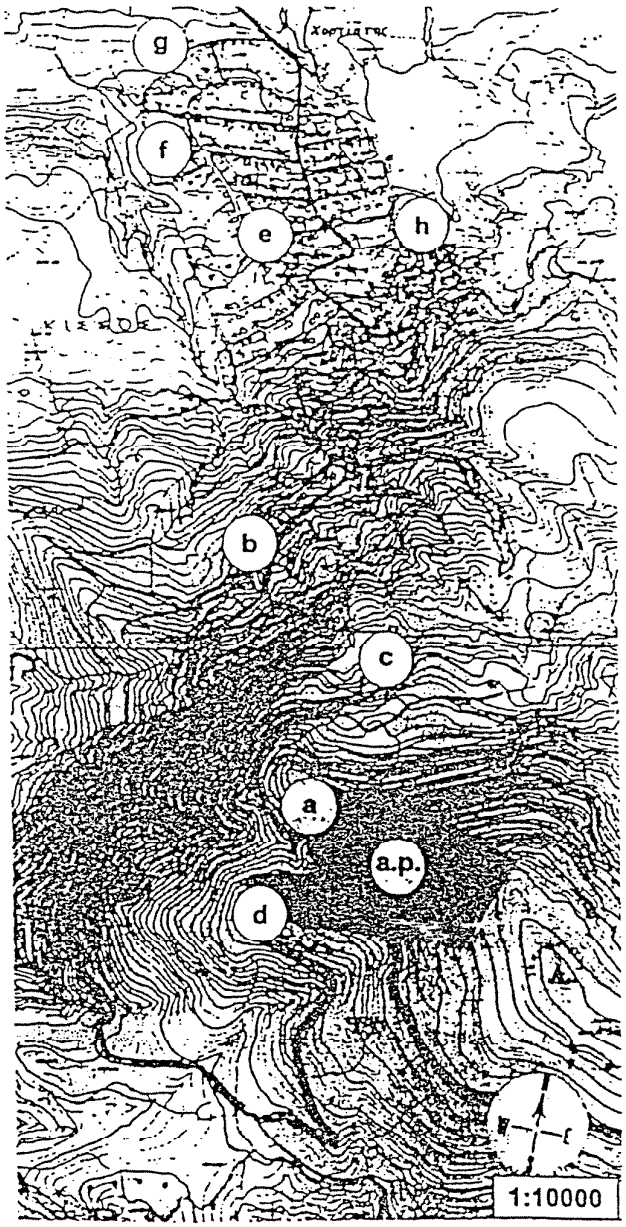

Fig. 1. Wide area of Chortiatis, where the fist four matings took place.

tion i), far from the "antenna park" in a more or less free-of-RF radiation environment.

It was extremely difficult to use RF-free controls at the mountain sites, because it was almost impossible to make "electromagnetically screened cages." Such a cage should ideally provide high (of the order of 30 dB) screening at the frequency range between 88.5 and 950 MHz (Commercial Radio FM band, UHF TV band, and Mobile Communication band), and therefore would require a very dense and well-grounded, highly conductive external metal grid. Obviously, mice could hardly survive in such cages for about 5 months.

The litter was considered to be the experimental unit for the analysis of data. We measured the crown-rump length, the body weight, the number of the posterior (lumbar, sacral, and coccygeal) vertebrae, the congenital malformations, and the ossification of the skeleton.

The RF power was measured in each position, using an electric field meter and a low gain (4 dB) wide-band (80–900 MHz) log-periodic antenna and spectrum analyser. To obtain comparable results the "IEEE std. C95.3.1991" was used. On the third floor of the public school, where the mice were situated, a 360 degree integration was also performed, due to the directivity of the measuring antenna together with the close proximity of the walls and metal furniture. Wherever iron bars or metal screens existed in front of the windows, two series of measurements were carried out: one on each side of the screen.

The collected newborns were killed for examination. Their crown-rump length was measured, and they were weighed and inspected under the dissecting microscope for external congenital malformations. Then they were fixed and subsequently cleared and stained in toto by a double staining of their skeleton [Peters, 1977]. The procedure was lightly modified as follows:

The newborns were fixed with alcohol 86% for 3 days; their skin, eyes, and viscera were removed; then they were immersed for 3 days in alcohol 100% and for 4 days in a mixture of alcohol 100% and ether 1:1. They were stained for 1–2 days with blue alcyan coloration [alcohol 86% 80 ml, acetic acid 20 ml, alcyan blue 20 mg] until the nonmineralised cartilagenous parts of the bones became blue. They were immersed in alcohol 100% for 4 days. Then they were stained for 12–24 days with red alizarin coloration [KOH 1 g, H_2O 100 ml, alizarin solution (alcohol 86% saturated with alizarin red S) 0.1 ml] until the ossified parts of the bones became red. They were immersed in solution Mall I (KOH 1 g, distilled water 80 ml, glycerine 20 ml) until the transparency of their body was completed. Finally, they were stored in a conservation solution (distilled water and glycerine 1:1, with some thymol crystals as contamination prevention). The stained newborns were inspected for skeletal defects as well as for the degree of ossification of their bones. The ossification of the skeleton and particularly of the vertebrae is an excellent and creditable indicator of the prenatal exposure to noxious agents and can be a measure of development delay.

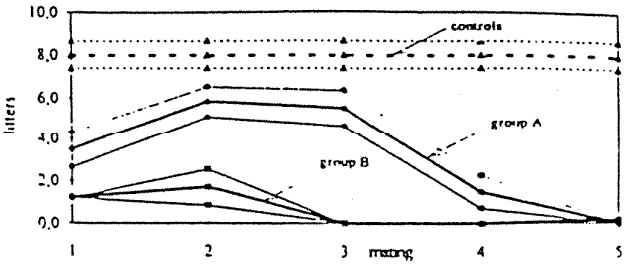

Fig. 2. Comparison of the mean values ± standard deviation of number of newborns per dam and mating from all experimental groups.

RESULTS

The RF power levels measured, although below the limits proposed by the "ENV50166-2" and the "IEEE C95.1.1991" standards, are high and well above the power levels that are likely to be measured in other European or U.S. residential areas. In fact, on the third floor of the public primary school (position h), an average power density of 1.053 $\mu W/cm^2$ was found, equivalent to a specific absorption rate of 1.935 mW/kg. In the Hypaithrios Life Refuge (position d) the average power density in which the mice were located was of the order of 168 nW/cm^2. This reduced level was due to the screening effect of the iron bars in front of the windows, which gave an 8–10 dB RF-power decrease. The average power density levels in position i (Laboratory of Anatomy, School of Veterinary Medicine, University of Thessaloniki), where the controls were placed and the fifth experimental matings were performed, was 40 dB weaker.

The number of the littered newborns by the experimental dams of groups A and B were, compared with those littered by the controls, progressively reduced from the first to the fifth pregnancy. This reduction is more evident in group B and is clearly shown in Table 2 and in Figure 2.

On the other hand, the rest of the four measured parameters, i.e., the crown rump length and the weight and the number of the lumbar, sacral, and coccygeal vertebrae increased in the newborns from groups A and B compared with the controls. This was more evident in group A than in group B (Table 2 and Fig. 3). A

TABLE 2. Statistical Characteristics of All Four Measurable Parameters per Dam, per Group, and per Gestation

Mating	Litters per dam mean ± s.d. median	Length (cm)	Weight (gr)	Vertebrae
Group A (6 dams)				
1st (25.05.1995)	3.5 ± 0.9	1.47 ± 0.13	2.71 ± 0.09	31.48 ± 1.43
	4.0	1.44	2.69	32.07
2nd (21.06.1995)	5.8 ± 0.7	1.25 ± 0.06	2.55 ± 0.05	24.28 ± 0.97
	7.0	1.22	2.50	24.29
3rd (08.09.1995)	5.5 ± 0.9	1.72 ± 0.25	2.71 ± 0.13	28.72 ± 1.92
	6.5	1.72	2.60	28.71
4th (07.10.1995)*	1.5	1.10	2.47	23.22
	0.0	1.10	2.47	23.22
5th (23.11.1995)*	0.0			
	0.0			
Mean value	3.3	1.39	2.61	26.93
Group B (6 dams)				
1st (25.05.1995)*	1.2	1.19	2.53	28.57
	0.0	1.19	2.53	28.57
2nd (21.06.1995)	1.7 ± 0.9	1.25 ± 0.04	2.60 ± 0.06	28.55 ± 1.14
	1.5	1.26	2.58	27.26
3rd (08.09.1995)*	0.0			
	0.0			
4th (07.10.1995)*	0.0			
	0.0			
5th (23.11.1995)	0.2	1.05	2.50	30.00
	0.0	1.05	2.50	30.00
Mean value	0.6	1.16	2.54	29.04
Controls (6 dams)				
1st (23.11.1995)	8.0 ± 0.07	0.96 ± 0.15	2.38 ± 0.02	19.59 ± 0.47
	7.5	0.97	2.37	19.52
Mean value	8.0	0.96	2.38	19.59

*Single or no gestation.

thorough external and internal examination under the dissecting microscope revealed only one case of extensive and two cases of limited malformation. No retardation of skeletal ossification worth mentioning was observed; only five cases out of 116 showed limited retardation. It has to be noted here, that the evaluation of the skeleton ossification was focused in the bones of the forelimbs and hindlimbs and in the lumbar, sacral, and coccygeal vertebrae.

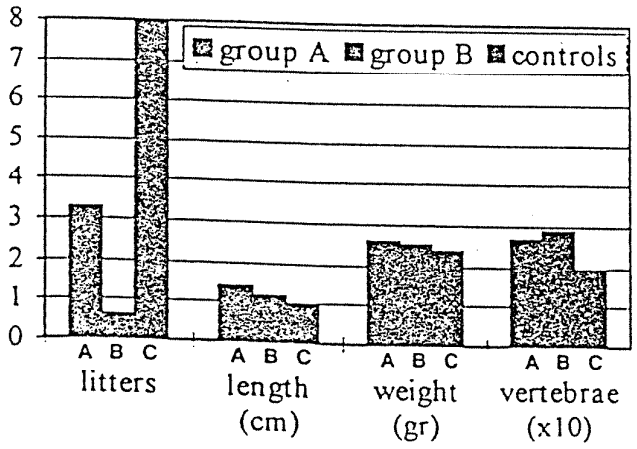

Fig. 3. Comparison of the mean values of all four measurable parameters for all gestations. Controls (C).

DISCUSSION

To study effects of a possibly noxious agent on a mammalian embryo, three groups should be considered: the embryos, the dams, and the males. In this work, all three have been studied: the infertility for dams and males, the lethality for embryos, the teratogenicity or the reduction in deformity for foetuses, or any combinations of them. They all have been considered by exposing male and female mice (before and during pregnancy) to an RF-radiation environment close to the "antenna park."

Infertility and lethality were assessed by counting the number of their newborns, whereas the possible

teratogenicity and the reduction deformity by autopsy was considered by the study of the embryonic skeletons. An important stage in this study was the examination of the skeletons, since the ossification of the bones is considered an excellent and creditable indicator of the prenatal exposure to noxious agents and can be a measure of development delay. In the beginning of organogenesis, the neural tube functions as a precursor of the cartilages and bones of the developing skeleton [Noden and Delahunta, 1985]. Teratogenic factors of any kind, that affect the embryonic nervous system, result in structural defects of the skeletal components. Therefore, to detect the teratogenic action of a factor on the embryonic nervous system, it is technically convenient to study the foetal skeleton rather than the embryonic nervous system itself.

A very important result of this experimental study (Table 2 and Fig. 2) is a progressive decrease of the number of the size of the litters of the dams of group A (position d) and group B (position h), compared with the controls (position i) and with the breeding history of these mice. Mice from the BALB/c/f breeding colony obtained from the "Theageneion Anticancer Institute of Thessaloniki" have been used for years in our laboratory for reproduction. Repeated pregnancies with a recovery period of 1–4 weeks for over a year, had never affected the fertility of the dams or any morphological parameters of the offspring, a fact that to our knowledge has not been questioned in the available literature.

It is worth noting that the RF power density levels, although very different from place to place, were very low and well below the CENELEC and IEEE relevant standards. Yet, it should be pointed out that:

(a) the experimental animals lived in this environment for 6 months, which is a long period of time.

(b) there was a considerable difference in power density levels of the order of 10 dB between the two main positions d and h and almost of 40 dB between d and i,

(c) there is a considerable difference between the volumes and consequently the body mass of the adult mouse and other experimental animals used as models in the international standards applied to humans.

The interpretation of our observations could follow various directions. The most popular view in numerous studies of the relevant literature, that this is a consequence of the overheating of the irradiated testis [Lary et al., 1986, 1987; O'Connor, 1980)] could be considered. On the other hand, the assumption that RF and microwave radiation effects are limited to heating has been questioned in a series of studies [Cleary, 1988, 1990]. The exposure conditions in these "in vivo" studies may suggest a thermal component of RF-induced testicular damage. However, interpretation of these data with respect to damage thresholds or interaction mechanisms is difficult. This difficulty is due to a number of factors, including the time, intensity, or both, the variations in species sensitivities, and the frequency-dependent non-uniform microwave energy absorption in tissue. Consequently, although these findings seem to be consistent with a hypothesis that the RF-induced heating is associated with testicular damages, the borderline between the "direct" effects of radiation and the effects that are indirectly associated with the tissue heating is not very clear.

Our observations could also be attributed to an intra-uterus death of the irradiated embryos in the early stages of the prenatal development, a speculation that could not be investigated in our experimental design because it required a postmortem autopsy of the dam. On the other hand, the prerequisite to these scenarios is a large RF power density, whereas the power densities we measured were of the order of $\mu W/cm^2$ or nW/cm^2, rather than mW/cm^2, or in terms of specific absorption rate (SAR), mW/kg rather than W/kg. Therefore, we cannot exclude the possibility of an indirect nonthermal mechanism focused on the endocrinological axon hypophysis-gonads that causes infertility to the males or the females [Thuery, 1991].

It should be noted here that the male experimental animals progressively developed a very bad physiological condition (rough hair, emaciation, etc.), not correlated to any other sickness symptoms, during their stay at the experimental positions a–g. Therefore, despite of the limited amount of data, the duration of the exposure to low intensity RF electromagnetic fields seems to be a repression parameter. In fact, chronic or long-term exposure to low intensity electromagnetic fields is generally associated with adverse results [Lary et al., 1983]. The most peculiar findings of this study were the increases in the crown-rump length, the body weight, and the number of the posterior vertebrae (lumbar, sacral, and coccygeal) of the experimental offsprings compared with the controls (Table 2, Fig. 3).

It must be noted that a study of mice [Jensh et al., 1977; 1978a; 1978b] under low levels of irradiation during the whole period of a single gestation (10 and 20 mW/cm^2) had no effect on maternal, foetal, or placental masses and no effect on the frequency of resorption, foetal death rate, size of litter, sex of the newly born, and their ability to perform. Other studies [Michaelson et al., 1976] reported a faster development of rat foetuses. This finding agrees with another report [Johnson et al., 1977] that noted an increase in the weight of newly born rats and a premature opening of the eyes after prenatal irradiation (5 mW/cm^2 at 918 MHz, for 380 h), as well as an impaired ability to learn. On the

other hand, other studies found lower average weight at birth. At medium power density levels (10, 20, and 50 mW/cm^2, at 2375 MHz), which are above the limits imposed by CENELEC and the relevant IEEE standard, the reproductive capacity of mice was somewhat impaired, with smaller litter size and a rise in neonatal mortality, which is a direct function of the power flux density [Il'Cevic and Gordodeckaja, 1976; McRee, 1980].

Although it is difficult to explain this foetal development increase, we believe that it could be due to a favourable placental nourishment of the foetuses during the pregnancy. In fact, this finding could be associated with:

(a) reproductive causes, i.e., blood-flow to a smaller number of foetuses, because of the reduction of the fertility of the irradiated males or females,

(b) thermal causes, i.e., possible increase of the blood flow of the dams, directly due to the RF irradiation,

(c) endocrinological causes, i.e., increase of the somatotrophic hormone because of the RF irradiation and

(d) environmental causes, i.e., the vasodilatation and partial increase of the blood pressure of the experimental dams because of the mountain altitude.

Of course combinations of these possibilities cannot be excluded.

According to various references [Tell and Harlen, 1979; Lu et al., 1980; Deschaux et al., 1983] discrepancies between the results of experiments may be due to different experimental conditions, random formation of hot spots in the glands and the hypothalamus, or a variety of other factors, as the cicardian rhythm and differences between species. With the exception of the high power effects on testicles, that do not belong to the endocrine ensemble, the interaction seems to involve the pituitary gland or even the central nervous system rather than the terminal glands.

We would close this discussion with what Jacques Thuery wrote (1991), that the true state of affairs is probably far more complex, but the available data are not sufficient to allow us to outline it more clearly, and that all attempts to extrapolate these results to humans lead to very high power densities, partly because geometric resonance effects are very significant in small animals. Consequently, taking into account the constant exposure of the human population living close to the "antenna park" to low intensity RF radiation, these adverse health effects in mice resulting from chronic or prolonged exposure may prove of importance in the near future. Indeed, there is evidence that chronic exposure to low-intensity RF radiation may be associated with health effects different to embryo-toxicity [Salford et al., 1992; Cleary, in press].

The findings of this preliminary experimental study have led to several conclusions. Of course, the final word to the problem in question has not been said as yet. Therefore, more work is called for; laboratory-based simulation might provide valuable information.

ACKNOWLEDGMENTS

The authors thank I. Grivas, G. Marangos, and V. Oiconomou, students of the Faculty of Veterinary Medicine of Thessaloniki, and Mr. I. Milarakis of the Department of Telecommunications of the School of Electrical Engineering and Computer Engineering, who followed this experimental study and offered their technical assistance.

REFERENCES

CENELEC ENV50166-2: Human exposure to electromagnetic fields. High frequency (10 kHz to 300 GHz).

Chemoff N, Roger JM, Kavet R (1992): A review of the literature on potential reproductive and developmental toxicity of electric and magnetic fields. Toxicology, 74:91–126.

Cleary SF (1988): Biological effects of non-ionising radiation. In Webster E (ed): "Encyclopaedia of Medical Devices and Technology," Vol. 1; New York: John Wiley & Sons, pp 274–303.

Cleary SF (1990): Biological effects of radio-frequency electromagnetic fields. In Gandhi OP (ed): "Biological Effects and Medical Applications of Electromagnetic Energy." Englewood Cliffs, NJ: Prentice Hall, pp 236–255.

Cleary SF (in press): Electromagnetic energy: Biological effects and possible health significance. In Craighead J (ed): "The Pathology of Human Environmental and Occupational Disease." Boston: Mosby YearBook.

Deschaux P, Jimenez C, Santini R, Pellissier J (1983): Effet d' un rayonnement micro-onde sur la reproduction de la souris male. Econ, progrs electr., No 8-9, Mars-Juin, 15–17.

IEEE std. C95.3.1991: "IEEE recommended practice for the measurement of potentially hazardous electromagnetic fields-RF and microwaves."

IEEE C95.1.1991: "IEEE standard for safety levels with respect to human exposure to RF electromagnetic fields, 3 KHz to 3 GHz."

Il'Cevic N, and Gordodeckaja S (1976): Effects of the chronic application of the electromagnetic microwave fields on the function and morphology of the reproductive organs of animals. US joint Pub Res Serv Rep, JPRS, L/5615, Feb. 5–7.

Jensh R, Ludlow J, Weinberg I, Vogel W, Rudder T, Brent R (1977): Teratogenic effects on rat offspring of non-thermal chronic prenatal microwave irradiation. Teratology 15/2, 14 A.

Jensh R, Ludlow J, Weinberg I, Vogel W, Rudder T, Brent R (1978a): Studies concerning the postnatal effects of protracted low dose prenatal 915 MHz microwave radiation. Teratology 17/2, 21 A.

Jensh R, Ludlow J, Weinberg I, Vogel W, Rudder T, Brent R (1978b): Studies concerning the effects of protracted prenatal exposure to a non-thermal level of 2450 MHz microwave radiation in the pregnant rat. Teratology 17/2, 48 A.

Johnson R, Mizumari S, Myers D, Guy A, Lovely R (1977): Effects of pre- and post-natal exposures to 918 MHz microwave radiation

on development and behaviour in rats. In International Symposium of biological effects of electromagnetic waves. Airlie.

Lary JM, Conover DL, Johnson PH, Burg JAR (1983): Teratogenicity of 27.12 MHz radiation in rats is related to duration of hyperthermic exposure. Bioelectromagnetics 4:249–255.

Lary JM, Conover DL, Johnson PH, Hornung RW (1986): Dose-response relationship between body temperature and birth defects in radio-frequency-irradiated rats. Bioelectromagnetics 7:141–149.

Lary JM, Conover DL (1987): Teratogenic effects of radio-frequency radiation. IEEE Engineering in Medicine and Biology Magazine, March.

Lu S, Lotz G, Michaelson S (1980): Advances in microwave induced neuroendocrine effects: the concept of stress. Proc. IEEE. 68. No 1:73–77.

McRee D (1980): Soviet and Eastern European research on biological effects on microwave radiation. Proc IEEE 68/1:84–91.

Michaelson S, Guillet R, Catallo M, Small J, Inamine G, Heggeness F (1976): Influence of 2450 MHz microwaves on rats exposed in utero. Proceedings of the IMPI Symposium 5A/3, Leuven.

Noden MD, Delahunta A (1985): The embryology of domestic animals. Baltimore: Williams & Wilkins.

O'Connor ME (1980): Mammalian teratogenesis and radio-frequency fields. Proc IEEE 68:56–61.

Peters PWJ (1977): Double staining of foetal skeletons for cartilage and bone. In Neubert D, Merker HJ, Kwasogroch TE (eds): "Methods in Prenatal Toxicology." Stuttgart: George Thieme.

Salford LG, Brun A, Eberhardt JL, Persson RR (1992): Development of rat brain tumours during exposure to continuous and pulsed 915 MHz electromagnetic radiation (meeting abstract). First World Congress for Electricity and Magnetism in Biology and Medicine, June, Lake Buena Vista, FL, 27–28.

Tell R, Harken F (1979): A review of selected biological effects and dosimetric data useful for development of radio-frequency safety standards for human exposure. J Microw Power 14, No 4:405–424.

Thuery J (1991): Microwaves: Industrial, Scientific, and Medical Applications. Grant EH (ed): London: Artech House Inc.

Salmon Divide

Bioelectromagnetics 13:379–393 (1992)

Increased Sensitivity of the Non-Human Primate Eye to Microwave Radiation Following Ophthalmic Drug Pretreatment

Henry A. Kues, John C. Monahan, Salvatore A. D'Anna, D. Scott McLeod, Gerard A. Lutty, and Samuel Koslov

The Johns Hopkins University Applied Physics Laboratory, Laurel (H.A.K., D.S.M., S.K.); Food and Drug Administration, Center for Devices and Radiological Health, Rockville, (J.C.M.); and Wilmer Ophthalmological Institute, The Johns Hopkins University School of Medicine, Baltimore, Maryland (S.A.D., G.A.L.)

Previous studies in our laboratory have established that pulsed microwaves at 2.45 GHz and 10 mW/cm² are associated with production of corneal endothelial lesions and with disruption of the blood-aqueous barrier in the non-human primate eye. In the study reported here we examined ocular damage in monkeys (*M. mulatta* and *M. fascicularis*) following topical treatment with one of two ophthalmic drugs (timolol maleate and pilocarpine) that preceded exposure to pulsed microwaves. Anesthetized monkeys were sham exposed or exposed to pulsed, 2.45 GHz microwaves (10 μs, 100 pps) at average power densities of 0.2, 1, 5, 10, or 15 mW/cm² 4 h a day for 3 consecutive days (respective SARs were 0.052, 0.26, 1.3, 2.6, and 3.9 W/kg). Immediately before microwave exposure, one or both eyes were treated topically with one drop of 0.5% timolol maleate or of 2% pilocarpine. Following administration of a drug, we observed a significant reduction in the power-density threshold (from 10 to 1 mW/cm²) for induction of corneal endothelial lesions and for increased vascular permeability of the iris. Diagnostic procedures (in vivo specular microscopy and fluorescein iris angiography) were performed following each exposure protocol. In addition, increased vascular permeability was confirmed with horseradish peroxidase tracer techniques. Although we did not measure intraocular temperatures in experimental animals, the results suggest that a mechanism other than significant heating of the eye is involved. Our data indicate that pulsed microwaves at an average SAR of 0.26 W/kg, if administered after pretreatment with ophthalmic drugs, can produce significant ocular effects in the anesthetized primate. ©1992 Wiley-Liss, Inc.

Key words: microwaves, glaucoma drugs, primates, corneal endothelium, iris

Received for review August 22, 1991; revision received February 21, 1992.

Address reprint requests to Henry A. Kues, JHU/APL, Johns Hopkins Road, Laurel, MD 20723.

INTRODUCTION

Approximately 35 years ago, serious concern arose regarding possible adverse health effects to humans exposed to microwave radiation from a variety of industrial and consumer applications including radar, communication equipment, and microwave ovens. Initially, most of the concern was focused on effects related to tissue heating, and extensive research efforts concentrated on the eye; an acceptable study organ because of its limited ability to dissipate heat [Elder, 1983; National Council on Radiation Protection and Measurements, 1986; Cleary, 1980; Lipman et al., 1988]. Of particular interest were high-level microwave exposures capable of producing thermal effects such as the induction of cataracts in the crystalline lens. Following microwave exposure, slit-lamp examination and histological evaluation of the lens were employed to assess the type and degree of changes. On the basis of these studies it was concluded that 1) cataract induction requires microwave exposure levels greater than 100 mW/cm^2, 2) temperatures in excess of 41 °C in the lens are necessary for cataract induction, 3) both continuous wave (CW) and pulsed microwaves have comparable thresholds for cataract induction, and 4) cataract induction is frequency dependent [Elder, 1983].

Studies in rabbits have revealed microwave-induced ocular effects other than cataract formation. Kinoshita et al. [1966] showed that the level of ascorbic acid in the rabbit lens is decreased after whole-body microwave exposure. Weiter et al. [1975] confirmed this in cultured rabbit lenses under strictly controlled exposures. Rosenthal et al. [1977], using slit-lamp biomicroscopy and electron microscopy, examined the effects of acute exposure to radiation (35 and 107 GHz) in rabbits. Both corneal epithelial and corneal stromal damage was observed following exposure, demonstrating that these effects occur at lower power levels than those required to produce lenticular damage.

Several microwave-ocular studies have been conducted on non-human primates. Kramar et al. [1978] exposed rabbits and monkeys to high-level 2.45 GHz microwaves, noting distinct differences in the effects observed in rabbits and monkeys. Earlier lenticular findings were confirmed in the rabbit, but cataract induction was not observed in the monkey, even at exposure levels that caused facial burns, lid edema, and changes in the anterior chamber. Kues et al. [1985], using rhesus and cynomolgus monkeys to examine effects of microwave radiation on the corneal endothelium, found that both pulsed and CW, 2.45 GHz microwaves produced endothelial lesions, 16 to 24 h post exposure. The lesions were comparable to corneal pseudoguttata [Krachmer et al., 1981], i.e., when viewed by specular reflection they had the appearance of dark spots interspersed in the regular endothelial mosaic, but they persisted for a few days only. Moreover, a distinct difference in threshold value for the two modalities was observed, with an approximate threefold increase in power (30 mW/cm^2) required for CW microwave exposure to induce lesions. A subsequent study [Kues and D'Anna, 1987] revealed that, in addition to corneal endothelial damage, an increase in the permeability of the iris vasculature occurred with pulsed radiation at levels (10 mW/cm^2) comparable to those used in the 1985 corneal study. It is important to note that this exposure level is 1/10th that reported to induce cataracts, and results in an ocular temperature increase that is less than 1 °C during a 4-h exposure.

The present study was undertaken to examine effects of combined treatment with microwaves and each of two drugs used clinically for the treatment of glaucoma.

Timolol maleate was selected because it has been shown to protect the eye against heat-induced disruption of the blood-aqueous barrier [Holmdahl and Bengtsson, 1981]. We chose to test timolol's potential as a protective measure against microwave-induced vascular leakage, assuming the possibility of a thermal mechanism. Pilocarpine was evaluated because of its ability to increase the permeability of the iris vasculature to fluorescein [Stocker, 1947], thus measuring pilocarpine's ability to potentiate this leakage.

MATERIALS AND METHODS

Adult rhesus and cynomolgus monkeys (*Macaca mulatta, Macaca fascicularis*), 4 to 18 years of age and ranging in body mass from 4 to 7 kg, were employed in this study. Tap water was available ad libitum and food (Purina Monkey Chow) was provided once a day.

Two similar microwave exposure systems were employed for ocular irradiation. Both the exposure systems and associated dosimetric procedures have been described previously [Kues et al., 1985].

Ocular specific absorption rates (SARs) were determined by in vivo temperature measurements during microwave exposure of three monkeys used for these determinations only. A nonperturbing fluoroptic (Luxtron 1000B System) thermal probe was surgically implanted in the anterior chamber with the probe tip abutting the corneal endothelial surface. A 4-h exposure at 20 mW/cm^2 yielded a temperature increase of 0.77 °C in the anterior chamber, resulting in a calculated SAR of 0.26 W/kg per mW/cm^2 of incident power [Kues et al., 1985]. This value indicates that even at an exposure of 20 mW/cm^2, a microwave-induced temperature elevation in the eye is less than that normally associated with thermal damage and is within the normal physiological range.

During each session of exposure or sham-exposure, each monkey was immobilized by an intramuscular injection of ketamine HCl (0.3 to 0.4 ml of 100 mg/ml). They were then intubated and maintained with halothane gas anesthesia for the 4-hour session and subsequent diagnostic procedures. Details of the tube routing for anesthesia and the positioning of the monkey within the anechoic chamber during exposure have been described previously [Kues et al., 1985]. During each exposure session the monkey's eyelids were held closed with surgical tape to prevent corneal drying.

The protocol for the present study consisted of ocular exposure of each monkey to pulsed, 2.45 GHz microwaves (10 μs, 100 pps) for 4 h a day for 3 consecutive days at a specific power density. Power densities of incident radiation as measured at the position of the eyes ranged from 0 to 15 mW/cm^2. To normalize any animal-to-animal variability in biological susceptibility each monkey was exposed in a random pattern at a range of power densities throughout the course of the study. In drug-treated eyes, ophthalmic solutions (1 drop of 0.5% timolol or 2.0% pilocarpine) were administered topically immediately before exposure. Intraocular pressures (IOPs) were measured in several monkeys with an Alcon surface-contact pneumatic tonometer. These measurements were obtained immediately before the instillation of timolol, and again 4 h after drug treatment and microwave exposure (10 mW/cm^2) or drug treatment alone. The time between groups of three exposure sessions was, at a minimum, 2 weeks. Prior to initiation of each expo-

sure protocol, routine diagnostic procedures (wide-field, corneal specular microscopy, fluorescein iris angiography, and slit-lamp examination) were performed to document the absence of preexisting or residual (from previous microwave exposures) corneal and iris abnormalities.

Immediately following the third exposure session, fluorescein iris angiography was performed to ascertain the integrity of the iris vasculature. Sodium fluorescein (0.4 ml of 25%) was injected into a saphenous vein, and the subsequent transit of the dye through the vessels of the iris was visualized and photographed by a modified Zeiss fundus camera [D'Anna et al., 1983]. The vascular integrity of the iris was independently evaluated by two researchers during a 15-min observation period following injection of the sodium fluorescein dye. The angiograms were obtained during this period for subsequent analysis and confirmation of assigned scores.

A score of 1 was assigned to an eye exhibiting no leakage of sodium fluorescein into tissue during a 15-min observation period. The appearance of a small amount of sodium fluorescein in tissue and the anterior chamber during a 15-min observation period represented minor leakage and was assigned a score of 2. A score of 3, or moderate leakage, was assigned to an eye exhibiting partial filling of the anterior chamber with sodium fluorescein more than 5 min after injection. Leakage was considered major and assigned a score of 4 if, within the first 3 min following injection, a significant amount of fluorescein exuded into the anterior chamber, causing the entire anterior chamber to fluoresce, completely obscuring visualization of the iris vessels.

Twenty-four hours after the last exposure session, the monkeys were anesthetized and corneal endothelial examinations performed with a Keeler-Konan (Model SP-1) wide-field specular microscope. During examination, an eyelid speculum was inserted and the cornea kept moistened with balanced salt solution. A central corneal field, 6 mm in diameter, was examined and photographed. Each photograph represents a microscopic field of the endothelial surface, approximately 2 mm^2. The degree of endothelial damage was evaluated from the photograph that demonstrated the highest number of visible lesions. These lesions had the appearance of pocks in the monolayer, resembling pseudoguttata. Two observers evaluated each photograph and assigned a score based on the total number of lesions.

A score of 1 was assigned to a healthy endothelium with less than three visible lesions (pseudoguttata). A score of 2 represented three to ten lesions, and a score of 3 represented 11 to 50 lesions. A score of 4 was assigned when counts exceeded 50 lesions. In scoring both corneal endothelial changes and iris vascular integrity, an intermediate value (i.e., 1.5, 2.5, or 3.5) was assigned if the observers disagreed on the score or if the evaluation of both observers clearly did not fit into a predefined category. Scores obtained for both the endothelial and vascular evaluations following the different drug treatments were analyzed statistically by a general linear model for analysis of variance (ANOVA) [SAS, 1988].

In addition to the diagnostic procedures described above, several monkeys were studied histologically to evaluate vascular permeability of the iris to horseradish peroxidase (HRP, a glycoprotein 100 times larger than sodium fluorescein) following microwave exposure, with or without timolol pretreatment. Following the final exposure and diagnostic procedures, 500 mg of HRP (Type II, Sigma Chemical Co., St. Louis, MO) per kg of body mass was administered intravenously and allowed to circulate for 15 min. The monkey was then euthanatized by an intravenous overdose

of sodium pentobarbital. The eyes were enucleated and fixed in quarter-strength Karnovsky's glutaraldehyde-paraformaldehyde fixative for 4 h at room temperature. The eyes were washed in three changes of 0.1 M sodium cacodylate, pH 7.4 (30 min/wash), overnight at 4 °C. The tissue was dehydrated, infiltrated, and embedded in JB-4 (Polyscience). HRP was detected in 2 μm iris sections by development with either diaminobenzidine (DAB) or tetramethyl benzidine (TMB) and counterstaining. Under light microscopy, sections were examined and evaluated for vascular integrity based on the relative amount of extravascular HRP.

RESULTS

A summary of the results of the diagnostic examination following exposure to various power densities of microwave radiation and drug pretreatment is presented in Tables 1 and 2. The iris vasculature and corneal endothelium appeared normal in monkeys exposed to microwaves at less than 10 mW/cm² (Tables 1 and 2), without drug pretreatment. Sham exposure (0 mW/cm²) for 3 days, without drug pretreatment, produced no increase in iris vasculature permeability to fluorescein (Fig. 1A) and no observable change in the corneal endothelium (Fig. 1B). Similar results were also observed in monkeys that received either timolol or pilocarpine pretreatment and were sham-exposed.

Table 1. Effects on Iris Vascular Permeability†

Power density (mW/cm²)	SAR (W/kg)	Mean ± S.E.M (N)*		
		No drug	0.5% Timolol	2.0% Pilocarpine
0	0	1.0 ± 0.00 (2)	1.0 ± 0.00 (9)	1.0 ± 0.00 (2)
5	1.3	1.0 ± 0.01 (8)	2.7 ± 0.31 (5)*	2.4 ± 0.55 (4)
10	2.6	2.1 ± 0.28 (6)*	2.7 ± 0.44 (3)*	2.8 ± 0.51 (5)**
15	3.9	2.8 ± 0.26 (6)*	3.5 ± 0.50 (2)*	4.0 ± 0.00 (2)**

†Mean values shown represent the relative vascular permeability of the iris to Na^{++} fluorescein dye based on a 15-min observation period immediately following injection. A value of 1 equals no visually observable leakage, and 4 equals major leakage (refer to Materials and Methods section for complete description of scoring system used).
*The number of eyes examined.
*$P < .001$.
**$P < .01$.

Table 2. Corneal Endothelial Changes†

Power density (mW/cm²)	SAR (W/kg)	Mean ± S.E.M (N)*		
		No drug	0.5% Timolol	2.0% Pilocarpine
0	0	1.0 ± 0.00 (3)	1.0 ± 0.00 (9)	1.0 ± 0.00 (4)
5	1.3	1.2 ± 0.13 (8)	2.8 ± 0.33 (4)*	2.9 ± 0.66 (4)*
10	2.6	1.9 ± 0.31 (8)*	4.0 ± 0.00 (3)*	3.2 ± 0.31 (6)*
15	3.9	2.8 ± 0.15 (6)*	4.0 ± 0.00 (2)*	3.0 ± 0.00 (2)*

†Mean values shown represent the numerical score assigned to denote a categorical number of lesions (pseudoguttata) per area of corneal endothelium. A value of 1 equals a normal endothelium with < three lesions per 2 mm² and a value of 4 equals > fifty lesions (refer to Materials and Methods section for a complete description of the scoring system used).
*The number of eyes examined.
*$P < .001$.

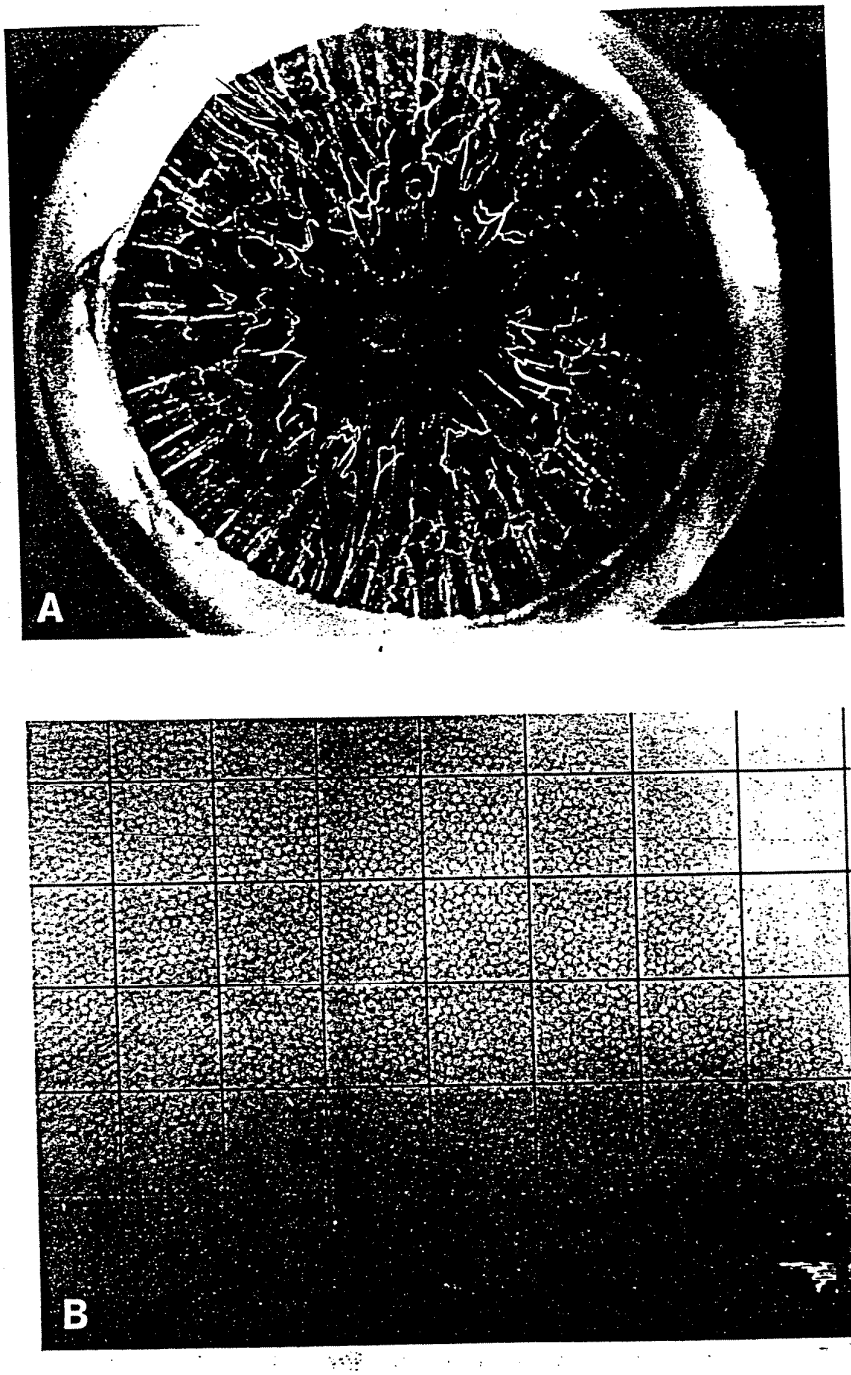

Fig. 1. A: Normal fluorescein angiogram of the iris (3 min post-injection); sham-exposed monkey. B: Wide-field specular micrograph of corneal endothelium; sham-exposed monkey.

Pulsed microwaves (2.45 GHz) at an average power density of 10 mW/cm² (SAR 2.6 W/kg) produced minor leakage of fluorescein (Fig. 2A) into the anterior chamber of the eye (a score of 2). Corneal endothelial lesions (Fig. 2B) were also observed. Peripheral areas of the cornea, as shown in this figure, also displayed posterior corneal rings or naturally occurring endothelial folds [Hirst, et al., 1983]. At a higher exposure level (15 mW/cm²) iris vascular leakage and the number of endothelial lesions also increased.

Exposure at average power densities of 5, 10, and 15 mW/cm² with timolol pretreatment increased the amount of fluorescein leakage from the iris vasculature (Fig. 3A) and increased the number of endothelial lesions (Fig. 3B) as compared with effects observed under a "microwave-only" exposure at these power densities. Monkeys pretreated topically with one drop of pilocarpine and exposed at these power densities also demonstrated an increase in fluorescein leakage and a concomitant increase in the number of endothelial lesions as compared with "microwave-only" exposed subjects. At an exposure level of 10 mW/cm², pretreatment with either timolol or pilocarpine increased effects, scoring from minor to moderate, as seen in Tables 1 and 2. When the power levels were decreased to 5 mW/cm² (a subthreshold "microwave-only" dose) moderate changes were observed following drug pretreatment and microwave exposure.

Timolol pretreatment combined with microwave exposure at 15 mW/cm² resulted in major changes as compared with microwave-only exposed monkeys in the degree of vascular leakage and number of corneal endothelial lesions (Fig. 4A, B). In two of the timolol-treated monkeys, IOP was measured before and after microwave exposure. The reduction of IOP, from 18 mm to 10 mm/Hg following administration of timolol, was similar in both the microwave-exposed and sham-exposed subjects. Because of the degree and consistency of ocular effects produced, few monkeys were exposed at the higher power level (15 mW/cm²) with drug pretreatment.

Our intent in this study was to alter microwave-induced ocular effects by administration of two ophthalmic drugs for which specific effects were anticipated. However, when timolol acted synergistically with microwaves the scope of this research was expanded in an attempt to determine a microwave threshold value following drug pretreatment. Several monkeys were therefore pretreated with timolol and exposed at power densities of 0.2 or 1 mW/cm². The results are summarized in Table 3. In monkeys that were sham-exposed or exposed at 0.2 mW/cm² following timolol pretreatment, iris angiography, and corneal specular microscopy failed to reveal any difference in the eyes as compared with normal, non-exposed eyes. When the exposure level was increased to 1 mW/cm² and the monkeys were pretreated with timolol, a moderate degree of iris vascular leakage (Fig. 5A) was observed. A moderate number of corneal endothelial lesions (11 to 50 lesions/field; Fig. 5B) were also observed under these exposure conditions. The data therefore indicate that with timolol pretreatment, a microwave-ocular damage threshold lies between 0.2 and 1 mW/cm² (SAR of 0.05 to 0.26 W/kg). To date, similar experimentation with pilocarpine pretreatment prior to microwave exposure has not been evaluated. The study of monkeys exposed to pulsed microwaves alone indicates the threshold of the ocular effect to be about 10 mW/cm² (SAR 2.6 W/kg).

The data presented in this study are composed of observations following initial exposure of the monkeys, as well as the results of subsequent exposures. We rec-

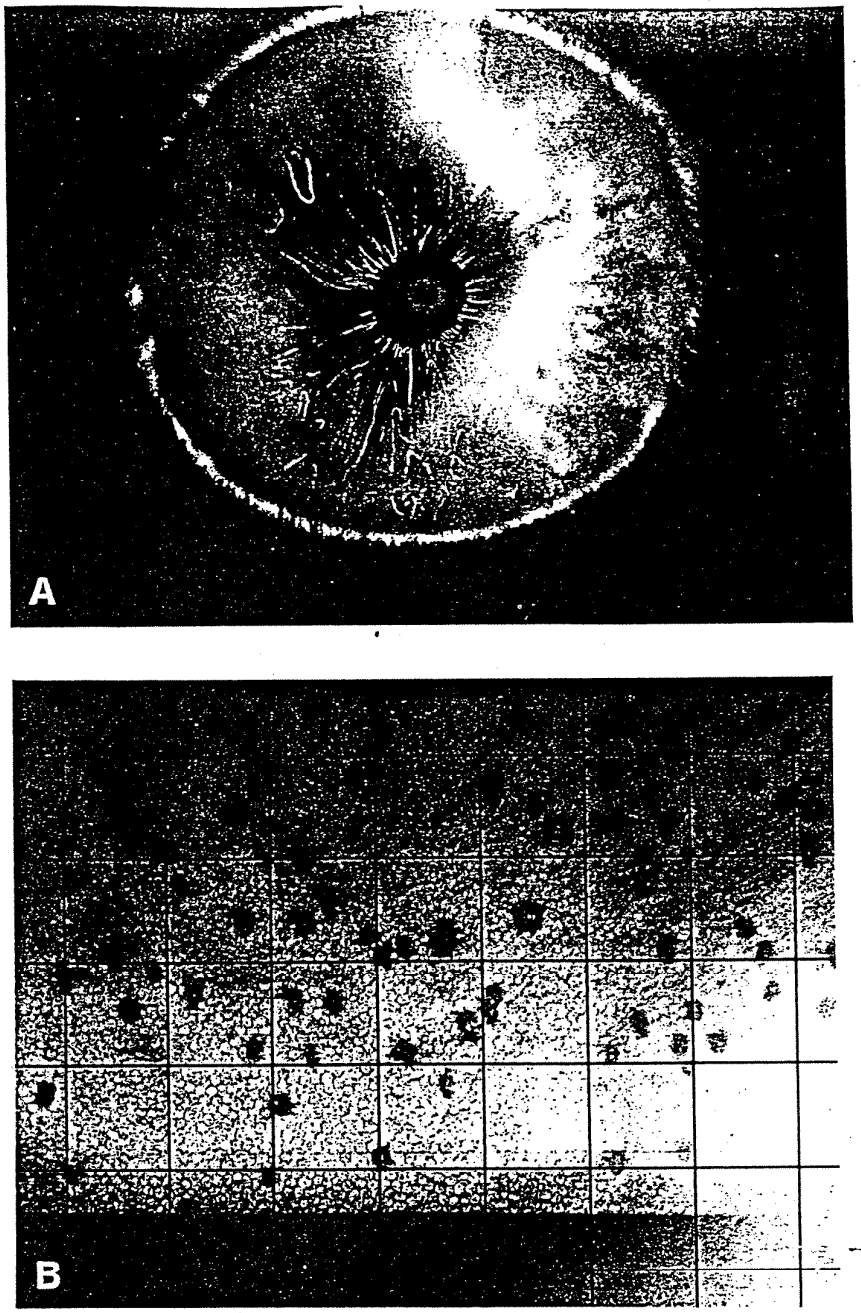

Fig. 3. **A:** Fluorescein angiogram of the iris (5 min post-injection), demonstrating a moderate increase in vascular permeability; monkey pretreated with timolol and exposed at 10 mW/cm². **B:** Wide-field specular micrograph of corneal endothelium demonstrating a major number of lesions; monkey pretreated with timolol and exposed at 10 mW/cm².

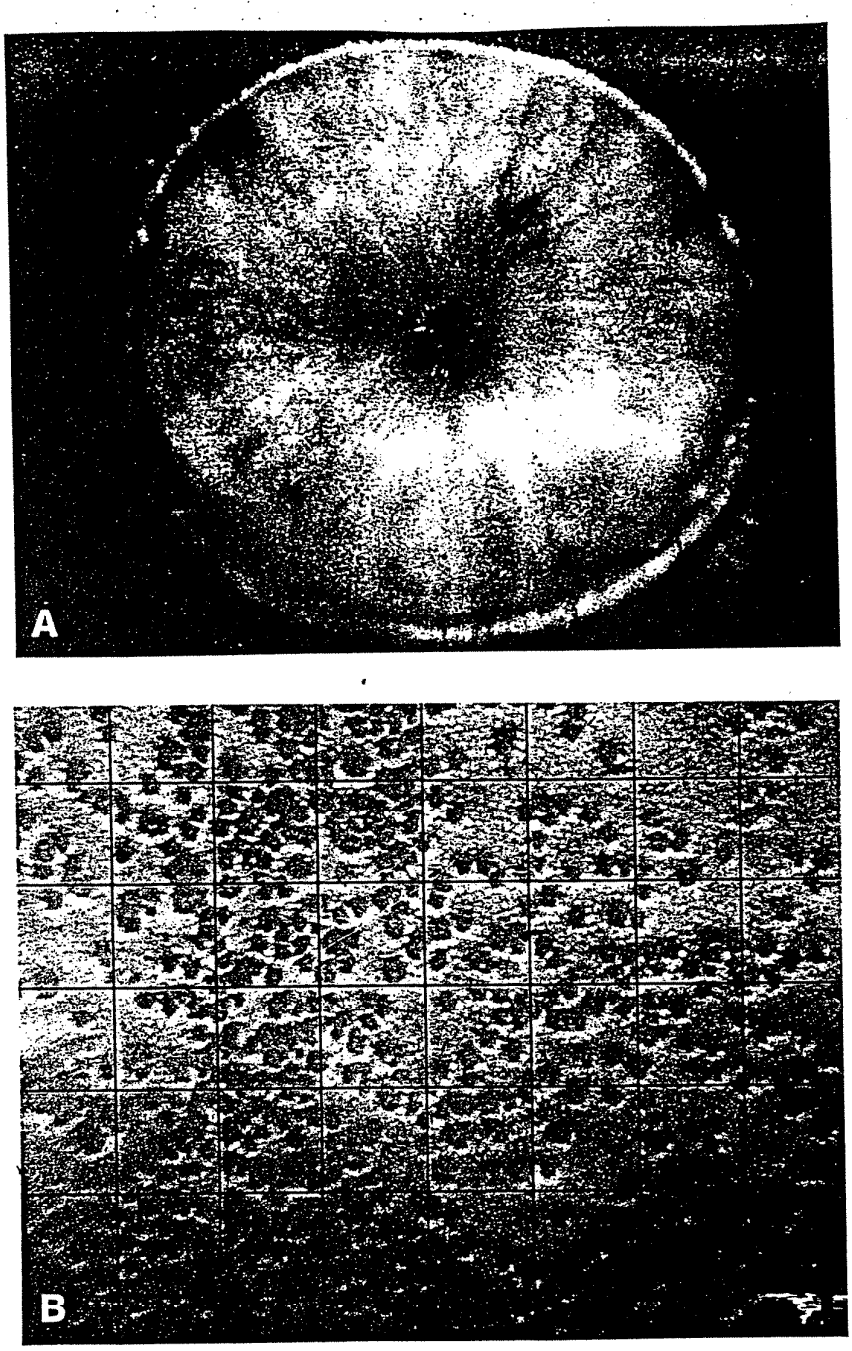

Fig. 4. A: Fluorescein angiogram of the iris (4 min post-injection) demonstrating a major increase in vascular permeability; monkey pretreated with timolol and exposed at 15 mW/cm². B: Wide-field specular micrograph of corneal endothelium demonstrating a major number of lesions; monkey pretreated with timolol and exposed at 15 mW/cm².

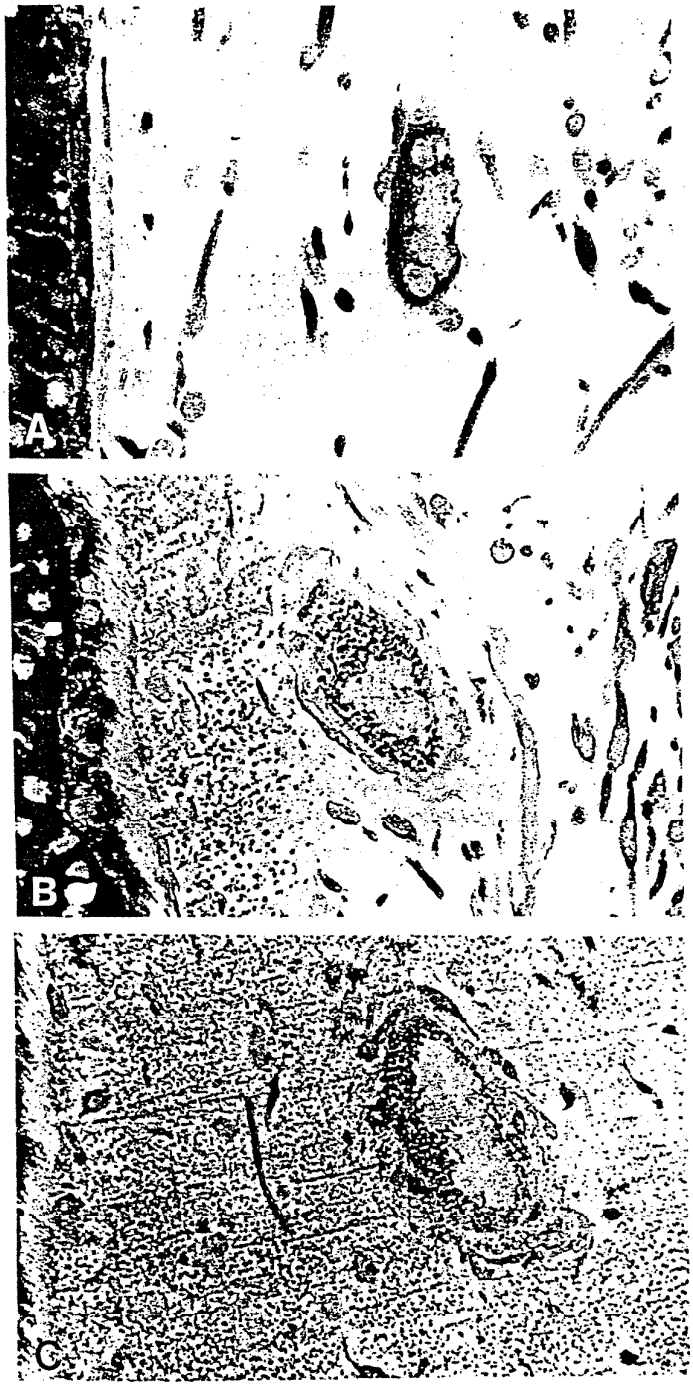

Fig. 6. **A:** Iris section demonstrating no extravascular HRP reaction product; from a non-drug-treated and sham-exposed monkey. **B:** Iris section demonstrating extravascular HRP reaction product; from a non-drug-treated monkey exposed at 10 mW/cm². **C:** Iris section demonstrating extensive extravascular HRP reaction product; monkey pretreated with timolol and exposed at 10 mW/cm².

at 0.2 mW/cm^2. Exposure of the eye at 1 mW/cm^2 resulted in an average SAR of 0.26 W/kg within the anterior chamber of the eye near the corneal endothelial surface.

The original hypothesis for this investigation was based on the reported ability of two specific ophthalmic drugs to alter vascular permeability in opposite directions. Holmdahl and Bengtsson [1981] demonstrated that timolol provides protection against thermal breakdown of the blood-aqueous barrier. This study led us to postulate that if the increased permeability of the blood-aqueous barrier was due to the thermal aspects of microwave exposure, timolol should reduce this permeability. Rather than decreasing the microwave-induced vascular permeability, timolol increased the permeability in a manner comparable to that observed with pilocarpine pretreatment. This finding suggests that a mechanism other than significant heating of the ocular tissue is involved in the observed results.

Both timolol and pilocarpine have a commonality that may explain why both drugs reduced the microwave threshold for ocular changes. It has been reported [Abrahamsson et al., 1988; Melikian et al., 1971] that both timolol and pilocarpine bind to ocular melanin. Microwave exposure of B-16 melanoma (melanin-containing) cells has been shown to affect change in membrane ordering, as measured by electron paramagnetic resonance-reporter techniques. This alteration is unique to the melanin containing, B-16 cells and due, at least in part, to the generation of oxygen radicals. No change in fluidity was observed in amelanotic B-16 cells [Phelan et al., 1992]. Another recent study [Kiel et al., 1990] has shown that microwave exposure of a melanin complex can also result in the release of free radicals. In a pilot, in vitro study in our laboratory we have observed also that there is a melanin-microwave interaction which generates free radicals (unpublished data). Such oxygen radicals are known to increase vascular permeability [Hull, 1985] and cause corneal endothelial damage [Hull, 1979]. Thus it is possible that microwave exposure of ocular tissue may result in either the generation or release of free radicals, which then cause increased vascular permeability of the iris. The corneal endothelial lesions, which do not appear until 24 h post-exposure, are probably a secondary effect. The initial leakage of iris vessels allows serum protein into the aqueous humor, which would result in the production of additional free radicals, and damage to the corneal endothelial cells. Although interaction between microwave radiation and the drug/melanin complex is speculative at this time, it does offer a possible explanation for the unexpected finding that both drugs lower the microwave threshold for ocular damage.

The non-human primate model used in this study is anatomically and physiologically similar to the human eye. Nevertheless, it must be recognized that the effects observed in this study were derived under laboratory conditions, including anesthesia and repeated prolonged exposures, and may not necessarily duplicate conditions found in the environment. However, the data indicate strongly that individuals may be subject to ocular changes from low-level microwave exposure when the average dose rate in the eye is 0.26 W/kg or greater if the exposure occurs while the individual is utilizing timolol therapy.

ACKNOWLEDGMENTS

The authors acknowledge the expert assistance of Jeaneen Jernigan and Terry Pfenning in the preparation of this manuscript. This work was supported in part by the Department of the Navy and by the Food and Drug Administration. The results

and opinions expressed in this paper are those of the authors and do not necessarily reflect the views of the Department of the Navy. No official endorsement should be inferred. In conducting the research on animals, the authors adhered to the "Guide for Care and Use of Laboratory Animals"(Department of Health and Human Services Publication No. NIH 85-23, 1985) and to the procedures prescribed by the Division of Comparative Medicine of the Johns Hopkins Medical Institutions. Laboratory work was performed at the Wilmer Ophthalmological Institute of the Johns Hopkins University School of Medicine.

REFERENCES

Abrahamsson T, et al. (1988): Binding of the ß-blockers timolol and H 216/44 to ocular melanin. Exp Eye Res 47:565–577.

Cleary, SF (1980): Microwave cataractogenesis. Proc IEEE 68:49–55.

D'Anna SA, et al. (1983): Fluorescein angiography of the heavily pigmented iris and new dyes for iris angiography. Arch Ophthal 101: 289–293.

Elder JA (1983): Special senses. In "Biological Effects of Radiofrequency Radiation." Elder JA, Cahill DF (eds). EPA 600/883-026F. Washington, DC: Environmental Protection Agency, pp 5–64–5–78.

Hirst LW, et al. (1983): Posterior corneal rings. Invest Ophthal Vis Sci 25:586–588.

Holmdahl G, Bengtsson E (1981): The effect of timolol maleate on the disruption of the blood-aqueous barrier in the rabbit eye. Invest Ophthal Vis Sci 20:726–732.

Hull DS (1979): Photodynamically induced alteration of the corneal endothelial cell function. Invest Ophthal Vis Sci 18:226–231.

Hull DS (1985): Effect of oxygen-free radical products on rabbit iris vascular permeability. Acta Ophthal 63:513–518.

Kiel JL, et al. (1990): Diazoluminomelanin: A conductive luminescent polymer with microwave and radiowave absorptive properties. Annual International Conference of the IEEE Engineering in Medicine and Biology Society 12:1689–1690.

Kinoshita JH, et al. (1966): Biochemical changes in microwave cataracts. Doc Ophthal 20:91–103.

Krachmer JH, et al. (1981): Cornea pseudoguttata: A clinical and histopathologic description of endothelial cell edema. Arch Ophthal 99:1377–1381.

Kramar PO, et al. (1978): Acute microwave irradiation and cataract formation in rabbits and monkeys. J Microwave Power 11:135–136.

Kues HA, et al. (1985): Effects of 2.45-GHz on primate corneal endothelium. Bioelectromagnetics 6:177–188.

Kues, HA, D'Anna SA (1987): Changes in the monkey eye following pulsed 2.45 GHz microwave exposure. Proc IEEE Ninth Annual Conf of the Engineering in Medicine and Biology Society, pp 698–700.

Lipman RM, et al. (1988): Cataracts induced by microwaves and ionizing radiation. Surv Ophthal 33:200–210.

Melikian HE, et al. (1971): Ocular pigmentation and pressure outflow responses to pilocarpine and epinephrine. Am J Ophthal 72:70–73.

National Council on Radiation Protection and Measurements (1986): Cataractogenesis. NCRP Report No 86, pp 191–206.

Phelan AM, et al. (1992): Modification of membrane fluidity in melanin-containing cells by low-level microwave radiation. Bioelectromagnetics 13:131-146.

Rosenthal SW, et al. (1977): Effects of 35 and 107 GHz CW microwaves on the rabbit eye. Proc USNC/URSI Annual Meeting 1:110–128.

SAS User's Guide (1988): OS SAS Release 6.01. Cary, NC: SAS Institute, Inc., pp 547–640.

Stocker FW (1947): Experimental studies on the blood-aqueous barrier. Arch Ophthal 37:583–590.

Weiter JJ, et al. (1975): Ascorbic acid changes in cultured rabbit lenses after microwave irradiation. Ann N Y Acad Sci 247:175–181.

Salmon Dinner

Bioelectromagnetics 6:177–188 (1985)

Effects of 2.45-GHz Microwaves on Primate Corneal Endothelium

Henry A. Kues, Lawrence W. Hirst, Gerard A. Lutty, Salvatore A. D'Anna, and Gregory R. Dunkelberger

Johns Hopkins University Applied Physics Laboratory, Laurel, Maryland (H.A.K.); Bethesda Eye Institute, St. Louis University, St. Louis (L.W.H.); and Wilmer Ophthalmological Institute, Johns Hopkins Hospital, Baltimore (G.A.L., S.A.D'A., G.R.D.)

Both eyes of anesthetized cynomolgus monkeys (*Macaca fascicularis*) were irradiated with 2.45-GHz microwaves, either pulsed or continuous wave. In vivo corneal endothelial abnormalities were observed by specular microscopy and confirmed through histologic techniques after a 16- to 48-hour postexposure period. Pulsed microwaves with an average power density of 10 mW/cm^2 (equivalent to a specific absorption rate (SAR) = 2.6 W/kg) produced these effects, while levels of 20–30 mW/cm^2 (equivalent to a SAR = 5.3 to 7.8 W/kg) with continuous wave irradiation were required to produce similar changes.

Key words: microwave irradiation, specular microscopy, monkey, corneal endothelium

INTRODUCTION

The three major ocular components in vision, cornea, lens, and retina, have been studied by bioelectromagnetic researchers investigating potential health hazards associated with microwave exposure [Carpenter et al, 1974; Williams et al, 1975]. In most previous experiments involving microwave irradiation of the eye, the lens was the primary target for investigation [Carpenter and Van Ummersen, 1968]. This ocular research established a direct relationship between microwaves at exposures exceeding 100 mW/cm^2 and lens opacification or cataract formation in test animals [Cleary, 1980]. The retina may also be susceptible to microwave irradiation [Aurell and Tengroth, 1973]. Ultrastructural degeneration of retinal neurons in rabbits has been reported at microwave power levels of 55 mW/cm^2 [Paulsson et al, 1979].

The cornea, with its stratified structure of epithelium, Bowman's membrane, stroma, Descemet's membrane, and endothelium, recieved scant attention in early microwave work [Richardson et al, 1951]. Rosenthal et al [1975], employing slit lamp

Received for review October 3, 1983; revision received November 30, 1984.

The results and opinions expressed in this paper are those of the authors and do not necessarily reflect the views of the Department of the Navy. No official endorsement should be inferred. In conducting the research on animals, the authors adhered to the "Guide for Care and Use Of Laboratory Animals" (DHEW Publication No. NIH 78-23, 1978) and to the procedures prescribed by the Division of Laboratory Animals Medicine of the Johns Hopkins Medical Institute.

Address reprint requests to H.A. Kues, Johns Hopkins University Applied Physics Laboratory, Johns Hopkins Road, Laurel, MD 20707.

examination and electron microscopy, found epithelial and stromal damage in rabbit corneas at microwave power levels below 10 mW/cm^2. The endothelium, unlike the other corneal layers, is composed of a single layer of approximately one-half million flat and mostly hexagonal cells. The endothelium, with its anatomic integrity and active cell "pumps," is the most important component in maintaining corneal dehydration and transparency [Smolin and Thoft, 1983]. Therefore, any serious damage to the endothelium can lead to corneal edema and visual loss. In spite of its anatomic importance, the corneal endothelium has long been ignored in microwave studies of the eye. Even the recent work of McAfee [1983] in part depended upon observations performed by slit lamp biomicroscopy, which at best gives poor quality images of corneal endothelium.

Specular microscopy [Laing and Sandstrom, 1975; Bourne and Kaufman, 1976; Koester et al, 1980], a recent development in the field of diagnostic and clinical ophthalmology, enables the endothelial cell monolayer to be photographed and studied in vivo with resolution of individual cells far exceeding that produced by the slit lamp biomicroscope. This technique proved to be ideal for studying the temporal effects of microwaves on the corneal endothelium.

The rabbit corneal endothelium is known to repair itself rapidly through mitosis, regaining its original anatomy within days to weeks [Mills and Donn, 1960]. The adult subhuman primate and human endothelium, unlike that of the rabbit, is not known to repair itself through cell division [Van Horn and Hyndiuk, 1975]. Because of the similarity of the simian corneal endothelium to that of the human, the monkey was chosen as a suitable model for the study of microwave irradiation effects. Once endothelial cells of these species are damaged, they are replaced by surrounding endothelial cells which enlarge and migrate to fill in defects in this monolayer of cells. An overall reduction in cell population results. Eventually, a serious reduction in endothelial cell density will cause marked swelling of the cornea with a resultant loss of transparency [Smolin and Thoft, 1983].

MATERIALS AND METHODS

The type of apparatus that was utilized for the animal exposures is shown in Figure 1. The 1.2 × 1.2 × 1.2-m anechoic chamber had all sides and top lined with AN-77 absorbing material, while the bottom was lined with SPY-12 absorbing material. The chamber door was ventilated in a manner to allow convective airflow around the animal and designed o minimize microwave reflections. Two exhaust ports were located at the top of the chamber. Temperature inside the chamber was measured during exposure sessions and was found to remain within ± 1.5 °C of room temperataure. Room temperature was held between 23 °C–25 °C during irradiation. The 2.45-GHz continuous wave (CW) microwaves were generated by an HP-8616B microwave signal source driving an ALFRED-5020 traveling wavetube amplifier (twt). The harmonic content of the HP-8616B signal generator and twt were measured. The second harmonic was found to be 48 dB down for the HP-8616B alone, and 15 dB down at the twt output. To decrease harmonic content, the microwave energy was then transmitted through an isolator and HP-360D low pass filter (>30 dB at 4.9 GHz). The microwaves were then passed by way of a coaxial cable to a bidirectional coupler to measure both forward and reflected power. The microwaves then traveled from the bidirectional coupler by means of a coaxial cable into an HP-

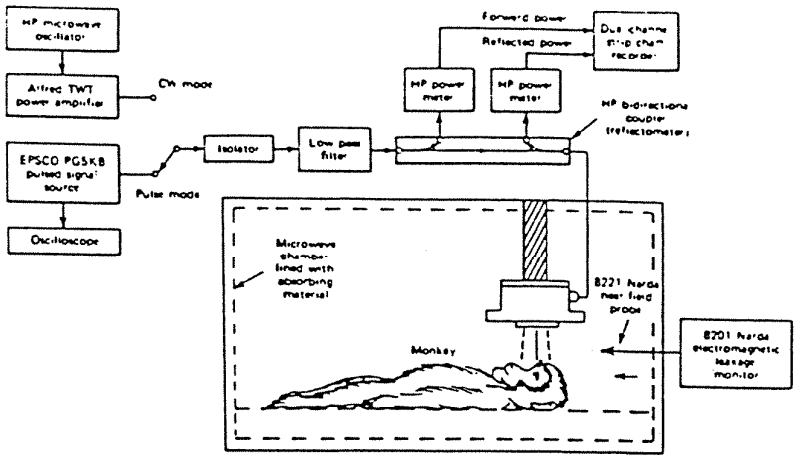

Fig. 1. 2.45 GHz primate exposure apparatus.

S281A coaxial-to-waveguide transition source located within the anechoic chamber. The source with its 7.214 × 3.404-cm aperture was positioned over the ocular area to be irradiated with the 7-cm plane crossing both eyes and centered on the nasal bridge at a height sufficient to allow a 10-cm gap between it and the ocular surface. System input and reflected power levels were measured (2.9 W input with 50–150 mW reflected for a 10 mW/cm^2 exposure) and recorded on a dual-strip chart recorder during each 4-hour exposure. The 2.45-GHz pulsed irradiations (10 μs at 100 pps) were performed as indicated above with the exception that an EPSCO PG5KB pulsed signal source was utilized in place of the CW source and twt power amplifier.

The microwave power density at the cornea was determined prior to each exposure through a 2.45 GHz calibrated Narda 8201 electromagnetic monitor. During initial system measurements, the probe was positioned from the bottom parallel to the direction of energy propagation at a point 10 cm from the source, approximating where the animal's nasal bridge and eyes would be located. This required the removal of the Styrofoam animal holder for each measurement. It was later discovered that by placing the 8221 probe in parallel alignment with the source's long plane and rotating the probe so the manufacturer's calibration mark faced the source at its center, a reading within a few percent of the perpendicular alignment was obtained. The accuracy of this alteration has since been measured and verified on site by an independent group, Athey and Allen from the Food and Drug Administration. The measured power densities were then compared against the prescribed input power settings of 2.9 W per 10 mW/cm^2 exposure. The prescribed system input was obtained by means of an independent evaluation of the incident power density using the transmission portion of the radar range equation, $PD = \frac{P_t G_t}{4\pi R^2}$. This was based upon measurement of transmitted power, antenna (emitter) gain, and field pattern, various line losses, and component standing wave ratio (SWR).

The use of the HPS281A coaxial cable to waveguide transition as an antenna may be questionable. Its use was necessitated by the required power densities and available equipment limitations. It was also found to be inappropriate to change the

source to something more conventional halfway through our study. We believe the following two facts must be recognized. First, at the close distance involved, a multiple reflection between the test animal and the antenna, primarily its waveguide flange, could alter the intensity of the incident field. This alteration in intensity could go in either direction. Measured specific absorption rate (SAR) indicates that this is probably not occurring. A second and lesser objection is that both the measured gain (5.7 dB) and the beam width imply that the active region of the antenna is slightly larger than the 7.214 × 3.404 cm waveguide opening. The 10-cm distance is just at the farfield boundary ($2d^2/\lambda$, where d is the aperture diagonal) for this opening. A larger area of radiation means that the far-field criterion may not be satisfied, although it may be violated by a factor of two without significantly degrading the accuracy of the inverse square law as used in our calibration. These facts and the realization that the presence of the animal may have introduced some change in field symmetry were accepted for the present experiment.

Equivalent SARs were based upon actual in vivo temperature measurements made during a 4-hour microwave exposure to 20 mW/cm^2. A nonperturbing fluoroptic (1000 B System) thermal probe was surgically implanted in the anterior chamber of the eye and butted up against the endothelial layer of the cornea. A baseline temperature of 34.5 °C was recorded just prior to exposure. Microwaves with a power density of 20 mW/cm^2 were then applied as in a normal exposure session. The temperature was recorded every 4 seconds for the first hour and then every minute for the remaining 3 hours. A 1-minute temperature rise of .09 °C was selected from the steepest part of the recorded 4-hour temperature increase of 0.77 °C. This reading of .09 °C/min was then applied to the equation 1 °C/min = 58.6 W/kg, which is based on a specific heat of tissue of 0.84 [Durney et al, 1980]. A calculated SAR of 5.27 W/kg per 20 mW/cm^2 of incident power or 0.26 W/kg per 1 mW/cm^2 was then assumed.

The animals were intubated and maintained under halothane gas anesthesia. The rubber anesthesia tubes were brought into the chamber through two aluminum fittings mounted in the fine mesh copper screen. A second set of rubber anesthesia tubes ran from the fittings parallel with the monkey, past its head and neck and across its chest. They then joined at a plastic "Y" fitting at the animal's neck, with a rubber endotracheal tube inserted through the mouth into the airway. No metal fittings were used after the connection to the aluminum wall fittings. The rubber tubes also remained outside the microwave exposed area. While in the microwave chamber, the monkeys rested in a supine position on a Styrofoam platform directing both eyes, with eyelids closed, toward the microwave source. Care was taken in positioning the animal in order to subject both eyes to the same microwave field intensity.

During several 10 mW/cm^2 pulses and sham exposures, body core temperature (rectal) was measured by means of an Electromedics Inc. M-99 digital thermometer. An average baseline temperature of 35.8 °C was measured just before microwave exposure. The temperature decreased an average of 2.4 °C after 4 hours in the microwave-exposed animals and 2.5 °C in the sham-exposed animals. This decrease was attributed to the effect of anesthesia.

Examinations were performed using a Keeler-Konan (Model SP-1) specular microscope on all monkeys while they were under halothane gas anesthesia or ketamine sedation. An eyelid speculum was inserted, and the cornea was kept moistened with balanced salt solution during the examination. The wide-field contact

specular microscope was used to scan and photograph the central 6 mm of cornea. Each photographic field at 120× covered approximately 1 mm^2 of cornea. Reported degree of endothelial damage was based upon the number of visible lesions present in the photographic field from each eye which demonstrated the greatest number of lesions. Each evaluation was then placed in one of four categories: no change, 0–2 lesions; minor change, 3–10 lesions; moderate change, 11–50 lesions; major change, greater than 50 lesions.

Fifteen juvenile cynomolgus monkeys (*Macaca fascicularis*) were subjected to specular microscopic examination prior to and subsequent to 2.45 GHz microwave exposure. Three basic protocols were used: one involved a once-a-week, 4-hour 5–30 mW/cm^2 exposure, repeated over a period of time, with specular microscopic examinations performed every 2 to 4 weeks; a second involved a series of single 10–30 mW/cm^2 exposures of 4 hours separated by one or more weeks and followed each time by specular microscopic examinations; a third protocol was employed in which four consecutive daily 4-hour exposures were performed. Exact exposure levels for each animal are given in Tables 1 and 2. For the series of single exposures, specular microscopic examinations were performed just before exposure and repeated 4, 24, 48, and in some cases 72 hours, after exposure. Late in the study, when a latent period was found to exist between microwave exposure and the onset of corneal changes, the examination at 4 hours was deleted from the protocol. When the four-consecutive-day protocol was used, specular microscopic examinations were performed just before exposure on day 1 and repeated on days 3, 4, and 5.

Five monkeys were used for a total of ten sham exposures. Three monkeys received two sham exposures each; of the remaining two monkeys, one received three and the other received one sham exposure. Four of the five sham monkeys were later placed into the exposure protocols.

Four monkeys were euthanatized by administration of an overdose of intravenous sodium pentobarbital immediately after an effect was confirmed by specular

TABLE 1. 2.45 GHz Continuous-Wave Microwave-Induced Endothelium Abnormalities

Primate number	Exposure levels (mW/cm^2)[a]	Minimum time between exposures	Number of exposure sessions	Number of examination sessions	Number of times abnormalities observed	Comments
1	5	1 week	44	10	0	No change
2	10	1 week	56	12	1	Minor change one eye only
3	10	1 week	10	3	0	No change
4	20	1 week	18	6	0	No change
5	30	—	1	1	1	Major change one eye, moderate in other
6	20	1 week	1	1	0	No change
	30	1 week	5	5	3	Moderate change
7	20	1 week	22	14	1	Minor change
	30	1 week	8	6	2	Minor-to-moderate change
	20	1 day	2[b]	2[c]	2	Major change

[a]Equivalent SARs are 0.26W/Kg per 1 mW/cm^2 incident power.
[b]Each session consisted of four consecutive daily 4-hour irradiations.
[c]Effect first appeared between 3rd and 5th day after start of protocol.

TABLE 2. 2.45 GHz Pulsed Microwave Induced Endothelium Abnormalities*

Primate number	Exposure levels (mW/cm^2 avg)[a]	Minimum time between exposures	Number of exposure sessions	Number of examination sessions	Number of times abnormalities observed	Comments
8	10	1 week	5	5	0	No change
	10	1 day	4[b]	4[c]	4	Minor change
9	15		1	1	1	Major change
10	10	1 week	5	5	5	Minor-to-major change
	15		1	1	1	Major change
11	10	1 week	5	5	2	Very minor change
	10	1 day	4[b]	4[c]	4	Major change
12	10	1 week	11	11	6	Minor-to-moderate change
13	5	1 week	2	2	0	No change
	10	1 week	4	4	4	Minor-to-major change
	10	1 day	1[b]	1[c]	1	Major change
14	10	1 week	4	4	1	Minor change
15	10	1 week	2	2	0	No change

[a]Pulses were 10 μs wide and had a 100 pps repetition rate.
[b]Each session consisted of four consecutive daily 4-hour irradiations.
[c]Effect first appeared between 3rd and 5th day after start of protocol.
*Equivalent SARs are 0.26W/kg per 1 mW/cm^2 incident power.

microscopy. The eyes were immediately enucleated, and one of the pair of eyes was submitted for vital staining and the other eye for transmission electron microscopy. For vital staining, the corneas were examined with a rim of sclera and processed according to the alizarin red–trypan blue method of Spentz and Peyman [1976]. For transmission electron microscopy, an incision was made in the enucleated eyes at the pars plana and the globe fixed in a standard glutaraldehyde-paraformaldehyde solution. The cornea with a 1-mm scleral ring was removed, postfixed in OSO_4, dehydrated, cleared, and embedded in Epon-812 (Electron Microscopy Sciences). Thin sections were cut, stained, and observed with a Jeol 100B transmission electron microscope.

RESULTS

Specular microscopic observations of normal primate corneal endothelium provided a clear view of hexagonal endothelial cells of uniform size (Fig. 2). Cell boundaries were distinctly delineated, and the nuclear regions were visible in most cells. When peripheral areas of the cornea were viewed, posterior corneal rings or naturally occurring endothelial folds were frequently seen [Hirst et al. 1983].

Abnormalities in the endothelial monolayer were also clearly observed by specular microscopy in primate corneas following controlled exposure to microwave irradiation. The lesions, unicellular to multicellular in size, were found to be widespread over the cornea and appeared to be areas where some cell death and subsequent loss had occurred (Figs. 3 and 4). Histologic vital staining confirmed endothelial damage and death by showing areas with swollen, trypan blue—stained nuclei, which were surrounded by enlarged cells, as well as pockets devoid of any cells (Fig. 5). Transmission electron microscopy also indicated endothelial cell abnormalities which

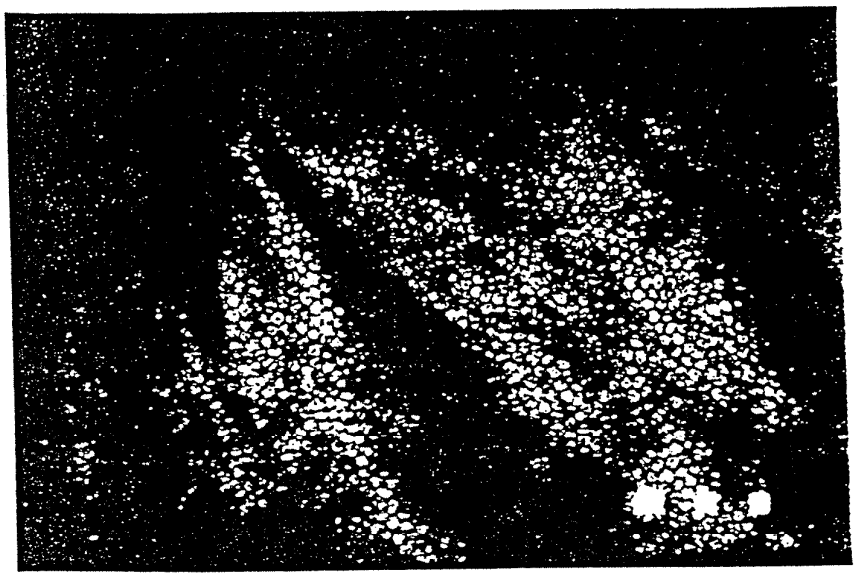

Fig. 2. Keeler-Konan wide-field specular micrograph (magnification ×120) of normal pre-irradiated monkey endothelium (animal #6).

included unusual vacuoles and an apparent separation of endothelium from Descement's membrane (Fig. 6).

The extent of microwave-induced endothelial abnormalities appeared to be influenced by actual power density, type of microwave mode, and exposure protocol (Tables 1 and 2). With both CW and pulsed microwave modes, increased power densities produced a greater number of endothelial lesions. Pulsed microwaves produced abnormalities at lower power densities than corresponding CW microwaves (Table 3). With a single 4-hour exposure at 20–30 mW/cm^2 of CW microwaves at 2.45 GHz, endothelial abnormalities were observed. Similar effects were observed following a single 4-hour exposure of 10 mW/cm^2 pulsed microwaves at 2.45 GHz. While each protocol produced some change under certain mode and power density conditions, major changes (a larger area of change and a higher concentration of individual lesions) were most frequently observed with the protocol using 4-hour exposures over four consecutive days. Sham-exposed primates which were anesthetized and treated identically to the other experimental animals, with the exception of not receiving any microwave irradiation, showed no detectable endothelial abnormalities.

Microwave-induced endothelial changes were first observed 16–48 hours after irradiation. A latent period of 16 hours or greater appeared to exist, since no endothelial abnormalities could be detected before this period. Both eyes of each primate were subjected to approximately the same microwave power level during each exposure. When endothelial changes occurred, they were observed in both eyes in all but one case. However, the degree of change and duration of the latent period frequently varied between the two eyes. The CW-exposed monkeys (irradiated once

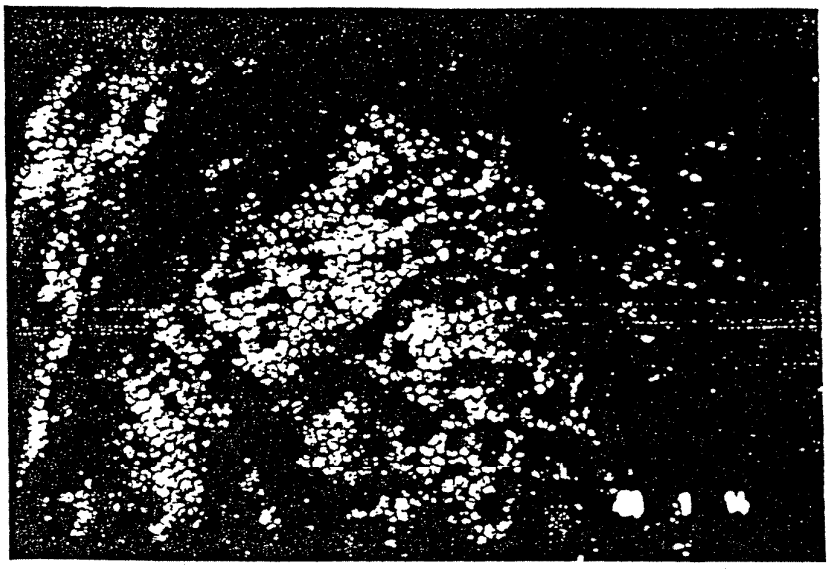

Fig. 3. Keeler-Konan wide-field specular micrograph (magnification ×120) of monkey corneal endothelium 48 hours after a 4-hour exposure to 2.45 GHz pulsed microwave of 10 mW/cm^2 average power (animal #10). There are approximately 50 lesions per square millimeter of central corneal endothelium. The individual lesions vary from abnormalities of single cells (arrow) to confluent cell abnormalities involving three to five cells (square). The lesions are relatively uniformly scattered over the central endothelial surface, with intervening areas of normal appearing corneal endothelium.

weekly with exposure levels of 20 mW/cm^2 or less) generally showed minor, if any, observable endothelial changes even over extended periods of time. The major effects from CW were generally the result of higher power density (30 mW/cm^2) exposures. All pulsed microwave exposed monkeys showed moderate-to-major levels of endothelial change at 10-15 mW/cm^2 exposures; the few 5 mW/cm^2 pulsed exposures produced no change. Again, a 16-48 hour latent period seemed to exist.

The most severe endothelial cell changes occurred during exposure protocols of four consecutive daily irradiations, which utilized both 20 mW/cm^2 CW and 10 mW/cm^2 pulsed microwaves. These abnormalities were first observed 72-96 hours after the initial irradiation in the 4-day series.

The damage to corneal endothelium probably was not due to thermal effects of microwaves, since only minimal changes in temperature at the endothelium-aqueous humor interface was observed during the 4-hour exposure. Within 72-96 hours following observation of microwave-induced endothelial lesions, the endothelium of all irradiated primates appeared normal. Occasionally, some large cells were noticed near areas where lesions had been found previously.

DISCUSSION

The transparency of the cornea is due to its ordered structure and is dependent upon its relative deturgescence. Deturgescence, the state of perfect hydration of the

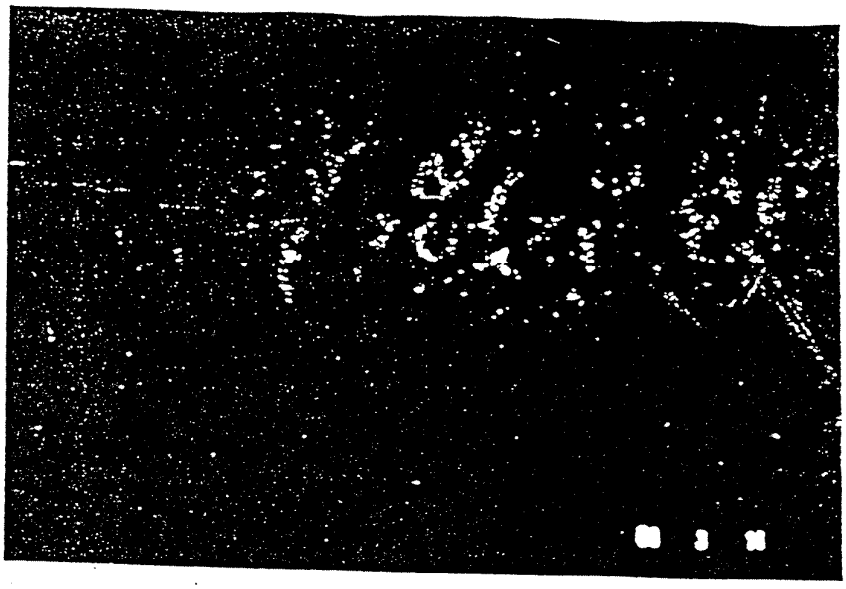

Fig. 4. Keeler-Konan wide-field specular micrograph (magnification ×72) of monkey central corneal endothelium 48 hours after a 4-hour exposure to 2.45 GHz pulsed microwave of 15 mW/cm$_2$ average power (animal #9). The widespread distribution of endothelial lesions and intervening normal endothelial mosaic can be appreciated. The corneal folds seen to the left of the micrograph are normal features of applanation by the specular microscope.

corneal tissue, is maintained by the anatomic integrity and active cell "pumps" of the endothelium. In this paper, we have reported a study that addresses the effects of 2.45-GHz microwaves on primate corneal endothelium, with the use of in vivo specular microscopy. Morphological change was found to occur in the endothelium after a post-exposure latent period of approximately 16 to 48 hours.

Based upon our findings, the following conclusions may be drawn: Under the conditions of the protocols presented, a 4-hour exposure at 20-30 mW/cm^2 to CW irradiation at 2.45 GHz can produce observable cellular effects (Table 1). A 4-hour exposure of pulsed microwaves at 2.45 GHz produces similar effects down to 10 mW/cm^2 average power (Table 2). Chronic exposure to pulsed microwave (10–15 mW/cm^2) produced a greater incidence of endothelial cell damage than chronic exposure to CW microwave of greater power density (20–30mW/cm^2) (Table 3). Short-term repeated daily exposures appear to be more likely to produce greater endothelial change than a larger number of individual exposures spaced more than one week apart. Within the limits of our exposure protocol, the observed endothelial changes appear reversible, but some cell loss does occur. The affected corneas in all cases appeared relatively normal within 72 to 96 hours after the observation of endothelial lesions. There were, however, large cells in areas of previous microwave damage suggesting a loss of cells. In support of the hypothesis that cell loss was occurring in the areas of large cell development, cell death was clearly documented by vital staining. Since there is cell loss, the question remains of what the long-term effect on the cornea would be after a large number of microwave exposures at levels capable of producing the reported endothelial lesions. We are extending our protocol

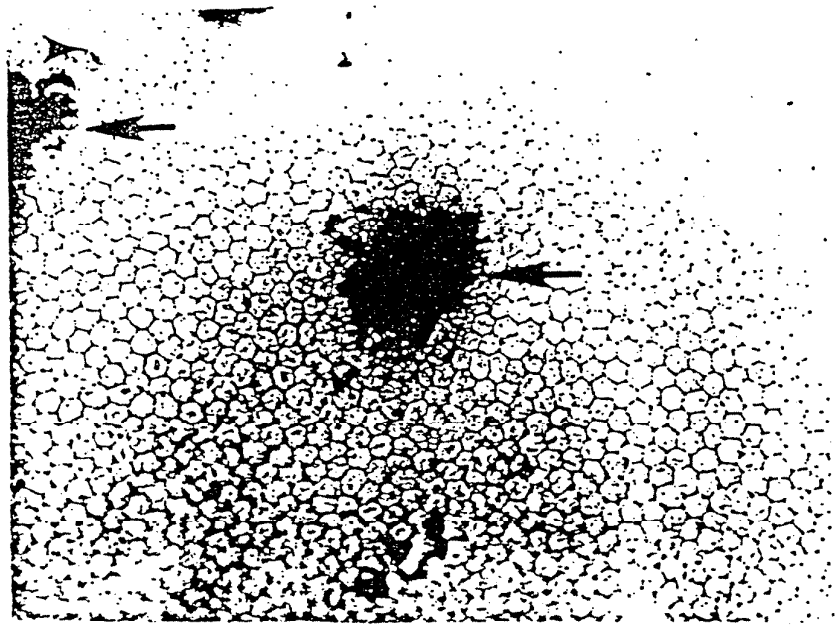

Fig. 5. Photomicrograph (×400) of alizarin red and trypan blue vital stained corneal endothelium from a monkey 48 hours after a 4-hour exposure to 2.45 GHz pulsed microwave of 10 mW/cm^2 average power (animal #10). The normal endothelium displays a well-defined hexagonal outline and oval, faintly stained nuclei. Two lesions are evident in which there is cellular uptake of trypan blue in areas lacking endothelial cells (solid arrows). Surrounding endothelial cells are distorted and stain faintly with trypan blue (star). Damaged adjacent individual endothelial cells display swollen, blue stained nuclei (arrow heads).

to examine the possibility of microwave-induced depletion of endothelial reserves and its resultant end point. We are presently using specular microscopy to study cell density changes as well as changes in cell shape and size. This work will be reported upon in a future publication.

Throughout our study, we have pondered the question of why previous researchers [Rosenthal et al, 1975; McAfee et al, 1983] had not observed this endothelial effect during the course of their investigations. One plausible explanation is that slit-lamp examination does not normally resolve the corneal endothelium with sufficient detail to detect the changes we have reported. During our study, changes observed with the specular microscope were not visible by slit-lamp examination. As for histologic examinations, our study has revealed that a time "window" may exist during which time the reported change is observable. Before and after this period, the endothelium probably would appear relatively normal. It was by use of the in vivo examination, that we were able to find this window of effect and then study the corneas histologically.

The monkey eyes used in this study are comparable biologically to the human eye. The experimental protocol, however, was not designed to match real-life human exposure conditions. To determine whether this reported effect presents a human ocular health hazard, considerable research remains to be conducted. Whether there

Fig. 6. Transmission electron micrograph (×4,000) of monkey corneal endothelium 48 hours after a 4-hour exposure to 2.45 GHz pulsed microwave of 10 mW/cm^2 average power (animal #10). Prominent intracellular vacuolization is present (star). Underlying Descemet's membrane and stroma remains normal, but a space exists between basal surface of endothelium and Descemet's membrane.

TABLE 3. Frequency that Damage was Observed

Mode	No. eyes	Average power level (mW/cm^2)	Total no. observations	No. times damage observed
CW	6	10-20	21	1
CW	6	20-30	27	7
Pulsed	16	10-15	38	20
Sham	10	0	10	0

is a microwave exposure level or frequency at which the present reversible damage becomes irreparable and what effect the anesthetic has on endothelial damage are questions unanswered at this time. The point of this paper is not necessarily to point out a possible health hazard, as in some previous ocular studies, but rather to report upon an interaction between microwaves and a naturally occurring biological tissue and to provide a methodology for its investigation. Studies of this nature remain crucial to the understanding of the interaction between microwaves and living organisms.

ACKNOWLEDGMENTS

The authors wish to thank Drs. Thomas Rozzell and Samuel Koslov for their help and encouragement. We also acknowledge the histological assistance of

Dr. W. R. Green and his staff, and critical measurements of the microwave system by R.C. Mallalieu, W. Athey, and S. Allen.

This work was supported in part by the Department of the Navy (through the Office of Naval Research and Naval Sea Systems Command under contract N00024-83-C-5301), by the National Eye Institute Grant EY 02476 (Hirst), and by the Electron Microscopy Grant EM 01765 (Wilmer Institute).

REFERENCES

Aurell E, Tengroth B (1973): Lenticular and retinal changes secondary to microwave exposure. Acta Ophthalmol (Copenh) 51:764-771.

Bourne WM, Kaufman HE (1976): Specular microscopy of human corneal endothelium in vivo. Am J Ophthalmol 81:319-323.

Carpenter RL, Van Ummersen CA (1968): The action of microwave radiation on the eye. J Microwave Power 3:3-19.

Carpenter RL, Ferri ES, Hagan GL (1974): Assessing microwaves as a hazard to the eye—progress and problems. Proc Int Symp Biologic Effects Health Hazards Microwave Radiation (Warsaw), pp. 178-184.

Cleary SF (1980): Microwave cataractogenesis. Proc IEEE 68:49-55.

Durney CH, Iskander MF, Massoudi H, Allen SJ, Mitchell JC (1980): "Radiofrequency Radiation Dosimetry Handbook." Report SAM-TR-80-32, pp 28-29.

Hirst LW, Dunkelberger G, Adams RJ, Kues HA (1983): Posterior corneal rings. Invest Ophthalmol Vis Sci 25:586-588.

Koester CJ, Roberts CW, Donn A, Hoefle FB (1980): Widefield specular microscopy: clinical and research applications. Ophthalmology 87:849-860.

Laing RA, Sandstrom MM (1975): In vivo photomicrography of the corneal endothelium. Arch Ophthalmol 93:143-145.

McAfee RD, Ortiz-Lugo R, Bishop R, Gordon R (1983): Absence of deleterious effects of chronic microwave radiation on the eyes of rhesus monkeys. Ophthalmol Vis Sci 90:1243-1245.

Mills NL, Donn A (1960): Incorporation of tritrum-labeled thymidine by rabbit corneal endothelium. Arch Ophthalmol 64:159-162.

Paulsson LE, Hamnerius Y, Hansson HA, Sjostrand J (1979): Retinal damage experimentally induced by microwave radiation at 55 mW/cm^2. Acta Ophthalmol 57:183-197.

Richardson AW, Duane TD, Hines HM (1951): Experimental cataract produced by three centimeter pulsed microwave irradiation. Arch Ophthalmol 45:382-386.

Rosenthal SW, Birenbaum L, Kaplan IT, Metlay W, Snyder WZ, Zaret MM (1975): Effects of 35 and 107 GHZ CW microwaves on the rabbit eye. Proc USNC/URSI Annual Meeting (Boulder, CO) 1:110-128.

Smolin G, Thoft R (eds) (1983): "The Cornea: Scientific Foundations and Clinical Practice." Boston: Little, Brown, pp 1-75.

Spentz DJ, Peyman GA (1976): A new technique for vital staining of the corneal endothelium. Invest Ophthalmol Vis Sci 15:1000-1002.

Van Horn DL, Hyndiuk RA (1975): Endothelial wound repair in primate cornea. Exp Eye Res 21:113-124.

Williams RJ, McKee A, Finch ED (1975): Ultrastructural changes in the rabbit lens induced by microwave radiation. Ann NY Acad Sci 247:166-174.